MEDACC

Demonstration and validation of innovative methodology for regional climate change adaptation in the Mediterranean area

LIFE12 ENV/ES/000536

Start date of project: 1 July 2013

Duration of project: 5 years

Methodology to assess the impacts of climate and global change in the LIFE MEDACC case study basins: Generation of scenarios, vulnerability maps and modelling

Due date of deliverable: 12-2016

Actual submission date: 12-2016

Organization name of lead contractor for this deliverable: CREAF, IPE – CSIC, IRTA

Dissemination level: Public

Authors

Diana Pascual, Javier Zabalza Martínez, Immaculada Funes, Sergio M. Vicente-Serrano, Eduard Pla, Robert Savé, Xavier Aranda and Carmen Biel

Cite as

Pascual D, Zabalza Martinez J, Funes I, Vicente-Serrano SM, Pla E, Savé R, Aranda X, Biel C (2016) Methodology to assess climate change impacts in the LIFE MEDACC case study basins: Generation of scenarios, vulnerability maps and quantification of impacts. Deliverable 13. LIFE MEDACC.

Executive summary

This deliverable explains the methodologies followed in the project LIFE MEDACC to assess the impacts of climate and global change in the three case-study basins: Muga, Ter and Segre.

The first section makes a general introduction to the deliverable objectives. The second section delves into the climate scenarios by giving a general background, explaining existent scenario data and going into detail about the downscaling methodology of the RCP4.5 scenario proposed for this project. The third section carries out specific socioeconomic scenarios drawn ad hoc for project purposes. We have developed three land cover scenarios for the headwaters (afforestation, fire and forest management scenarios) and two water use scenarios for the medium and low basin courses (rational use of water resources and increased demand scenarios). The fourth section presents the hydrological modelling needed to assess the impacts of the scenarios in the water cycle. We have calibrated and validated two hydrological models (RHESSys and SWAT) and, then, introduce the climate and socioeconomic scenarios into the models to evaluate future impacts. The fifth section shows the methodology of the agriculture modelling. This project assesses agriculture suitability using net irrigation needs (NIR) of major crops and uses a set of agroclimatic parameters capable of indicating the consequences of climate change for crop production and growing cycle. Finally, the sixth section goes in depth into an analysis of climate change impacts on forests. We have applied a forest growth process-based model (GOTILWA+) and an index of forest fire risk (Drought Code of the Canadian Forest Fire Weather Index) for this analysis.

This deliverable delves into the methodologies followed by the project and the input data used in the modelling. The results, analysis of the results and conclusions of the application of these methodologies can be consulted at the *Deliverable 14 Impacts of climate and global change on the ecological, hydrological and agriculture systems in the LIFE MEDACC case study basins* (Pascual et al. 2016)

Contents

1. Introduction

One of the objectives of LIFE MEDACC project is the assessment of the impacts of climate and global change in the three case-study basins: Muga, Ter and Segre. This deliverable explains the methodologies followed to achieve this aim.

The Mediterranean region might become one of the most vulnerable areas in Europe and even in the world regarding climate change (IPCC 2007a). Observational studies have already revealed a global trend toward warmer conditions during the last decades and changes in rainfall seasonal patterns (IPCC 2007b, Bates et al. 2008, Ludwig et al. 2011). Besides, recent climatic models predict that the climate of the Mediterranean region will become warmer and drier at the end of the 21st Century, with changes in precipitation seasonal distribution (IPCC 2007a, EEA 2012). At the same time, land cover change processes are showing a general increase of the forests and the irrigated lands in the Northern rim of the Mediterranean basin, which have increased the water demand, given the increased evapotranspiration rates of these land cover types (Iglesias et al. 2007). All these processes are driving a decrease of the water availability in large regions of the Mediterranean, which is expected to be more severe in the coming decades, affecting the supply for industries, agriculture, urban uses and natural systems (Bates et al. 2008, Mariotti et al. 2008).

Water resources are directly affected by climate change, and the management of these resources affects the vulnerability of natural ecosystems, socio-economic activities and human health. Water management is also expected to play an increasingly central role in adaptation jointly to the management of water-related sectors like agriculture and forestry. At the regional level, not all of the Earth’s regions will be affected by the same changes in environmental conditions, and consequently, more exposed places will be potentially more vulnerable to climate change.

The significant vulnerability of water resources, agriculture and forestry to climate variability makes these sectors highly susceptible to climate and global change projections for Catalonia. For this reason, an accurate quantification of the impacts of climate and global change scenarios on these sectors, using a **multidisciplinary approach is essential to identify vulnerabilities and design adaptation measures**, ensuring a successful impact of the project results.

For our multidisciplinary approach, we have developed the following steps:

- Regional downscaling at basin scale of the IPCC RCP4.5 scenario.
- Design of ad hoc of socioeconomic scenarios: three land cover scenarios for the headwaters (afforestation, fire and forest management scenarios) and two water use scenarios for the medium and low basin courses (rational use of water resources and increased demand scenarios).
- Calibration and validation of two hydrological models (RHESSys and SWAT), one agriculture model, one forest model (GOTILWA+) and one index of forest fire risk (Drought Code of the Canadian Forest Fire Weather Index).
- Incorporation of climate and socioeconomic scenarios into the models to evaluate future impacts of climate and global.

This deliverable delves into the methodologies followed by the project and the input data used in the modelling. The results, analysis of the results and conclusions of the application of these methodologies can be consulted at the *Deliverable 14 Impacts of climate and global change on the ecological, hydrological and agriculture systems in the LIFE MEDACC case study basins* (Pascual et al. 2016).

2. Generation of climatic series

2.1. Introduction

The evaluation of main impacts of climate change in the selected basins is an aim of LIFE MEDACC project (Action B.1). Thus, it is needed to generate a robust climate series database for the period established (2012-2050) which can feed the hydrological models SWAT (Soil Water Assessment Tool) and RHESsys (Regional Hydro-Ecological Simulation System). This is needed for the analysis about the impacts, the vulnerability and the trends of different variables in the study area. As explained below, the series have been developed based on the Third Inform on Climatic Change in Catalonia (Martín-Vide, J. in press).

Nowadays, the generation of climatic series are based on 5th IPCC Inform, published in 2015, where the Representative Concentration Pathways (RCPs) are adopted and describe four possible climate futures, depending on the amount of greenhouse gases emitted in the following years. In the case of Catalonia the RCP4.5 was adopted, which is comparable to B1 scenario (from the 4th IPCC Inform), and assumes that is possible to have a range of radiative forcing values in the year 2100 relative to pre-industrial values of +4.5 W/m^2.

The climate models reproduce the observed patterns about temperature in a global scale and the trends of the last decades; while the precipitation models have improved from the last AR4 (4th Assessment Report of the IPCC) they are not as good as the temperature ones. There is a general coherence between projections from AR4 and AR5 in terms of large-scale patterns and the magnitude of the uncertainty has slightly changed, but now the characterization is complete and rigorous (IPCC 2014).

2.2. Background

After different meetings and workshops organized by the IPCC, the last report about global climate changes and its implications across the earth was developed in 2015. Nowadays, the Fifth Assessment Report (AR5) is a positive step to the knowledge about climate change, probably the most comprehensive analysis from the Fourth Assessment Report (AR4) in 2007. AR5 is made up by a huge multidisciplinary team, has some innovations and is based on several contributions as the physical science basis of climate change, the impacts, adaptation and vulnerability or the mitigation of climate change. AR5 has a great focus on the study of socioeconomic aspects of climate change and its implications for sustainable development.

In the Fifth Assessment Report (AR5) the Representative Concentration Pathways (RCPs) replace the Special Report on Emissions Scenarios (SRES) and are divided in four groups: RCP8.5, RCP6, RCP4.5 and RCP2.6. “The name representative concentration pathways was chosen to emphasize the rationale behind their use. RCPs are referred to as pathways in order to emphasize that their primary purpose is to provide time-dependent projections of atmospheric greenhouse gas (GHG) concentrations. In addition, the term pathway is meant to emphasize that it is not only a specific long-term concentration or radiative forcing outcome, such as a stabilization level of interest, but also the trajectory that is taken over time to reach that outcome. They are representative in that they are one of several different scenarios that have similar radiative forcing and emissions characteristics" (Moss, R. et al, 2008).

As explained before, in AR5 a new set of scenarios can be found (RCPs) with chapters dedicated to sea level change, carbon cycle and climate phenomena. Also is included a detailed climate change impacts report on a regional scale and adaptation and mitigation interactions. Related to the stabilization of greenhouse gas concentrations, can be founded a risk management and response framed to prevent dangerous anthropogenic interference with the climate system. The contents of the AR5 Working Group reports can be found at www.ipcc.ch.

2.3. Scenarios definition

The projections about changes in the climatic system are developed under a climatic models hierarchy, from simple models and other with intermediate complexity to complete ones and earth system models. All of them simulate changes under anthropogenic forcing and are based on a set of scenarios. Nowadays, with the new scenarios (RCPs), one of the most important changes is the combination of adaptation and mitigation, which are one of the key aspect in the report.

The anthropogenic emissions with another forcing agents, as land use changes, depend on socioeconomic factors and can be affected by global geopolitical agreements. This is another innovation included in AR5, with the inclusion of objectives based on the Framework Convention of the United Nations on Climate Change. In summary, the scenarios were developed under different criteria as socioeconomic factors, greenhouse gas emissions, land use changes, etc. The results are applied on a simple model to obtain temporal series of concentration of greenhouse that can be implemented in Atmosphere-Ocean General Circulation Models (AOGCMs).

For each category of emissions, an RCP has a set of values to start the series and the estimated emissions until 2100, which are based on results and assumptions about socioeconomic factors, population, economical activities, etc. While the socio-economic information is included in the process of generation of the scenarios, the result does not contain it.

The different scenarios are established just to make the same assumptions for every team who are working in climate modelling. In this way, the different studies can be comparable, making more robust the analysis and conclusions. But the main objective of a scenario is not to predict the future, actually is to know the uncertainties and different possibilities and take them into account to make more accurate the decisions under a wide range of possible futures (IPCC Scenario process for AR5).

The climate scenarios are used in project LIFE MEDACC by three reasons: (i) to study the effects of global warming, (ii) to combine information from diverse fields of study (agriculture, forest and hydrology) and (iii) to analyse the vulnerabilities establishing adaptive measures.

RCP4.5 was developed by the GCAM modelling team at the Pacific Northwest National Laboratory, Joint Global Change Research Institute (JGCRI) in the United States. It is a stabilization scenario in which total radiative forcing is stabilized shortly after 2100, without overshooting the long-run radiative forcing target level (Clarke et al. 2007, Smith and Wigley 2006, Wise et al. 2009).

2.4. Methodology

The temporal series developed for LIFE MEDACC project are based on comments about the Third Report on Climate Change in Catalonia (TICCC, Martín-Vide et al. in press). As this report is still in press, in this deliverable we only explain the changes applied to temperature and precipitation and some observations about the main changes and the spatial distribution of them.

In this case, the studied period is until 2050 and is based on different projects developed at different spatial scales (international, national and regional).

On the Second Report on Climate Change in Catalonia (SICCC) a regionalization was developed of the meteorological stations (Figure 1) in order to apply the different changes in temperature and precipitation, which will remain on the TICCC.

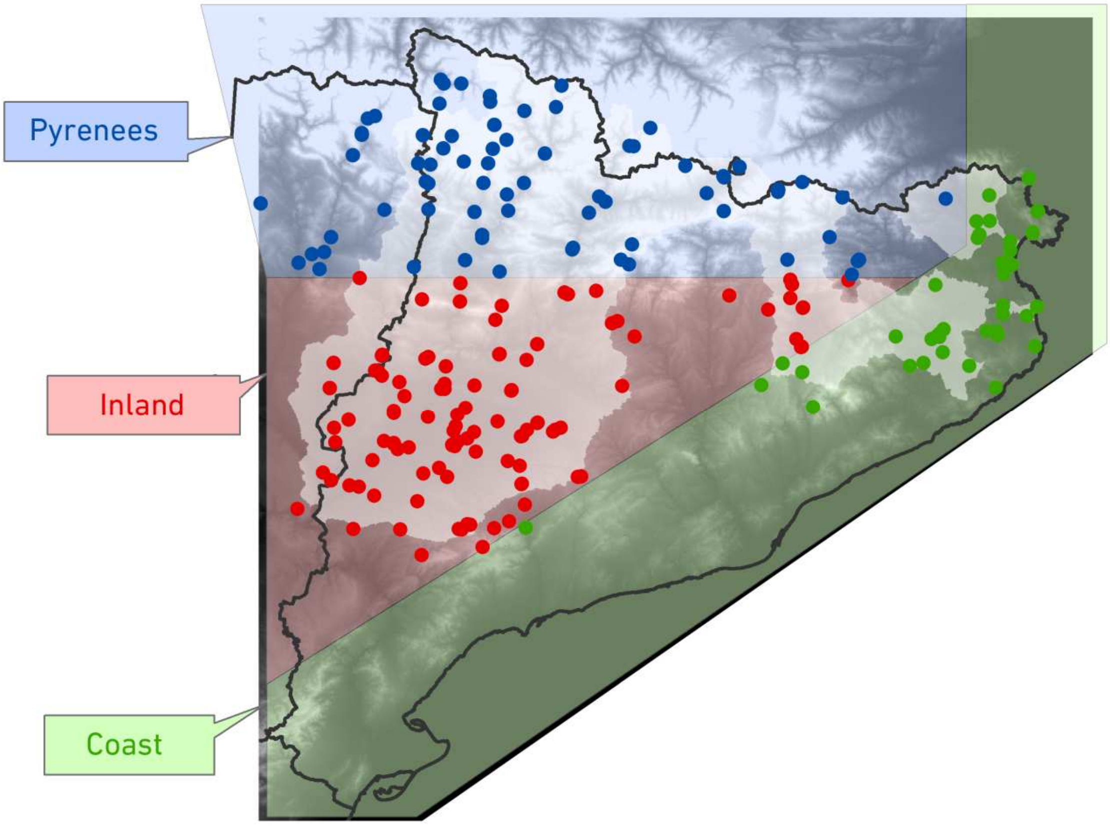

Figure 1. Spatial distribution of the meteorological stations in Catalonia.

The Table 1 shows a clear and spread temperature increase in all the spatial areas and seasons. The median values for Catalonia are: an increase of temperature of 0.8 and 1.4 ºC for 2012-2021 and 2031-2050 periods, respectively, and a decrease of precipitation of -2.4% and -6.8% for the same periods respectively. The increase of temperature are more accentuated in the Pyrenees, while the decrease of precipitation is more important on the Coastal area. The showed changes are based on scenarios (RCP4.5). Maybe, as the scenario is moderate (similar to B1), the changes are not as higher as expected. Anyway, the effect of a scenario more intensive would not be clear until the second half of the 21st century. All of these changes are always related to the reference period, 1971-2000.

		TEMPERATURE			PRECIPITATION		
		Pyrenees	Inland	Coast	Pyrenees	Inland	Coast
2012-2020	winter	0.5	0.6	0.7	2.7	2.1	-5.7
	spring	-0.1	0.1	-0.2	-1.3	-6.3	-6.9
	summer	0.6	0.5	0.1	-2.6	-1.6	-1.8
	autumn	0.1	0.3	0.2	-3.1	-4.6	-8.2
2021-2030	winter	0.9	0.9	1	0.5	0.4	-6
	spring	0.2	0.3	0.1	-5.1	-9.1	-9.7
	summer	1.1	1	0.6	-5.8	-5.8	-6.7
	autumn	0.7	0.8	0.7	-6.4	-6.9	-8.8
2031-2050	winter	1.2	1.2	1.3	-1.8	-1.3	-6.3
	spring	0.5	0.5	0.3	-8.9	-11.9	-12.5
	summer	1.6	1.5	1	-9.1	-9.9	-11.6
	autumn	1.2	1.2	1.1	-9.7	-9.2	-9.4

Table 1. Temperature and Precipitation changes for the different areas in Catalonia, based on RCP4.5 scenario.

The changes showed in Table 1 were applied to the observed temperature and precipitation series for the calibration period used in the project (2002-2011) year by year at daily scale. To avoid temporal patterns the results of this changes were randomly distributed (year by year) along the different periods, 2012-2020, 2021-2030 and 2031-2050. In this manner, we ensure that the proposed changes are kept accurately.

3. Generation of socioeconomic scenarios

3.1. Introduction

Global change refers not only to the changes in climate (climatic scenarios) but also to socioeconomic changes that include land use and land cover changes, demographic changes or changes in resource (water, energy, food) uses, among others. Global change scenarios draw alternative plausible options for different future socioeconomic developments (narrative storylines). These scenarios provide different views on the future of a certain study area by exploring what might happen given certain assumptions about the development of society and about environmental changes. Many international organizations and projects make use of scenarios that help them to plan an uncertain future. Some examples of global change scenarios that have been used as reference for this work are:

- IPCC emissions scenarios (SRES http://www.ipcc.ch/)
- Scenarios from the Global Environment Outlooks (3-4-5) developed by the United Nations Environment Programme (http://www.unep.org/GEO/geo3, http://www.unep.org/geo/geo4.asp, http://www.unep.org/geo/geo5.asp)
- Scenarios proposed by the Organisation for Economic Co-operation and Development (OECD) in the environmental perspective (http://www.oecd.org/env/cc/49082173.pdf, http://www.oecd.org)
- Scenarios from the Millennium Assessment Reports proposed by the United Nations (http://www.millenniumassessment.org/en/index.aspx)
- European projects: ALARM scenarios (http://www.alarmproject.net/alarm/), ESPON scenarios (http://www.espon.eu), PRELUDE scenarios from the European Environment Agency with a territorial focus (http://www.eea.europa.eu/media/audiovisuals/interactive/prelude-scenarios).

For Life MEDACC project purposes, we considered key to include not only climate change scenarios but also global change scenarios. Initially, we planned to use land use change projections (2030) and demography and water demands projections (2030) based on scenarios developed in other European, national or local projects. Nevertheless, we did not find any existent scenario that taken into account the characteristics and dynamics of the case-study basins or that had enough spatial resolution to be appropriate for the project objectives. Therefore, we decided to develop socioeconomic scenarios designed ad hoc for the project.

3.2. Definition of socioeconomic scenarios

The socioeconomic scenarios were developed based on experts' knowledge on main socio-economic sectors. A specific meeting was hold in May 19th 2015 where different experts discussed and agreed different plausible futures of the three basins. Experts covered the following areas: water management (partners from OCCC and IPE), forest sector (partners from IPE and CREAF), agriculture (partners from IRTA and an adviser of the DAAM, Ministry of Agriculture, Livestock, Fisheries and Food of Catalonia), demography (an expert from the Girona University) and adaptation policies and strategies (partners from the OCCC).

Different ideas, reflections and perspectives arose along the expert' meeting. Discussions can be followed in the minutes of the meeting, included in Annex 1. The following premises were agreed:

- Temporal time frame of the scenarios. The scenarios were drawn for 2050. We considered that long temporal time frames had less capacity to predict reliable changes. But also that short temporal time frames increases the difficulty to see changes when comparing with the reference (2002-2011). We also considered that time frame of the territorial policies affecting the area (land planning, irrigation plans...) or the available projections in the literature referring to the territory (demographic scenarios ...)

- Spatial frame of the scenarios. The scenarios were drawn at basin scale. Nevertheless, each basin was divided in two spatial areas with different implications for the scenario design:
  - Headwaters were identified to be more sensible to changes in land use and cover. Past trends have shown a rural abandonment of the headwaters, leading to afforestation and to the increase of forest density, and increasing the area affected by forest fires.
  - Medium and low basins courses are not subjected to significant changes in land cover, because the uses are more consolidated. Nevertheless, these areas are subjected to changes in water demands, due to changes in water consumption in the agricultural, industrial and touristic sectors.

The following narrative storylines of the socioeconomic scenarios were drawn:

- Land cover scenarios applicable to the headwaters:
  - *Afforestation scenario (**AFOR**):* This scenario shows an increase in the forest area of the headwaters. This process includes the colonization by conifers of (1) grassland and shrubland areas at high altitudes and (2) shrubland areas on slopes.
  - *Fire scenario (**FIREFOR**):* The forest area decreases as a result of an increased incidence of forest fires. Fires affect mainly coniferous forests and shrublands. The burnt areas would cover 10-15% of the current forest area that would pass mainly to shrublands and areas regenerated with holm oak and oaks.
  - *Forest management scenario (**MANAGEFOR**):* The forest area does not vary but there are internal changes due mainly to forest management and the replacement of species. The aim of the Catalan Ministry of Agriculture, Livestock, Fisheries and Food is to increase the current 28% forest area of Catalonia under management to the 50%. This current forest management (which includes use of biomass, the valorisation of forest products ...) occurs primarily in the mountainous areas. We use this target as reference for this scenario: the 50% of the current forest area of the headwaters will be managed by 2050, acting first in the more dense forests according to the Third National Forest Inventory (IFN3).
- Water use scenarios to the medium and low basin courses:
  - *Rational use of water resources scenario (**RATUS**):* This scenario has different implications depending on the basin:
    - *Water reuse scenario in the Muga basin*: Major water demand pressures in the Muga basin are caused by irrigation (62 hm^3/year, compared with the 147 hm^3/any of Muga renewable water resources). Water management has been key to reduce the impact of historical droughts in the basin, where some events put the basin in hydrological emergency in 1983, 1999, 2008 and 2010. In those situations, water restrictions for irrigation, urban (tourism users) and ecological flows were applied. The basin is, as a result, affected recurrently by water scarcity, due to high water demands, low water contribution and low capacity of water regulation (mainly through the Boadella reservoir). However, the basin has a high potential for using non-conventional water, mainly from reuse of regenerated water (4.7 hm^3/year in Figueres, 3.8 hm^3/year in Roses and 1.1 hm^3/year in Empuriabrava treatment plants). This scenario takes into account the reuse of this 9.6 hm3/year for irrigation during the summer period by reducing the water abstraction in the Pont de Molins dam.
    - *Water transfer reduction scenario in the Ter basin:* The Ter basin is highly affected by the water transference to the Metropolitan Region of Barcelona, quantified in 160 (5.3 m^3/s) to 210 hm^3/year. The system Ter-Llobregat, which supplies water demand for the Metropolitan Region of Barcelona (365 hm^3/year), has not enough capacity to supply current urban uses. Once every four years, the demands are higher than available resources, being necessary the use of reservoir storages, which only has capacity to supply demand for one year. For this reason, during the last drought episodes in 1999, 2001-02, 2005 and 2007-09, it was necessary to apply water restrictions, resulting in an

important domestic and industrial effort to reduce consumption and in the reduction of ecological flows. This scenario takes into account the increase of alternative water sources for supplying the Metropolitan Region of Barcelona that will imply the water return to the Ter basin. In this scenario the average volume is reduced to 110 hm^3 / year (3.6 m^3/s) as a result of the containment of urban demand in the Metropolitan Region of Barcelona (hereinafter RMB), total integration of desalinated water produced at La Tordera and Llobregat's ITAM (Installations for marine water treatment) and improved the efficiency of municipal distribution networks (reduced losses).

- *Canal d'Urgell modernization scenario:* The Segre basin is highly affected by the demand for agriculture irrigation. The two main irrigation channels, Urgell (more than 150 years old) and Segarra-Garrigues (in construction), involves a water demand about 972 hm^3/year to supply 140,000 ha of irrigation. Thus, the Segre stream flows are reduced by 63% after Oliana and Rialb reservoirs and the water derivation to Balaguer and Seròs channels. Hydroelectric power demand is also very high, with about 1,800 hm^3/year. Moreover, the Segre basin has shown a reduction of stream flow of about 20% since 1985 as a consequence of land cover changes and climate change processes in the headwaters. In addition, the water abstraction for agricultural uses is producing large environmental damages in the course of the main stream, which is affected by contamination and water anoxia. In order to achieve good ecological status of water bodies in the Segre basin, it is necessary to improve the use of water in agriculture through modernization of irrigation. This scenario takes into account the release of 150 hm^3/year of water to the Segre river for implementation of the Modernization Plan of the Canal d'Urgell. The remaining volume of water will flow downstream Oliana-Rialb reservoirs feeding into the Segre river.

o *Increased demand scenario (**DEMINC**):* This scenario has different implications depending on the basin:

- *Increase water storage scenario in the Muga basin:* This scenario considers the enlargement of the Boadella reservoir, from the current 57 hm^3 capacity to 85 hm^3 (maximum capacity from 62 to 90 hm^3). This enlargement is as a result of increasing agricultural demands and increasing urban demand (tourism).
- *Water transfer increase scenario in the Ter basin:* This scenario considers the increase of the average transferred volume to 200 hm^3/year as a result of increased demand for urban and industrial.
- *Canal Segarra-Garrigues development scenario:* This scenario implies the end of the construction and the consolidation of the Canal Segarra-Garrigues. It also accounts that the modernization of the Canal d'Urgell is finished. The Segarra-Garrigues plan has a concession of 342 hm^3/year for irrigation purposes, divided as follow: a concession of 100 hm^3/any extracted directly by the river, a transfer of 150 hm^3/year obtained by the Canal d'Urgell modernization, and a transfer of 92 hm^3/any form the Noguera Pallaresa affluent.

3.3. Land cover scenarios

The headwaters of each case-study basin were initially identified. For LIFE MEDACC project purposes, we delimitated headwaters as the area of the basin upstream of the main reservoirs. Then, the headwaters can be considered as unregulated sub-basins meanwhile downstream of the headwaters the river is highly regulated.

Figure 2 shows the headwater delimitation per basin and Table 2 shows the area occupied by each headwater.

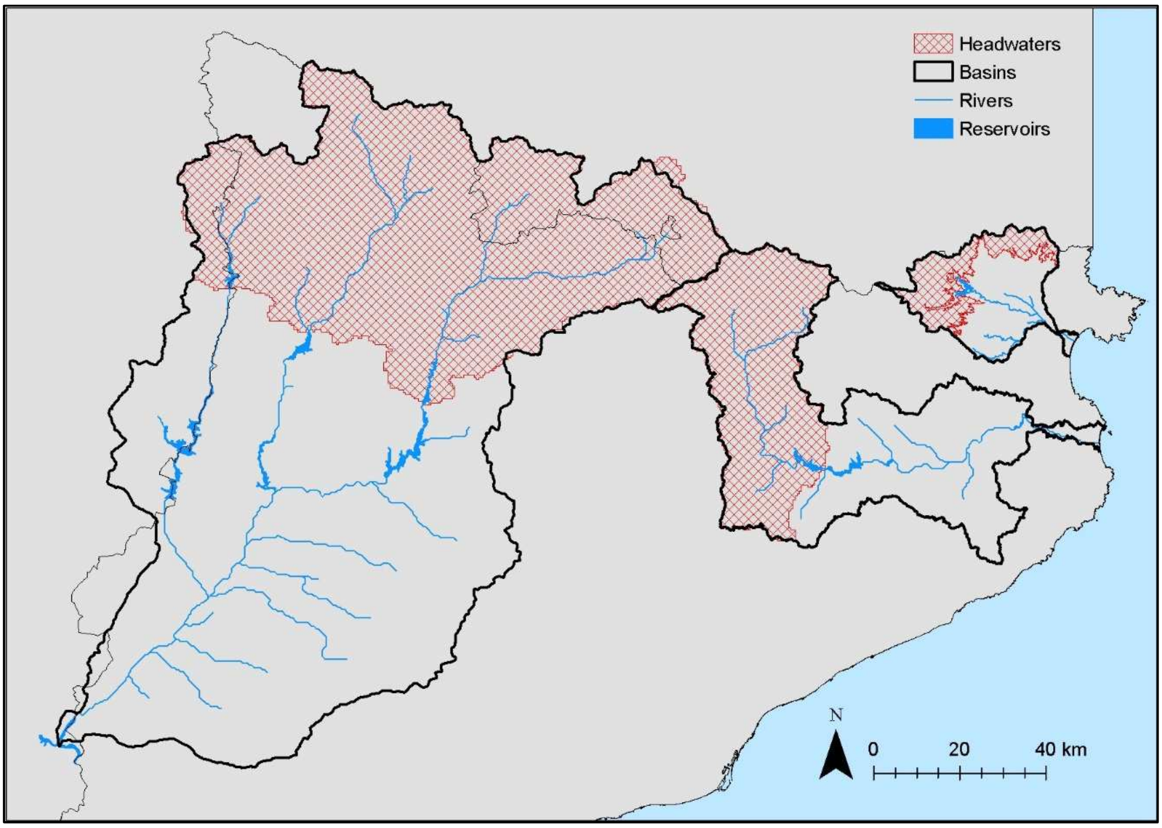

Figure 2. Headwaters delimitation per case study basins.

Basin	Total surface (km^2)	Headwaters' surface (km^2)	Percentage (%)
Muga	758.8	311.6	41.1%
Ter	2960.2	1525.0	51.5%
Segre	13005.0	5339.3	41.1%

Table 2. Surface occupied by each basin, headwater and relation in %

3.3.1. Afforestation scenario (AFOR)

This scenario foresees more forested headwaters by 2050. The initial hypothesis of this scenario is that forests, mainly conifers, will colonize grass and shrub areas at high altitudes and shrub areas on slopes. The scenario has been generated using a random forest algorithm.

Random forests (hereafter, RF) are algorithms that apply ensemble learning methodologies to classification and regression problems (Breiman 2001). The idea of the RF classification procedure is based on finding an efficient algorithm which turns a set of weak learners into a strong learner. Random Forest are a further development from decision trees methodologies, incorporating techniques such as bootstrap aggregating sampling, or “bagging” (see e.g. James et al. 2013). As a result, the predictive power of the RF methodology is, in general, superior to that of other statistical techniques (Kamusoko and Gamba 2015). It has been used in the past to study land use/cover dynamics (e.g. Gislason et al, 2006; Rodriguez-Galiano et al. 2012; Reynolds et al, 2016; Wessels et al. 2016), sometimes in conjunction with cellular automata techniques (Kamusoko and Gamba 2015). Due to their flexibility and power, their usage has seen a dramatic increase in recent years.

In this work we have used RF techniques to derive a predictive model for land cover dynamics in Catalonia. To derive that RF model we used the 1st (Burriel et al. 2001) and 4rd (CREAF 2009) land cover maps of Catalonia (MCSC) in vector format. Those MCSC maps were built from aerial orthophoto images obtained in 1993 and 2009. Time interval for land cover dynamics was therefore 16 years. MCSC datasets can be retrieved from www.creaf.uab.es/mcsc. The objective of our modelling exercise was to model how each pixel in those maps of Catalonia had changed its land cover class between 1993 and 2009, as a function of a set of predictor variables. Such a model could then be used to simulate future land cover maps.

As drivers of land cover dynamics in Catalonia we chose three different predictor types: topographic, climatic and landscape-based.

- Topographic: the influence of local topography is key in driving land cover changes. The dependence on topography is demonstrated by noticing how human-induced landscape structures (e.g. cities, roads and croplands) tend to show up at low or middle elevations, and preferably in flat lands, whereas forested and/or natural areas appear at higher elevations. We used the following two topographic predictor variables:
  1. Height: information about elevation per pixel was obtained from the Digital Elevation Model (DEM) of Catalonia at a spatial resolution of 15 m (Cartographic and Geologic Institute of Catalonia, ICGC, http://www.icgc.cat/Administracio-i-empresa/Descarregues/Elevacions/Model-d-Elevacions-del-Terreny-de-Catalunya2). The DEM was resampled to 40 m.
  2. Slope: slope map was calculated from the DEM map with the aid of the ArcGIS program.
- Climatic: climate is a crucial factor that determines the natural dynamics of ecosystems and, therefore, may drive changes in the observed landscape. We selected the following two climatic predictor variables:
  3. Total Annual Precipitation: we obtained precipitation maps from the Digital Climatic Atlas of Catalonia with a spatial resolution of 180 m per pixel (Ninyerola et al. 2000)
  4. Average Annual Temperature: temperature maps were also retrieved from the Digital Climatic Atlas of Catalonia, with the same spatial resolution of 180 m per pixel.
- Landscape-based: we assumed that previous landscape history at pixel level could play an important role in determining future cover dynamics. In addition, that dynamics has been shown to be driven, to a large degree, by the characteristics of the surrounding landscape (e.g. Molowny-Horas et al. 2015). However, accounting for this dependence is usually a difficult task since, a priori, there is not a unique way of describing how landscape itself influences future landscape dynamics. Consequently, we chose 5 different predictor variables within this category:
  5. Previous land cover class: previous land cover class at each pixel was selected as predictor variable.
  6. Distance to urban centres: we assumed that cover dynamics may be driven partly by the proximity to cities, villages or other urban centres. Therefore, at every pixel we calculated its distance to the closest urban-classified pixel.
  7. Distance to main roads: land cover changes in a given pixel may also be determined by its adjacency to a transportation network. Consequently, at each pixel we calculated its distance to the closest road-classified pixel.
  8. Distance to nearest land cover pixels: surrounding landscape may arguably be important in determining land cover dynamics at pixel level. Thus, at every pixel we computed its distance to the closest pixels per cover class.
  9. Number of adjacent pixels per class: at every pixel we calculated the number of surrounding (i.e. distance≤3) pixels per cover class.

Furthermore, predictors 1, 2, 3, 4, 6 and 7 were squared and included also in the model.

RF classification calculations were carried out with the “ranger” package (Wright 2016) of the R software (R Core Team 2016). We chose the default value of 500 as the total number of trees to be calculated. Given our limited computing facilities we increased the size of the pixels in all maps (i.e. 1993, 2009 and predictor maps) from 40x40 m to 200x200 m. This pixel aggregation procedure was done with the modal pixel value, for the categorical land cover maps, and the mean pixel value, for the quantitative predictors.

Interactions between predictors, as used and implemented in regression approaches, were not included. However, it is worth noticing that the RF methodology may account automatically for interactions between predictors, although exactly how those interactions are calculated inside the RF algorithm is beyond the scope of this study (Boulestiex et al. 2014).

Before the RF classification calculation, our dataset was split into a training and test datasets, containing 70% and 30% of all points, respectively. The RF algorithm was then applied to the training test. Goodness of fit was evaluated with the Cohen’s Kappa index, calculated with the test dataset, giving a value of 0.8. The corresponding confusion matrix of the test dataset is also shown in Table 3. As we can see, the largest percentage values are noticeably clustered along the diagonal, corresponding to corrected guesses by the predictive RF model.

		Predicted 2009 land cover map					
		Forest	Shrub	Open	Urban	Crop	Other
Actual 2009 land cover map	Forest	40.51	1.87	0.19	0.14	1.81	0.07
	Shrub	2.73	7.34	0.33	0.11	0.86	0.08
	Open	0.32	0.40	2.35	0.07	0.37	0.23
	Urban	0.40	0.09	0.01	3.89	1.11	0.02
	Crop	0.90	0.35	0.04	0.25	30.91	0.01
	Other	0.14	0.13	0.25	0.05	0.10	1.56

Table 3. Confusion matrix of the RF classification model. Values are in percentage of the total number of pixels (241,470) of the test dataset.

We show in Figure 3 variable importance in the RF model (Archer and Kimes 2008). Not surprisingly, variable importance of previous land cover class turned out to be highest. Next came two other landscape-based variables, i.e. distances to closest crop and to closest forest pixels. These three variables clearly stood out when compared with the others. Variable importance of the slope predictor then came fourth but, surprisingly, the DEM predictor only appeared as the 11th in Figure 3. Further, of the two climatic variables, variable importance of annual total precipitation was noticeably higher than that of temperature. Predicted MCSC maps (i.e. future predicted simulated land cover images) were finally simulated with the RF model.

Figure 4 shows the input raster (2009 Land Cover Map, up) and the model output raster (2057 AFOR scenario, down) for Catalonia. The AFOR scenario map was done for 2057 because the RF models in time-step equivalent to the period between the land cover maps used as input: 17 years from 1993 to 2009. Then, predicted MCSC maps were generated for 2009, 2025, 2041 and 2057. We used the 2057 map as AFOR scenario. The RP model predicts an afforestation of 2,074 km^2 (a 6.5% more than in 2009) in Catalonia. This afforestation occurs on current shrubland (5.4%), grassland (1.0%) and agriculture (1.2%) areas (Table 4).

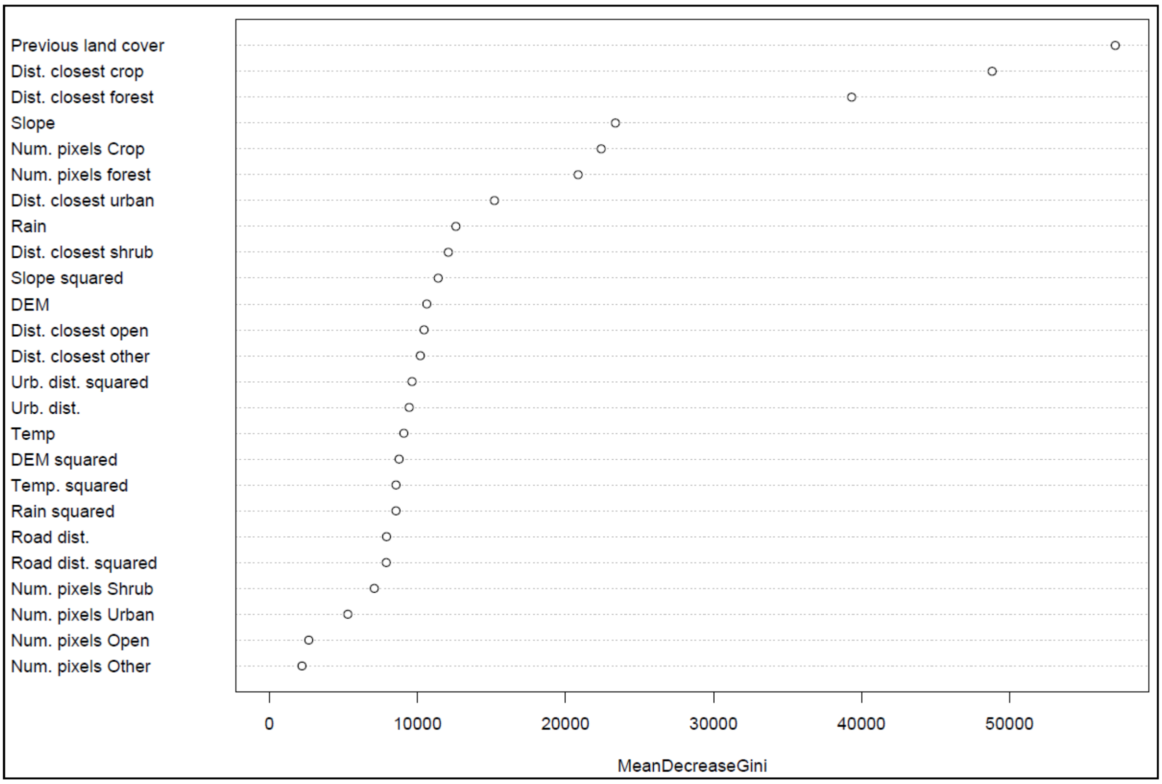

Figure 3. Importance of predictor variables used in the RF calculation.

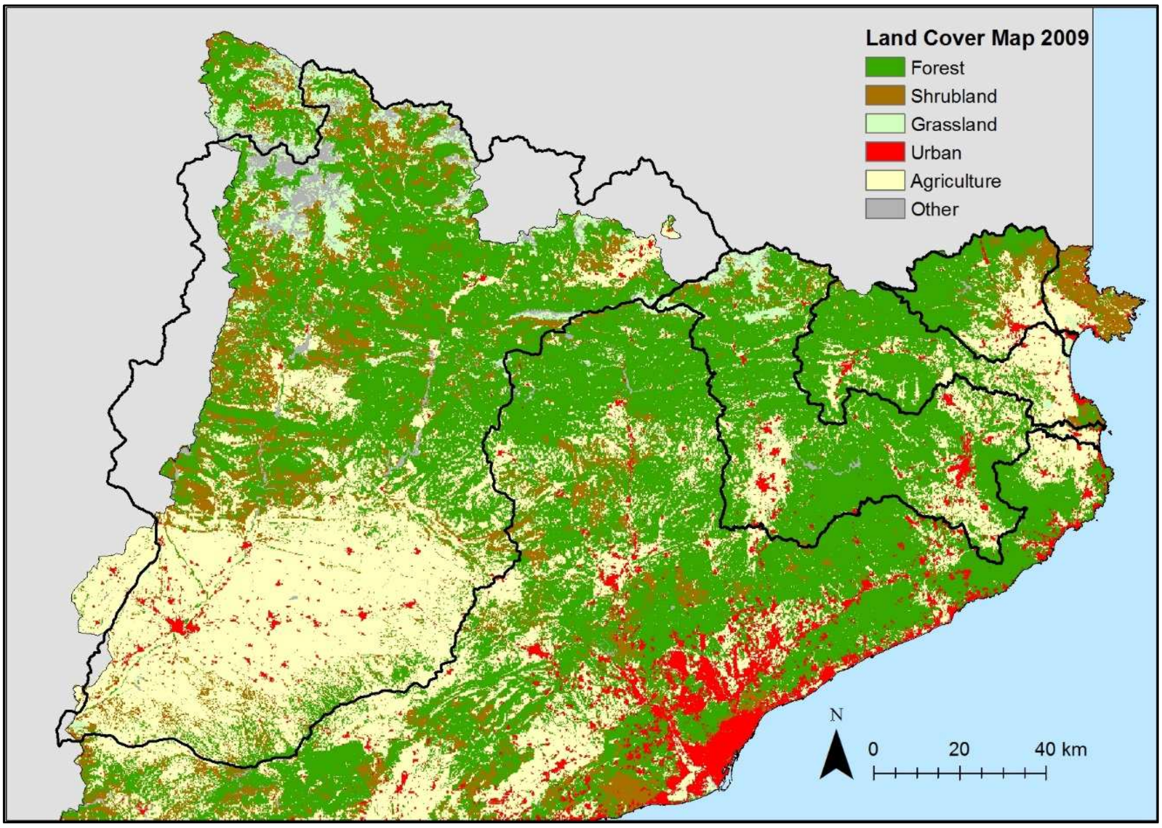

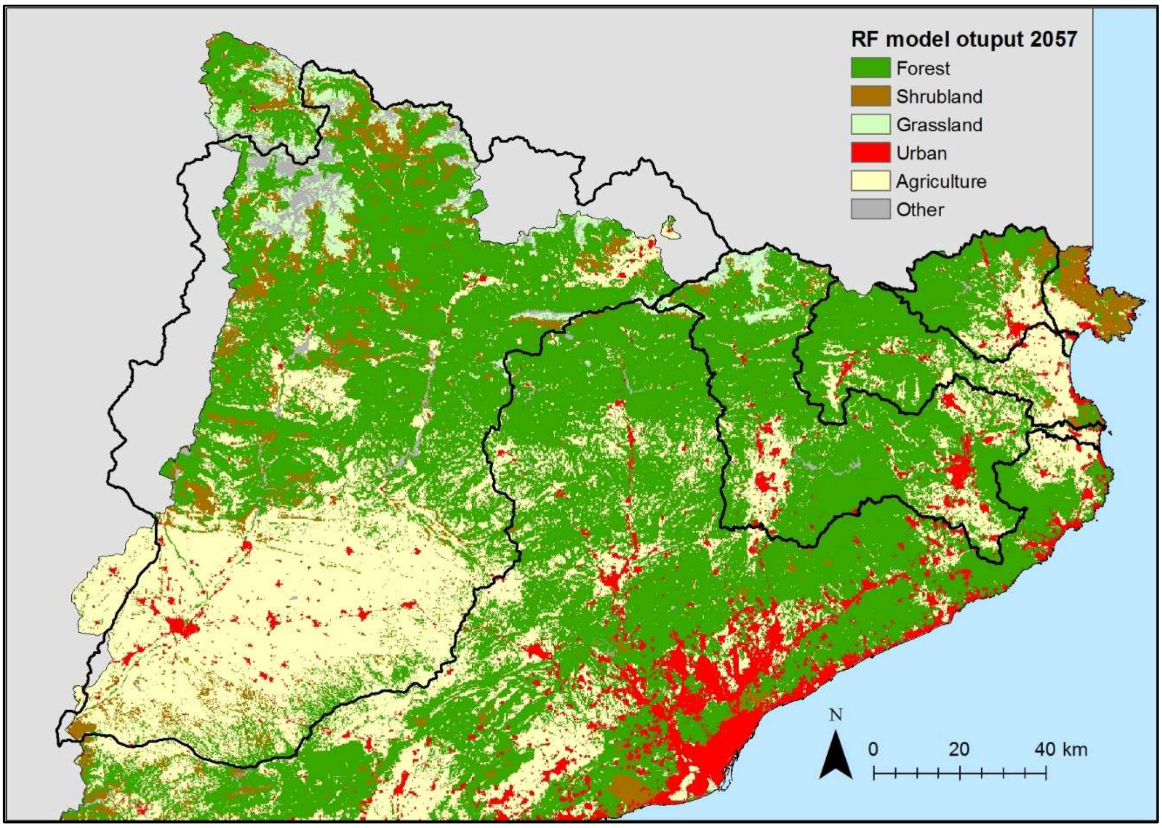

Figure 4. Land cover map (2009) (up) and RF model output (2057) (down) for Catalonia. Case-study basins are represented with black lines.

	Surface 2009 LCM (km^2)	Surface 2057 RF model output (km^2)	Change (%)	Change (km^2)
Forest	14,330.0	16,403.9	6.5%	2,074
Shrubland	3,685.4	1,933.8	-5.4%	-1,752
Grassland	1,202.2	871.8	-1.0%	-330
Urban	1,782.2	2,211.5	1.3%	429
Agriculture	10,525.2	10,135.7	-1.2%	-390
Other	727.6	651.5	-0.2%	-76

Table 4. Changes per land cover between the 2009 LCM and 2057 RP model output in percentage and surface (km2) per Catalonia.

We used the 200m-raster of the 2057 RF model output for drawing the AFOR scenario. For this purpose, we have to adapt the RF model output with the socioeconomic scenarios defined in the LIFE MEDACC project. Thus, the RF model output raster is used in the headwaters of the case-study basins, meanwhile the LCM 2005 is used in the medium and low courses. The results are available at *Deliverable 14 Impacts of climate and global change on the ecological, hydrological and agriculture systems in the LIFE MEDACC case study basins* (Pascual et al. 2016).

3.3.2. Fire scenario (FIREFOR)

This scenario foresees a less forested headwaters by 2050 as a result of an increased incidence of forest fires. Our initial hypothesis is that the fires would affect mainly coniferous forests and shrublands that would be converted by the middle of the 21st century to shrublands and areas regenerated with evergreen forests. The scenario has been generated using the MEDFIRE model (Brotons et al. 2013).

We have used an existent model, MEDFIRE model, which has been recently applied in Catalonia to predict changes in forest landscape composition under the effects of different fire regime scenarios (Brotons et al. 2013). MEDFIRE is a spatially explicit landscape dynamics model at 100-m resolution that allows to examine the spatial interactions between wildfires, landscape vegetation dynamics, climate change, and fire suppression strategies in Mediterranean ecosystems, and it is parameterized for Catalonia (Brotons et al. 2013). MEDFIRE allows predicting yearly changes of forest landscape composition as a function of fire regime, post-fire regeneration, and afforestation.

For LIFE MEDACC project purposes, we have used the scenarios created by the model developers (Brotons L, Gil-Tena A and the Biodiversity and Landscape Ecology Lab members from the Forest Sciences Centre of Catalonia, CTFC) ad-hoc for MEDACC project for 2050. For MEDFIRE modelling, first it is needed to set the reference fire regime and to calibrate it with the historical fire regime occurred during the reference period (1980-2000). To set up the reference fire regime, the model uses a top-down approach based on varying the percentage of adversely climatic years, that is, years with abound number of days with a high fire meteorological risk when fires affecting big areas occur. Normal and adverse years have been classified using the Thornthwaite aridity index, an indicator of water shortage in summer. For the reference period 1980-2000, a 40% of the years has been identified as climatically adverse (Gil-Tena et al. 2016). Then, this 40% has been induced during the period 2010-2050. The ignition probability is modelled depending on the climate, neighbouring land covers including interfaces among them, and human infrastructures (Gil-Tena et al. 2016) and the post-fire regeneration transitions is based on Rodrigo et al. (2004) and constrained by the presence before the fire of the tree species within 1 km radius. The input data is the Land Cover Forest Map of Catalonia (2010, based on the Catalan Land Cover Map 2009) reclassified in 16 classes: 1*) Pinus halepensis*, 2) *Pinus nigra,* 3) *Pinus pinea,* 4) *Pinus sylvestris,* 5) *Quercus suber,* 6) *Quercus faginea* and other marcescense oaks, 7) *Quercus ilex*, 8) Other conifers, 9) Other arboreal species, 10) Shrublands, 11) Grasslands, 12) Agriculture, 13) Extensive cereals, 14) Bare rocks, 15) Water, 16) Urban. Different levels of fire risk - probability of burning, probability of fire recurrence and probability large fire (>500ha) – can be computed from the MEDFIRE spatial outputs over 100 replicates and the simulated period (2010-2050).

We used the 100m-raster of the 2050 forest landscape for drawing the FIREFOR scenario. MEDFIRE model generated 100 replicas of the future forest landscape raster and model developers provide LIFE MEDACC project with 10. From these 10 replicas, we selected one (ForestMap3) that predicted landscape changes similar to the mean of the predicted landscape changes of the 10 replicas. For the project purposes, we reclassified the raster into 8 categories: 1) Conifer forest (including *Pinus halepensis*, *Pinus nigra, Pinus pinea, Pinus sylvestris* and other conifers categories), 2) Evergreen forest (including *Quercus suber* and *Quercus ilex* classes), 3) Deciduous forest (including *Quercus faginea* and other marcescense oaks, and other arboreal species), 4) Shrublands, 5) Grasslands, 6) Agriculture (including agriculture and extensive cereals), 7) Others (including bare rocks and soils) and 8) Urban. Figure 5 shows the input raster (2010 Land Cover Map, up) and the model output raster (2050 FIREFOR scenario, down) for Catalonia. The MEDFIRE model predicts a reduction of the area occupied by conifer forest (959 km^2 surface reduction, a 3% less than in 2010) in Catalonia. This conifer forests reduction favours the expansion mainly of shrublands (610 km^2 and 1.9%), but also of deciduous forest (298 km^2 and 0.9% increase) and evergreen forests (50 km^2 and 0.2% increase) after post-fire regeneration processes (Table 5).

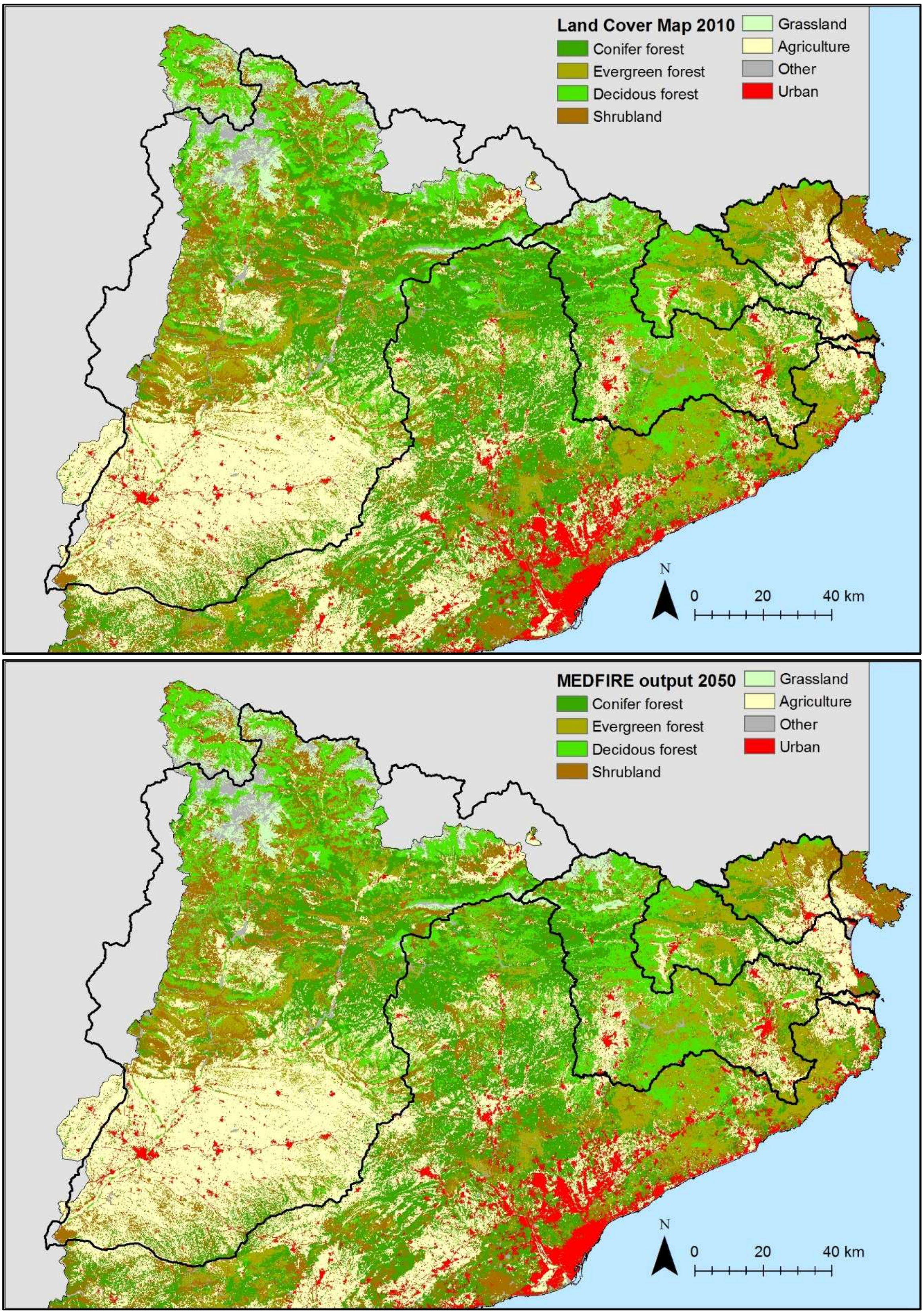

Figure 5. Land cover map (2010) (up) and fire scenario (2050) (down) for Catalonia. Case-study basins are represented with black lines.

	Surface 2010 LCM (km^2)	Surface 2050 MEDFIRE output (km^2)	Change (%)	Change (km^2)
Conifer forest	7,309	6,350	-3.0%	-959
Evergreen forest	3,064	3,114	0.2%	50
Deciduous forest	3,492	3,790	0.9%	298
Shrublands	4,718	5,328	1.9%	610
Grassland	795	795	0.0%	0
Agriculture	10,011	10,011	0.0%	0
Other	935	935	0.0%	0
Urban	1,786	1,786	0.0%	0

Table 5. Changes per land cover between the LCM 2010 and FIREFOR scenario 2050 in percentage and surface (km2) per Catalonia.

Similar to the AFFOR scenario, we have to adapt now the MEDFIRE model output with the socioeconomic scenarios defined in the LIFE MEDACC project. Thus, the MEDFIRE 2050 forest landscape raster is used in the headwaters of the case-study basins, meanwhile the LCM 2005 is used in the medium and low courses. The results are available at *Deliverable 14 Impacts of climate and global change on the ecological, hydrological and agriculture systems in the LIFE MEDACC case study basins* (Pascual et al. 2016).

3.3.3. Forest management scenario (MANAGEFOR)

This scenario foresees a change in forest structure (instead of in forest cover area, as previous scenarios) due mainly to forest management and the replacement of species. The aim of the Catalan Ministry of Agriculture, Livestock, Fisheries and Food is to increase the current 28% forest area of Catalonia under management to the 50%. We use this target as reference for this scenario: the 50% of the current forest area of the headwaters will be managed, acting first in the more dense forests according to the Third National Forest Inventory (IFN3).

We have combined two types of information: 1) the land cover map of 2005 to identify forest areas in the basin headwaters (Figure 6) and 2) the Third National Forest Inventory (IFN3) to select the forest areas with higher density. The IFN3 is part of an extensive national database of forest surveys distributed systematically across the forested area of Spain that was conducted from 1997 to 2008. Both information are deeply explained in Deliverable 12 of the LIFE MEDACC project (Vicente-Serrano et al. 2016).

We have selected the forests located in the basin headwaters (Muga 255 km^2, Ter 861 km^2, Segre 2,526 km^2) (Table 6). Then, we have combined this information with forest density data coming from the IFN3 (Figure 7). Thus, we have identified the higher density forests in the headwaters until reaching the 50% of the headwater forest surface (Muga 133 km^2 under forest management, Ter 427 km^2, Segre 1,261 km^2).

	Forest area in the basin (km^2)	Forest area in the headwaters (km^2)	Managed forest area (km^2)	Managed forest (%)
Muga	403	255	133	33.0%
Ter	1,782	861	427	24.0%
Segre	4,527	2,526	1,261	27.9%

Table 6. Area occupied by forests in the basin and headwaters, and managed area in percentage and surface (km2) per basin.

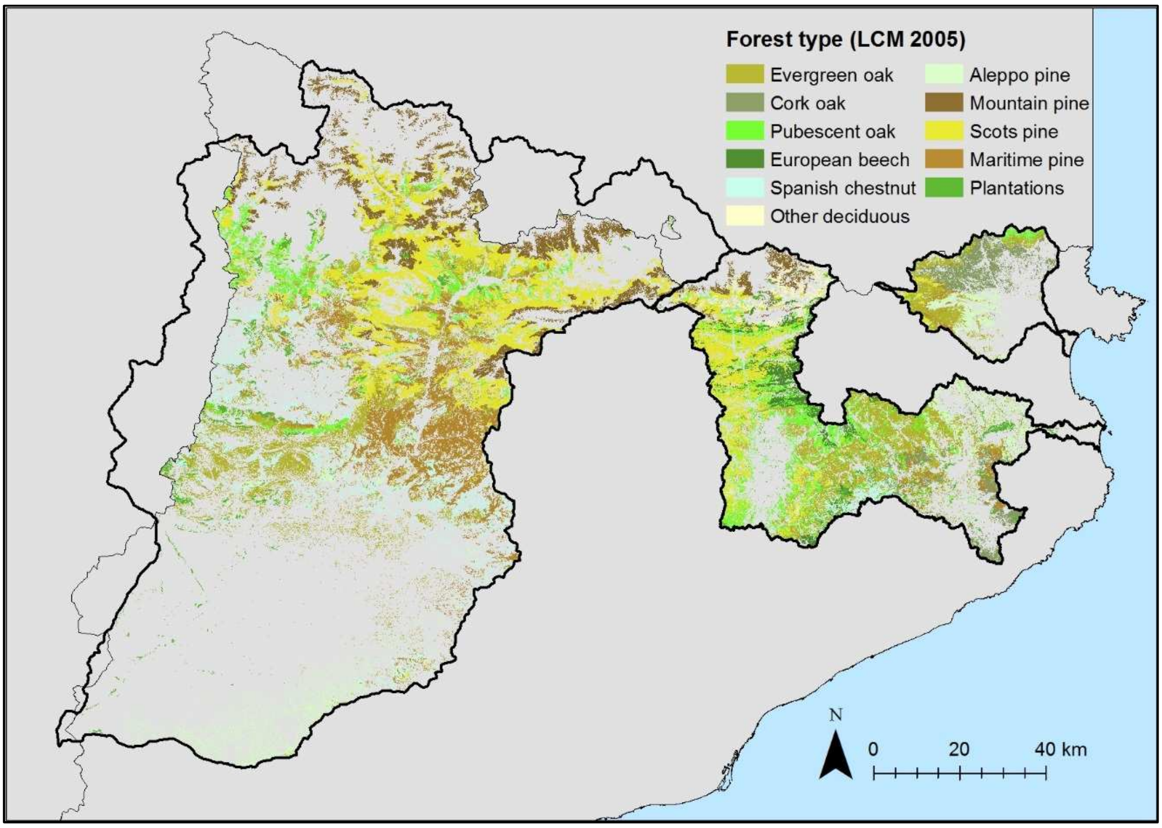

Figure 6. Distribution of forest type in case-study basins based on the 2005 land cover map of Catalonia

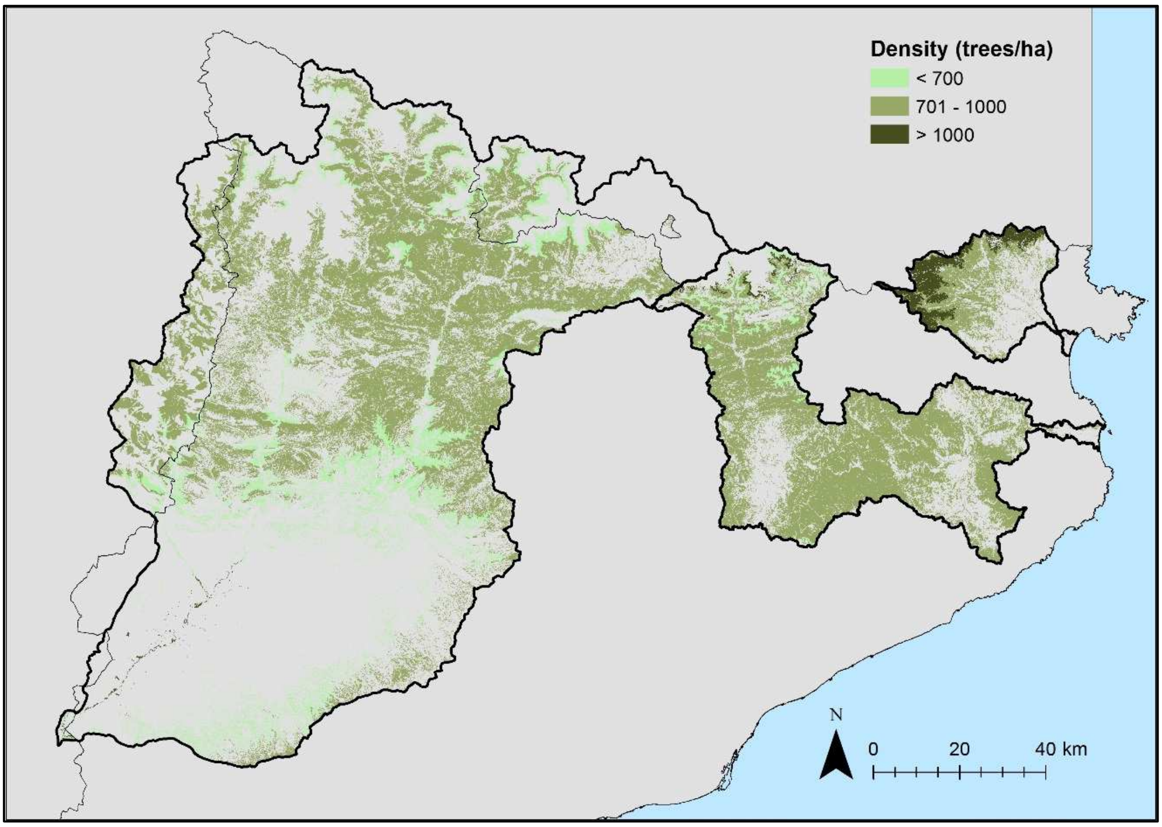

Figure 7. Density (tree/ha) per altitudinal range based on the IFN3 data.

The mosaic of this information in the headwaters with the LCM 2005 in the medium and low courses gives as a result the MANAGEFOR scenario. The results are available at *Deliverable 14 Impacts of climate and global change on the ecological, hydrological and agriculture systems in the LIFE MEDACC case study basins* (Pascual et al. 2016).

3.4. Water management scenarios

Water management scenarios were designed for medium and low basins courses, where not significant changes in land cover are expected. Nevertheless, changes in water demands are expected due to the increased pressures on water resources of the agricultural, industrial and touristic sectors.

In comparison with land cover scenarios, the water management scenarios are not represented as maps, but as changes in the magnitude of water extractions. These changes are directly applied to the hydrological models used to evaluate the impacts of the water management scenarios on the water cycle (see section 4). For this reason, we do not present in this section maps or tables, only the description of the scenarios.

3.4.1. Rational use of water resources scenario (RATUS)

This scenario foresees a reduction in water consumption by 2050 as consequence of using alternative water sources for covering water demands in the case-study basins. The released water is left into the rivers to improve their quality, restore their functionality and recover the provision of environmental services. This scenario has different implications depending on the basin.

Water reuse scenario in the Muga basin

Major water demand pressures in the Muga basin are caused by irrigation (62 hm^3/year, compared with the 147 hm^3/any of Muga renewable water resources). In a basin recurrently affected by water scarcity, this water demand is often difficult to satisfy. Together with a low water contribution and low capacity of water regulation (57 hm^3 in Boadella reservoir), the basin has suffered frequent water restrictions for irrigation, urban (tourism users) and ecological flows. Alternative water sources are key to cover water demands without risking the good ecological status of the river. In this sense, the basin has a high potential for using non-conventional water, mainly from reuse of regenerated water coming for three different treatment plants: Figueres (4.7 hm^3/year), Roses (3.8 hm^3/year) and Empuriabrava (1.1 hm^3/year).

This scenario foresees a reduction of 9.6 hm^3/year in the water abstraction of the Pont de Molins dam. This water abstraction flows into the Right and Left Irrigation channels, which irrigates approximately 4,000 ha and feeds the urban supply of 36,436 to 58,099 inhabitants (Cadaqués, Llançà, Roses, Empuriabrava, Mancomunitat de Pau, Palau Saverdera, Vilajuïga, Garriguella, Pedret and Marzà). The re-used water will directly feed into the irrigation fields, reducing the pressure over the water collection. The reduction of 9.6 hm^3/year in the water abstraction will be applied during the summer period, reducing 3.2 hm^3 in June, July and August, when maximum irrigation demands take place.

Water transfer reduction scenario in the Ter basin

The Ter basin is highly affected by the water transference to the Metropolitan Region of Barcelona, quantified in 160 (5.3 m^3/s) to 210 hm^3/year. Recurrently, the system Ter-Llobregat that supplies Barcelona has not capacity to satisfy the demands, incurring in water restrictions that affect the domestic and industrial consumptions and the maintenance of the ecological flows. Alternative water sources are needed to satisfy current and future water demands without risking the good ecological status of the river. In this sense, the basin has a high potential for finding alternative water sources as a result of the containment of urban demand in the RMB, the total integration of desalinated water produced at ITAM's La Tordera and Llobregat and the improvement of the efficiency of municipal distribution networks (reduced losses).

This scenario foresees a reduction of 50 hm^3/year in the water transference to the RMB. The reduction will be applied proportionally along the year (4.2 hm^3/month).

Canal d'Urgell modernization scenario

The Segre basin is highly affected by the demand for agriculture irrigation. The two main irrigation channels, Urgell and Segarra-Garrigues (in construction), involves a water demand about 972 hm^3/year to supply 140,000 ha of irrigation. The modernization of the Canal d'Urgell, with more than 150 years, is already planned and its implementation will reduce water consumption in about 150 hm^3/year. This water release is key to achieve a good ecological status of water bodies in the Segre basin, currently affected by contamination and water anoxia.

This scenario foresees a reduction of 150 hm^3/year in the water abstraction of the Canal d'Urgell. The reduction will be applied proportionally along the irrigation months (May, June, July, August and September), at the rate of 30 hm^3/month.

3.4.2. Increased demand scenario (DEMINC)

This scenario foresees an increase in water consumption by 2050 as consequence of not applying measures to reduce the pressures over the water cycle. This scenario puts at risk the good ecological status of the case-study water bodies. This scenario has different implications depending on the basin.

Increase water storage scenario in the Muga basin

The low water regulation capacity of the Muga basin, depending mainly on the Boadella reservoir (57 hm^3), with difficulty can cover irrigation demands (62 hm^3/year) during dry years. The mean water abstraction from the Pont de Molins dam to feed irrigation and urban demands is approximately 28 hm^3/year (mean value for the period 2002-2011 including Canal de la Dreta, Canal de l'Esquerra, Rec del Molí and Costa Brava Consortium – Nord (CCBN) supply).

This scenario foresees the enlargement of the Boadella reservoir to increase the capacity in 28 hm^3, from the current 57 hm^3 capacity to 85 hm^3 (maximum capacity from 62 to 90 hm^3). This enlargement is as a result of increasing agricultural demands and increasing urban demand (tourism).

Water transfer increase scenario in the Ter basin

The system Ter-Llobregat, which supplies water demand for the metropolitan region of Barcelona (365 hm^3/year), has not enough capacity to supply current urban uses. Once every four years, the demands are higher than available resources, being necessary the use of reservoir storages, which only has capacity to supply demand for one year. Moreover, Ter's river water has a better quality that the Llobregat one, favouring that the processes to make water drinkable be more affordable. This difference increases the pressure over the Ter's resources.

This scenario foresees an increase of 40 hm^3/year in the water transference to the RMB. The increase will be applied proportionally along the year (3.3 hm^3/month).

Canal Segarra-Garrigues development scenario

The Canal Segarra-Garrigues is currently under construction and has an approved water concession of 342 hm^3/year. The objective of the channel is to transform to irrigable land 70,150 ha in Lleida province. Considering the strong pressures over the Segre river, this concession is expected to be extracted from: 100 hm^3/any extracted directly by the river after the Rialb reservoir, 150 hm^3/year obtained from the modernization of the Canal d'Urgell Canal; and a transfer of 92 hm^3/any from the Noguera Pallaresa.

This scenario foresees an extraction of 250 hm^3/year from the Rialb reservoir into the Canal Segarra-Garrigues and a transfer of 92 hm^3/any from the Noguera Pallaresa. This extraction will be applied proportionally along the irrigation months (May, June, July, August and September), at the rate of 50 hm^3/month from the Segre river and 18.4 hm^3/month from the Noguera Pallaresa. A reduction of 150 hm^3/year in the water abstraction of the Canal d'Urgell is also included along the irrigation months (May, June, July, August and September), at the rate of 30 hm^3/month.

4. Hydrological modelling

4.1. Introduction

Hydrological models reproduce the processes that occur in a basin in the most rigorous way, so that, subsequently, can be used to know the evolution of water resources under different scenarios of change. There are many hydrological models currently available, distinguishing between global models (calculations are done at basin level), semi-distributed (at sub-basin level) and distributed (at pixel level).

The calibration and validation processes of the hydrological models are key to obtaining acceptable results compared with the reality. These processes are done through the comparison of the model results with observed data from gauging stations of the basin under study. The calibration involves adjusting the model so output values are close or similar to values recorded at the gauging station. The validation measures the model prediction capacity through the comparison between simulated results and observed data in a time period different from the calibration.

One of the LIFE MEDACC project objectives is to evaluate future impacts of climate and global change scenarios on water resources in three case-study basins. This process includes three main steps: 1) calibrating and validating the hydrological models for a historical period with observed stream flow and climate data; 2) generating climatic and socioeconomic scenarios (sections 2 and 3); and 3) incorporating climatic and socioeconomic scenarios into the calibrated and validated hydrological models to evaluate the future effects of the scenarios in the water cycle.

In this project we have used two different methodological approaches depending on the hydrological model used: RHESSys and SWAT models.

4.2. Hydrological models

4.2.1. RHESsys model

RHESsys is a hydro-ecological model spatially distributed and designed to display the fluxes between the hydrological and vegetal processes in a basin (Tague et al. 2004). The processes related on hydrological and biochemical aspects are combined and distributed spatially that allows to the user to choose the size and shape of the modelled unities. The spatial partition of the landscape provides a useful tool to show the significant variations of those factors at different scales (Band et al. 1993). RHESsys can be defined as an assembly of three models: MTN-Clim for aspects related with topography and meteorology, BIOME-BGC estimates storage and flux of carbon, nitrogen and water in an ecosystem and TOPMODEL for soil moisture and runoff. The RHESsys methodology is explained in Tague and Brand (2004).

RHESsys has been used in many environmental analysis with different tasks as snow and its implication on flow regimes (Godsey et al. 2014), water balance (Morán-Tejeda et al. 2015), water management implications in a climate change context (Lopez-Moreno et al. 2014), the effect of the drought stress on mortality in silver fir forests (Vicente-Serrano et al. 2015), runoff sensitivity to land cover changes in a mountain environment (Mohammed and Tarboton 2014), pastures productivity (Mitchel et al. 2005) or climate, topography and vegetation relationship in a mountain environment (Christensen et al. 2008).

GRASS (Geographic Resources Analysis Support System) software is required to manage the spatial information, which is used to build the base information (topography, spatial unities, streamflow network, relationships between different spatial partition, the establishment of hierarchy, etc.). RHESsys manages the space in a hierarchical way where a basin contains minor unities nested one inside the other to the minor spatial entity (patch) where vegetation information is associated. In each patch different processes (hydrological, meteorological and vegetation) are involved and all the unities are closely bound up with each other through bidirectional interactions defined within the model.

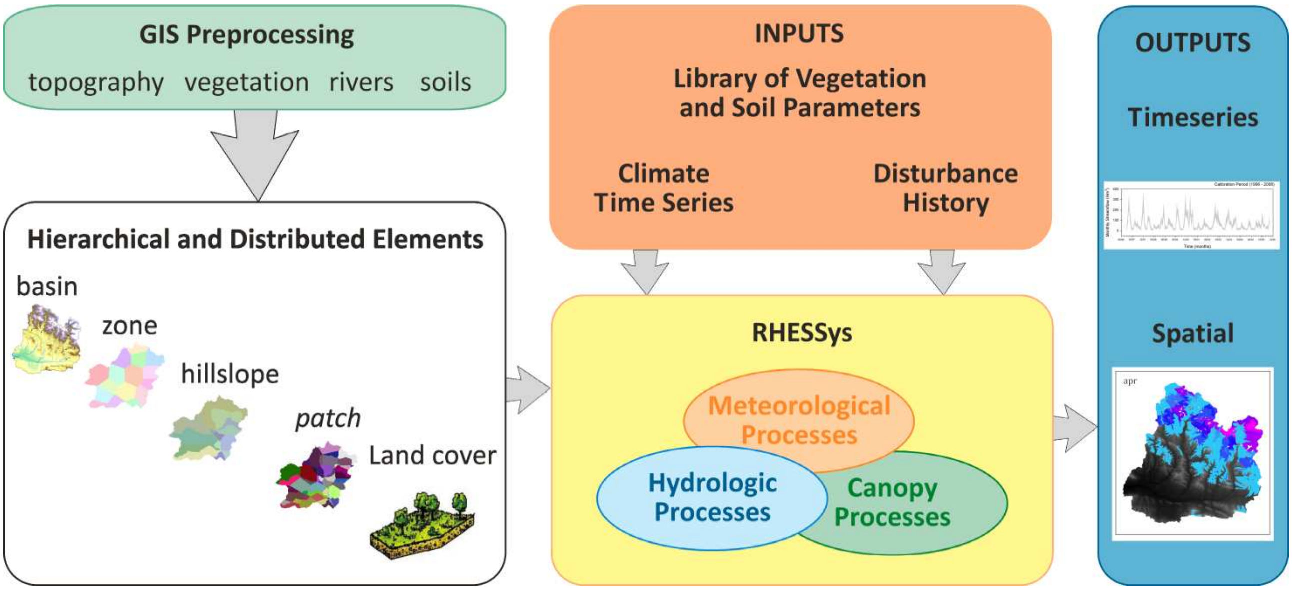

Figure 8. RHESsys workflow.

This structure allows a better solution to model the different processes at a different scales, as well as to the different spatial unities separated, what improves the flexibility to simulate the processes and to obtain results spatially distributed. The possibility to model at different scales and different resolutions improves the general process of simulation and ensures a very good spatial adjust of the processes and interactions within a basin.

4.2.2. SWAT model

The Soil and Water Assessment Tool (SWAT) (Arnold et al.1998) is a physically based, semi-distributed and continuous hydrological model that estimates surface and subsurface flow, erosion, sediment deposition and nutrient movement within the catchment, at a daily time step (Gassman et al. 2007). The model is able to make predictions of the long-term behavior of complex basins, especially to evaluate the effects of different management scenarios and changes in the environmental conditions. The model can be connected to GIS (ArcSWAT version), allowing the spatial parameters and input variables of the model at each point of the basin. Although the model is widely applied, it has been rarely used in Mediterranean basins (Nunes et al. 2008).

SWAT is based on the water balance equation in the soil, including processes such as interception, infiltration, surface runoff, evapotranspiration, percolation, lateral flow and groundwater recharge. Precipitation may be intercepted by vegetation or reach the soil surface (Neitsch et al. 2005). Water on the soil surface may infiltrate or flow over the surface as runoff contributing to surface drainage. Infiltrated water is stored in the soil profile and later evaporates, is uptaken by plants, contributes to the streams through lateral flow or percolates into the groundwater system. Groundwater can be stored in the aquifer, but it can also leave the soil and discharge into the streams, move upward in the soil profile or percolate to a deeper aquifer. For a full description of SWAT and its methods, see Neitsch et al. (2005). For LIFE MEDACC project, the surface runoff volume was estimated using a modification of the curve number (CN) method used by the Soil Conservation Service (SCS). PET was calculated using the Thornthwaite method, whereas lateral flow was predicted through a kinematic storage model and channel flood routing was estimated using the Variable Storage method.

SWAT model divides the study are into sub-basins, which allows to distinguish areas with similar land use, soil types and altitudinal range that influence in processes such as evapotranspiration or the distribution of precipitation. Meanwhile, the sub-basins are divided into hydrological response units (HRU), which are areas with the same land cover, soil type and slope. SWAT considers that these units have a similar hydrological response and estimates the main physical processes (runoff, actual evapotranspiration, soil moisture ...) at this level.

4.2.3. Comparison between RHESSys and SWAT models

Assessing the impacts of climate change on water cycle has to deal with a series of uncertainties related, among others, with the internal variability of climate, the future projections, the downscaling methods and the use of different hydrological models (Senatore et al. 2011, Koutroulis et al. 2013). We selected two different hydrological models with different methodological approaches in order to reduce the uncertainties associated to the selection of the models: SWAT and RHESSys. Both are process-based hydrological models with a different conception and applicability.

Morán-Tejeda et al. (2014) compared the performance of both models in a mountain basin on the Pyrenees (Spain) using climate and land-use change scenarios. Both models are distributed models that work with similar spatial partitioning, which makes results comparable at different spatial scales. Input data are also similar in content and format, and output variables are also comparable. Morán-Tejeda et al. (2014) concluded that the SWAT model was more sensitive to climate change scenarios, whereas RHESSys showed to be more sensitive to changes in land cover. They also found that the choice of the model does not impact in the direction of the predicted change, but it has a substantial effect in the magnitude and intra-seasonal patterns of the changes among the models. In this way, under their case study, they found that SWAT had larger sensitivity of water dynamics to changes in climate variables, whereas RHESSys model shower greater sensitivity to changes in land cover (Morán-Tejeda et al. 2014). They also found that both models showed a linear pattern of the response of stream flows to changes in precipitation and temperature; but SWAT showed a linear response to changes in land cover whereas RHESSys exhibits a nonlinear response. Nevertheless, they did not compare models outputs with observed data in order to determine which model provides better estimates.

4.3. Input data

Hydrological models require climate, topography, land use, soil type and stream flow data as inputs for the assessment of water resources. The quality and level of detail of the input data will determine the capacity of the model to adequately simulate the water cycle.

4.3.1. Climate data

Modelling water resources requires long climate series with continuous and reliable precipitation and temperature data (Pascual et al. 2015). Daily meteorological data were obtained from stations managed by the Spanish State Meteorological Agency (AEMET) and by the Meteorological Service of Catalonia (SMC). Some of the meteorological stations also provided data on radiation, relative humidity and wind speed. The stations were chosen according to their locations within or close to the basins, considering climatic heterogeneity and continuity in data series. Climate data was subjected to a process of quality control, filling gaps and homogenization. The procedure followed can be obtained from Vicente-Serrano et al. (2014).

We used 317 precipitation series, 340 temperature series, 8 radiation series, 10 wind speed series and 12 relative humidity series (Figure 9). The detail of the meteorological used can be consulted from Annex 4, 5, 6, 7 and 8 of Vicente-Serrano et al. (2014).

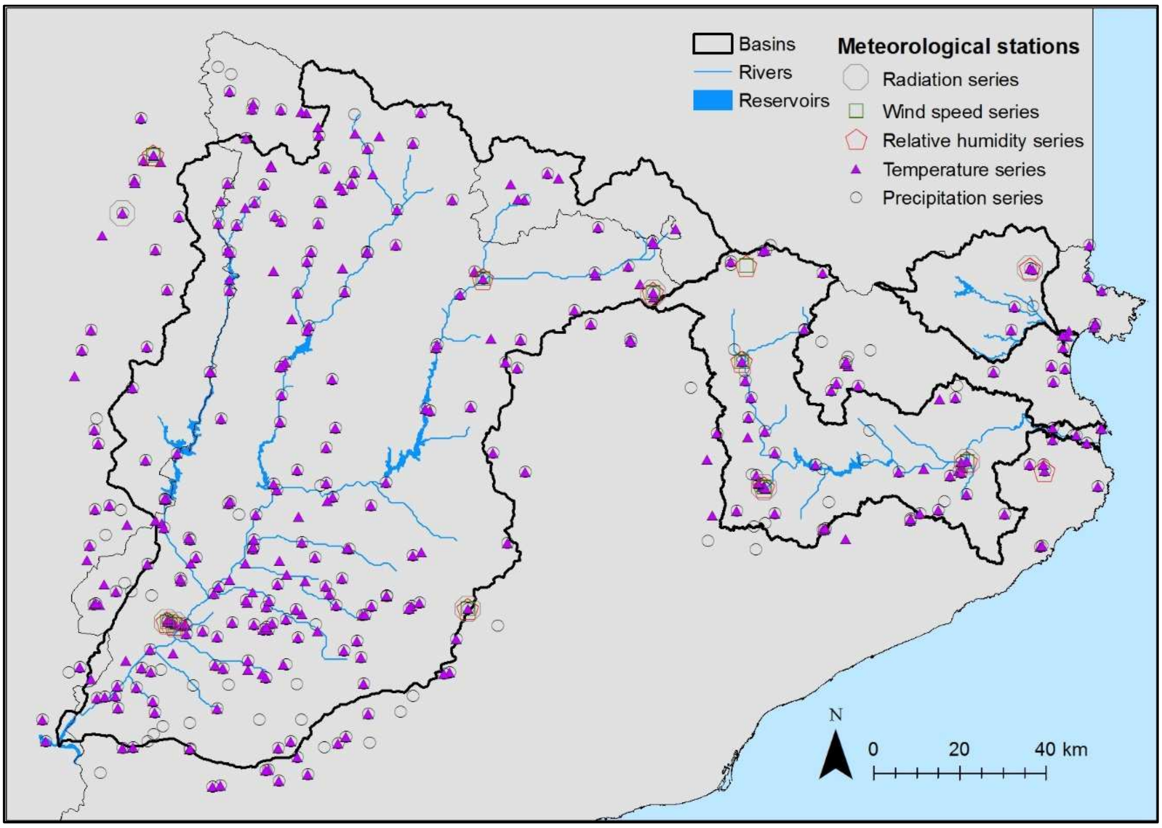

Figure 9. Location of meteorological stations used in the hydrological modelling.

4.3.2. Digital elevation model

The Digital Elevation Model (DEM) was provided by the Catalan Government (Cartographic and Geologic Institute of Catalonia, ICGC) at a spatial resolution of 15 m. Digital Elevation Model is the basic information for almost all the hydrological models, since it allows to obtain different essential information: slope, aspect, hydrologic response unit (HRU), wetness index, etc. Spatial resolution was resampled according to the needs of the project (i.e. 100m for Muga basin and 500m for Ter and Segre ones). Figure 10 shows the spatial distribution of elevation according to the available DEM at the spatial resolution of 500 m.

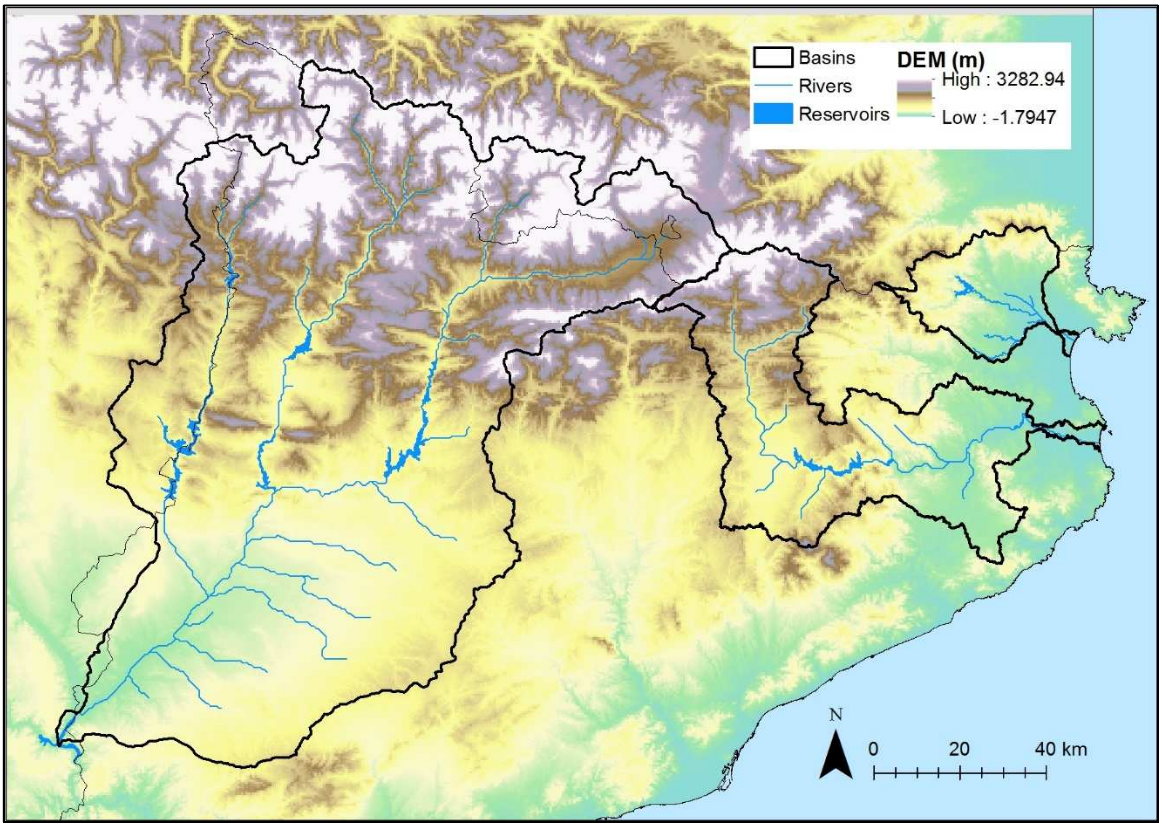

Figure 10. Digital elevation model.

4.3.3. Land use and land cover data

Land use and land cover data were obtained from different sources of information: a) the land cover map of Catalonia for 2005 (MCSC2005) at the spatial scale of 1:5000; b) the 2006 CORINE land cover at the spatial scale of 1:100000; c) the Spanish Land use System for 2005 (SIOSE2005) at the spatial scale of 1:25000; and d) the 2006 National forestry inventory III (IFN) from the Spanish Agricultural Ministry at the scale of 1:50000. We used different sources because of the territorial distribution of the three basins: although the majority of the studied territory belongs to Catalonia, which is covered by the MCSC2005, some parts of the three basins correspond to areas outside Catalonia, in Aragon and France, and were completed with SIOSE2005 and CORINE. The different data sources contained different legends, which were in some cases excessively detailed. For this reason, we unified and reclassified the different thematic information in 16 land use categories: 1) woody crops; 2) herbaceous crops; 3) irrigated herbaceous crops; 4) unproductive; 5) conifer forest; 6) deciduous forest; 7) evergreen forest; 8) shrublands; 9) meadows and grasslands. More details about the process can be consulted from Vicente-Serrano et al. (2014 and 2016) (Figure 11).

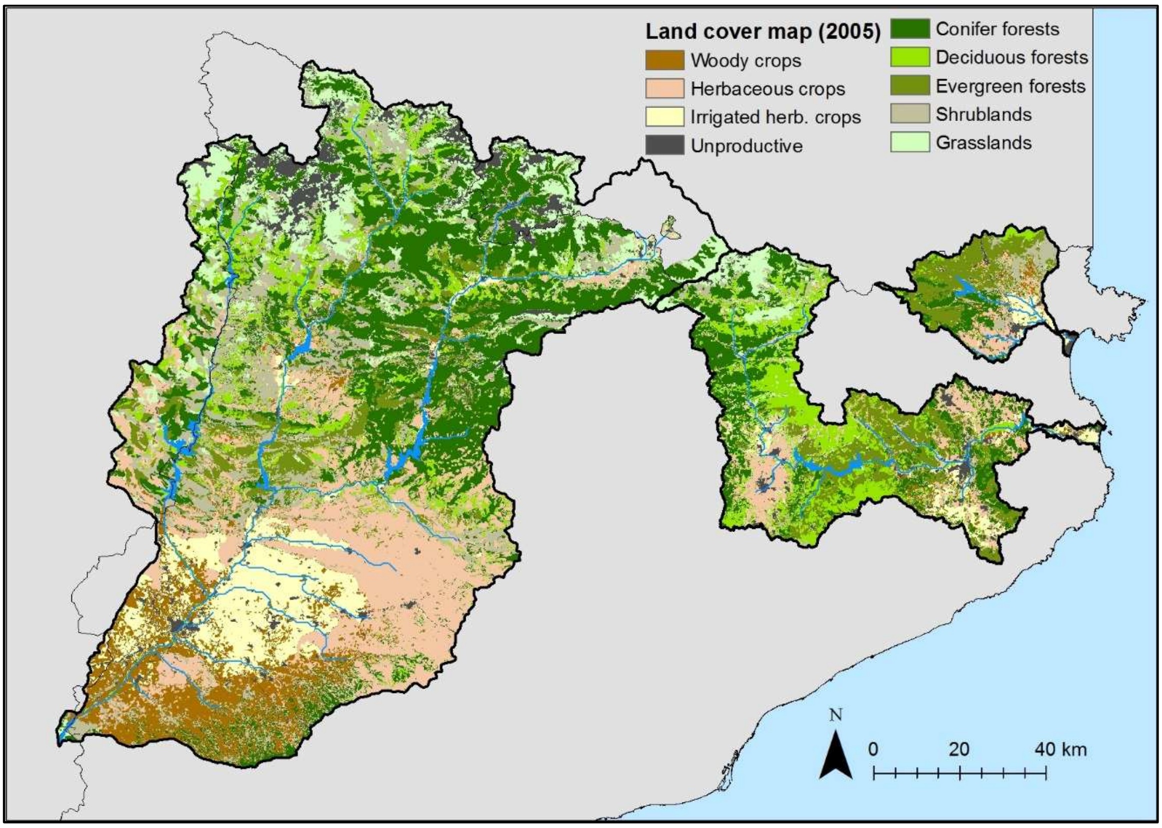

Figure 11. Land cover map 2005.

4.3.4. Soil data

Soil data were specifically created for LIFE MEDACC project purposes, since these data were not available for the three basins. Existent soil data within the three basin were fragmented and specific for agricultural areas. The methodology followed up and the input data needed to create the soil data are deeply explained in Vicente-Serrano et al. (2014).

4.3.5. Hydrological data

Daily stream flows data from gauging stations, reservoir management data and water abstraction through channels and collections are needed to calibrate and validate the hydrological models.

Daily stream flow data (m^3/s) used by LIFE MEDACC project were provided by the Catalan Water Agency (ACA, for Muga and Ter basins) and the Ebro Hydrographical Confederation (CHE, for Segre basin). Data availability depended on the basin: 3 gauging stations in Muga, 9 in Ter and 16 in Segre (Figure 12 and Table 7). Stream flow data were subjected to a process of quality control, filling gaps and homogenization. The procedure followed can be consulted at Vicente-Serrano et al. (2014).

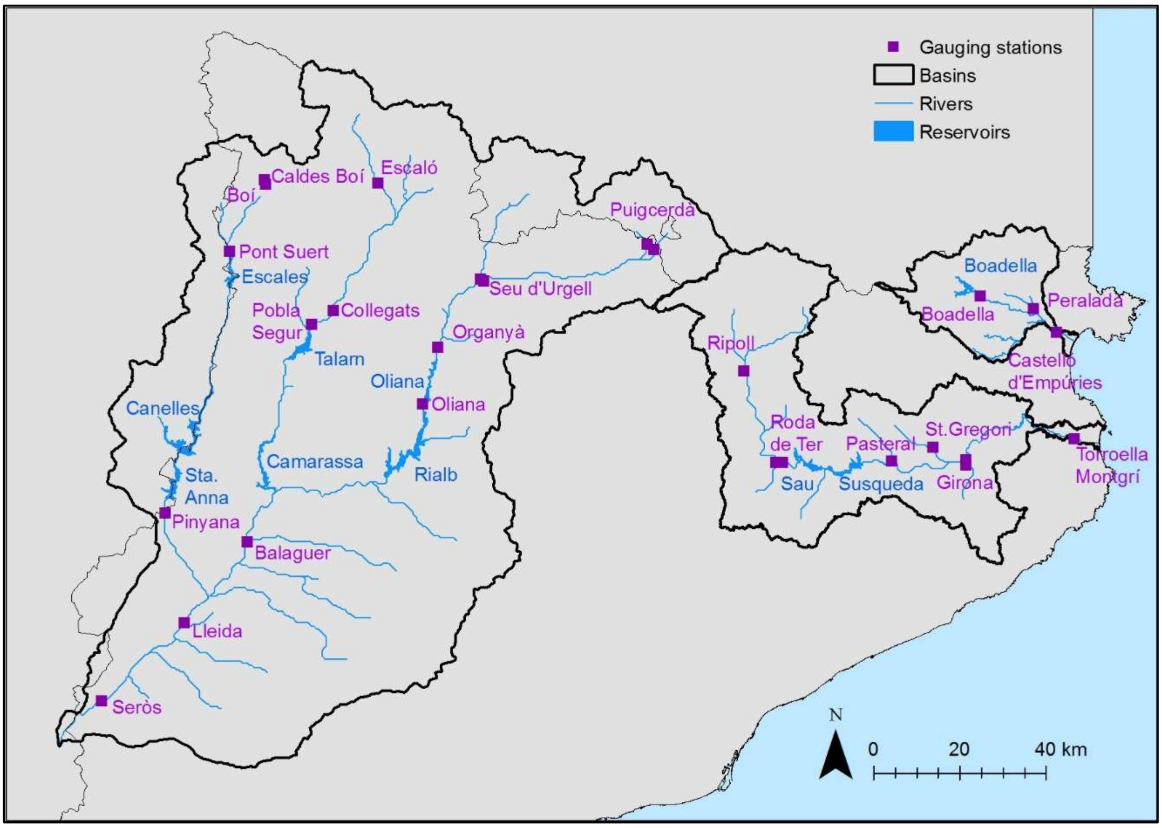

Figure 12. Location of the gauging stations and reservoirs used in the hydrological modelling.

	ID	Gauging station	X_UTM	Y UTM	Starting year
Muga	EA012	Boadella	488,400	4,686,700	1912
	EA052	Castelló d'Empúries	506,080	4,678,325	1972
	EA088	Perelada	500,770	4,683,770	1997
Ter	EA80	Torroella de Montgrí	510,378	4,653,688	2001
	EA33	Ripoll	433,600	4,669,450	1916
	EA19	Roda de Ter	442,600	4,648,300	1927
	EA85	Les Masies de Roda (Ter)	441,195	4,648,340	2000
	EA120	Les Masies de Roda (Gurri)	441,195	4,648,340	2000
	EA60	El Pasteral	468,000	4,648,600	1967
	EA09	Ginestar (Llémena)	477,500	4,651,800	1912
	EA10	Girona (Ter)	485,220	4,648,910	1986
	EA20	Girona (Onyar)	485,234	4,647,730	1959
Segre	A9024	Lleida (Segre)	303,722	4,610,793	1913
	A9083	Oliana (Segre)	358,993	4,661,577	1952
	A9021	Puigcerdà (Segre)	412,690	4,697,400	1922
	A9023	Seu d'Urgell (Segre)	373,190	4,690,149	1913
	A9022	Seu d'Urgell (Valira)	372,416	4,690,646	1913
	A9097	Pinyana (Noguera Ribagorzana)	299,252	4,636,313	1946
	A9111	Organyà (Segre)	362,524	4,674,728	1950
	A9096	Balaguer (Segre)	318,255	4,629,590	1969
	A9025	Seròs (Segre)	284,384	4,592,662	1925

	ID	Gauging station	X_UTM	Y UTM	Starting year
	A9137	Pont de Suert (Noguera Ribagorzana)	314,186	4,696,963	1952
	A9020	Puigcerdà (Arabó)	411,097	4,698,729	1922
	A9116	Caldes de Boí (Noguera de Tor)	322,333	4,713,637	1946
	A9117	Boí (San Nicolas)	322,583	4,712,597	1946
	A9102	Collegats (Noguera Pallaresa)	338,344	4,683,352	1969
	A9146	La Pobla de Segur (Noguera Pallaresa)	333,219	4,680,066	1952
	A9252	Escaló (Noguera Pallaresa)	348,717	4,712,793	1989

Table 7.Gauging stations used in the hydrological modelling.

Reservoir management data used by LIFE MEDACC project were provided by the Catalan Water Agency (ACA, for Muga and Ter basins) and the Ebro Hydrographical Confederation (CHE, for Segre basin). The provided data included: volume (hm^3), inflow (hm^3 and m^3/s) and outflow (hm^3 and m^3/s). Data were available daily or monthly, depending on the reservoir and the period. Segre basin is highly regulated and has a notable number of reservoirs and dams in the main river courses. Due to modelling constrictions, we only included reservoirs with a capacity higher than 100 hm^3. We considered one reservoir in Muga basin (Boadella), two in Ter (Sau and Susqueda) and 7 in Segre (Escales, Canelles and Santa Anna in Noguera Ribagorzana river, Talarn and Camarassa in Noguera Pallaresa river, and Oliana and Rialb in Segre river (Figure 12 and Table 8).

	Reservoir	Capacity (hm3)	Surface (ha)	Construction year	Available data
Muga	Boadella	62.0	364.0	1969	Monthly (1971-2008), daily (2003-2013)
Ter	Sau	169.0	570.0	1966	Monthly (1995-2007), daily (2003-2012)
	Susqueda	233.0	466.0	1968	Monthly (1995-2007), daily (2003-2012)
Segre	Escales (Noguera Ribagorzana)	152.3	400.0	1960	Daily (1960-2009)
	Canelles (Noguera Ribagorzana)	679.3	1,569.0	1965	Daily (1965-2009)
	Sta. Ana (Noguera Ribagorzana)	236.6	792.0	1961	Daily (1961-2009)
	Talarn (Noguera Pallaresa)	226.7	927.0	1958	Daily (1958-2009)
	Camarassa (Noguera Pallaresa)	163.4	624.0	1958	Daily (1958-2009)
	Oliana (Segre)	101.0	443.0	1958	Daily (1958-2009)
	Rialb (Segre)	403.6	1,505.0	1999	Daily (1999-2009)

Table 8. Reservoirs used in the hydrological modelling.

Water abstraction used by LIFE MEDACC project were provided by the Catalan Water Agency (ACA, for Muga and Ter basins) and the Ebro Hydrographical Confederation (CHE, for Segre basin). Data from Muga and Ter basin included water abstraction from reservoirs, dams and river courses in hm^3 at daily or monthly time step, depending on the water abstraction and the period. Data from Segre basin included mean monthly abstraction for the period 1986-2006 per sector (supply-industry, irrigation and other concessions) and per stretch of river (Table 9).

	Location of the abstraction	Water supply	Demand (hm3/year)	Available data
Muga	Boadella reservoir	Urban supply (Figueres)	4.99*	Monthly (2002-2012), daily (2006-2013)
	El Pasteral dam	Irrigation (Canal de la Dreta, Canal de l'Esquerra, Rec del Molí) and urban supply (CCB Nord)	28.72*	Monthly (2002-2012), daily (2006-2013)
Ter	Ponts de Molins dam	Urban supplies (ATLL, CCB Centre, Girona)	192.57*	Monthly (2002-2012)

	Location of the abstraction	Water supply	Demand (hm3/year)	Available data
	Ter River and wells	Irrigation (Pardina, Vilanna, Anglès, Sèquia Monar, Sant Julià de Llor, Cervià, Vinyals, Sentmenat, Pals)	115.23*	Monthly (2002-2012)
Segre	Noguera Pallaressa river	Urban and industrial supply	3.33+	Monthly mean value based on the Hydrologic Plan
	Noguera Pallaressa river	Irrigation	34.75+	
	Segre river	Urban and industrial supply	17.45+	
	Segre river	Irrigation	176.71+	
	Canal d'Urgell	Urban and industrial supply	16.41+	
	Canal d'Urgell	Irrigation	712.02+	
	Noguera Ribagorzana river	Urban and industrial supply	28.71+	
	Noguera Ribagorzana river	Irrigation	4.27+	
	Canal d'Aragó	Urban and industrial supply	12.38+	
	Canal d'Aragó	Irrigation	817.02+	
	Canal de Pinyana	Irrigation	169.21+	

*Table 9. Main water abstraction used in the hydrological modelling. * Water abstraction from Muga and Ter has been estimated as the mean annual value from 2002-2012. + Water abstraction from Segre has been provided by the CHE and only mean monthly values for the period 1986-2006 are available*

Hydrological data were highly diverse, and incomplete and of poor quality in some periods. We needed to select a common reference period for the calibration of the three basins. On one hand, the most restricted data were water abstractions, with daily data availability from 2006 and monthly data from 2002. On the other hand, stream flow data from gauging stations managed by ACA had problems of quality and data gap from 2011, due to budget problems caused by the crisis. Both reasons force us to set the reference period between 2002 and 2011 (10 years). Both models, RHESSys and SWAT were calibrated for the same period and with the same input data, although the gauging stations used for the calibration were not necessarily the same.

4.4. Calibration of the hydrological models

The first phase of the modelling and the most important part of the process is the calibration of the hydrological model. This process is done by comparing model results with observed data at gauging stations. Model calibration implies to modify the model parameters to obtain stream flow values similar to those registered in the gauging station, especially in regard to peak flows and base flows.

Model calibration was carried out with three main objectives: (1) to obtain simulated stream flow curves comparable with observed stream flow curves; (2) to obtain mean stream flow values and total contributions similar between simulated and measured data; and (3) to check the quality of simulated data with the Nash-Sutcliffe efficiency (NSE) coefficient, the RMSE-observations standard deviation ratio (RSR) and the percent bias (PBIAS, %), following Moriasi et al. (2007). The NSE coefficient, the RSR ratio and PBIAS equations and the statistics performance ratios are shown in Table 10.

Performance rating	$RSR = \left[\frac{\sqrt{\sum_{i=1}^{n} \left(Y_i^{obs} - Y_i^{sim} \right)^2}}{\sqrt{\sum_{i=1}^{n} \left(Y_i^{obs} - Y^{mean} \right)^2}} \right]$	$NSE = 1 - \left[\frac{\sum_{i=1}^{n} \left(Y_i^{obs} - Y_i^{sim} \right)^2}{\sum_{i=1}^{n} \left(Y_i^{obs} - Y^{mean} \right)^2} \right]$	$PBIAS = \left[\frac{\sum_{i=1}^{n} \left(Y_i^{obs} - Y_i^{sim} \right) * (100)}{\sum_{i=1}^{n} \left(Y_i^{obs} \right)} \right]$
Very good	0.00 ≤ RSR ≤ 0.50	1.00 ≤ NSE < 0.75	PBIAS < ± 10
Good	0.50 < RSR ≤ 0.60	0.75 ≤ NSE < 0.65	± 10 ≤ PBIAS ≤ ± 15
Satisfactory	0.60 < RSR ≤ 0.70	0.65 ≤ NSE < 0.5	± 15 ≤ PBIAS ≤ ± 25

Unsatisfactory	RSR > 0.70	NSE ≤ 0.5	PBIAS ≥ ± 25

Table 10. Equations for the statistics Nash-Sutcliffe efficiency (NSE) coefficient, RMSE-observations standard deviation ratio (RSR), Percent bias (PBIAS) and general performance ratings for the statistics for a monthly time step. Y_i^{obs} is the ith observation values sample for the constituent being evaluated, Y_i^{sim} is the ith simulated sample for the constituent being evaluated, Y_{mean} is the mean of observed data for the constituent being evaluated, and n is the total number of observations.

4.4.1. RHESSys model

Model calibration consists of modifying values of model input parameters in an attempt to match field conditions within some acceptable criteria. The four independent parameters that are typically calibrated in RHESsys are the decay of hydraulic conductivity with depth (m), saturated soil hydraulic conductivity at the surface – Ksat0 (K), and two groundwater parameters which control the proportion of infiltrated water that bypasses soil (via macropores and fractures) to a deeper groundwater table (gw1), and the rate of lateral flow from a hillslope scale groundwater table (modelled as a linear reservoir) to the stream channel (gw2).

However, prior to calibrating or running model simulations for predictive purposes, values for the state variables in the world file must be initialized. This process in RHESsys is called ‘spin-up’. The 'spin-up' period in RHESsys is the time of adjustment it takes for the model to reach a state of equilibrium in vegetation and soil carbon (C) and nitrogen (N) stores. After the ‘spin-up’ process it is time to determine reasonable values for the calibrated parameters (m, K, gw1 and gw2 in this calibration) by measuring the correspondence of modelled streamflow to observed streamflow for goodness of fit. Equifinality refers to an observation that different initial conditions (combinations of parameter values) may generate similar, or equivalent, output from a model. The interactions between the components of such a complex system cannot be considered independently, and so different parameter combinations may arrive at the same end result. Testing a large number of parameter sets across a wide range of possible parameter space helps to reduce uncertainty.

There are different methods of generating and sampling from the possible parameter space and calculating uncertainty. RHESsys generally employs the Monte Carlo method - a statistical sampling technique used to generate random parameter values from probability distributions, and the Nash-Sutcliffe efficiency metric - which measures the correspondence of modelled streamflow to observed streamflow for goodness of fit.

Nine sub-basins were monthly calibrated for LIFE MEDACC project: two basins in Muga river (Boadella and Castelló d’Empúries), two sub-basins in Ter river (Roda de Ter and Torroella de Montgrí) and five sub-basins in Segre river (Valira, Organyà, Escalés, Escaló and Seròs).

<u>Calibration of Muga basin</u>

Figure 13 shows calibration outputs for monthly stream flow and reservoir inflow (m^3/s) for two gauging stations: Boadella reservoir and Castelló d’Empúries. The graphical comparison between simulated and observed data showed a good fit, although in Castelló simulations overestimated low flood and underestimated flow peaks. The main reason to explain this is that RHESsys, in general, simulate in a not very good way the artificial streamflow. It is one of the main handicaps of this model, designed especially for mountainous areas. Assuming that the water demand data and the data about management of the Boadella-Darnius are good, the result of the calibration is satisfactory.

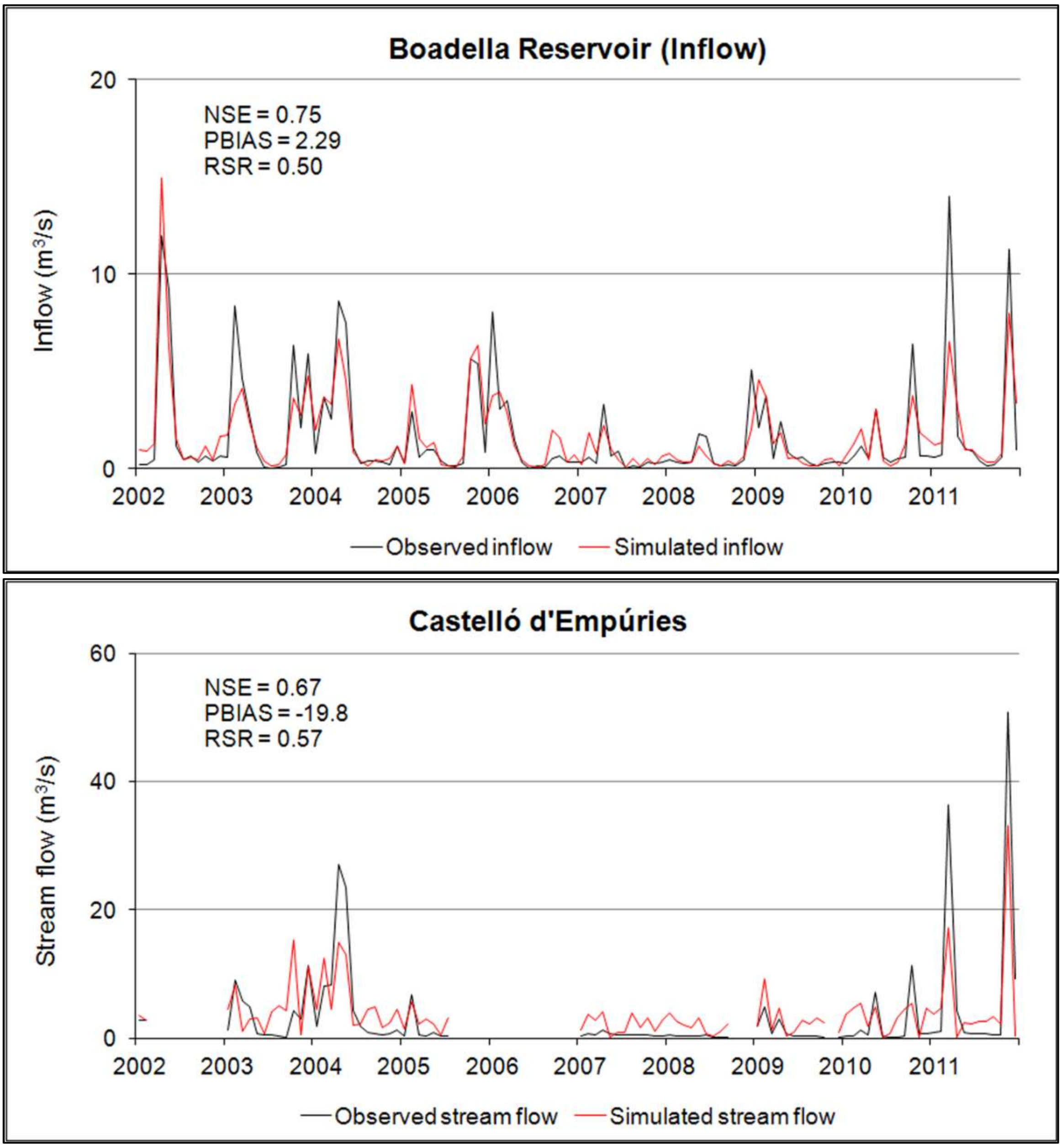

Figure 13. Calibration results: observed (black line) and simulated (red line) dam inflow or stream flow at two points of the basin: Boadella reservoir (headwaters) and Castelló d'Empúries (river mouth).

Table 11 compares simulated and measured dam inflow and stream flow data per gauging station. In Castelló, simulations overestimated mean stream flow values (by 19.8%). In Boadella, simulations overestimated observed data in a 2.3%. The NSE, PBIAS and RSR statistics show a very good fit for Boadella and a good/satisfactory in Castelló (Moriasi et al. 2007).

	Simulated Qm ($m^{3/}s$)	Observed Qm (m^3/s)	Statistics		
			NSE	PBIAS	RSR
Boadella Dam	1.64	1.68	0.8	2.295	0.5
Castelló d'Empúries	3.89	3.25	0.7	-19.8	0.57

Table 11. Calibration results at a monthly time step: dam inflow or stream flow values (Qm) from both simulated and observed data and statistics in each gauging station. Yellow color identifies unsatisfactory performance ratio for the statistic, yellow identifies satisfactory, light green good and dark green very good, following Moriasi et al. (2007).

Calibration of Ter basin

Figure 14 shows calibration outputs for monthly stream flow (m^3/s) for two gauging stations: Roda de Ter and Torroella de Montgrí. The graphical comparison between simulated and observed data showed a good fit, although, in the case of Torroella de Montgrí, at the end of the calibration period the simulations tend to underestimate peak flows, meanwhile the opposite trend is observed at the beginning of the period. The calibration in Roda Ter shows that RHESsys can replicate the streamflow evolution very well both, the low flow and high flow.

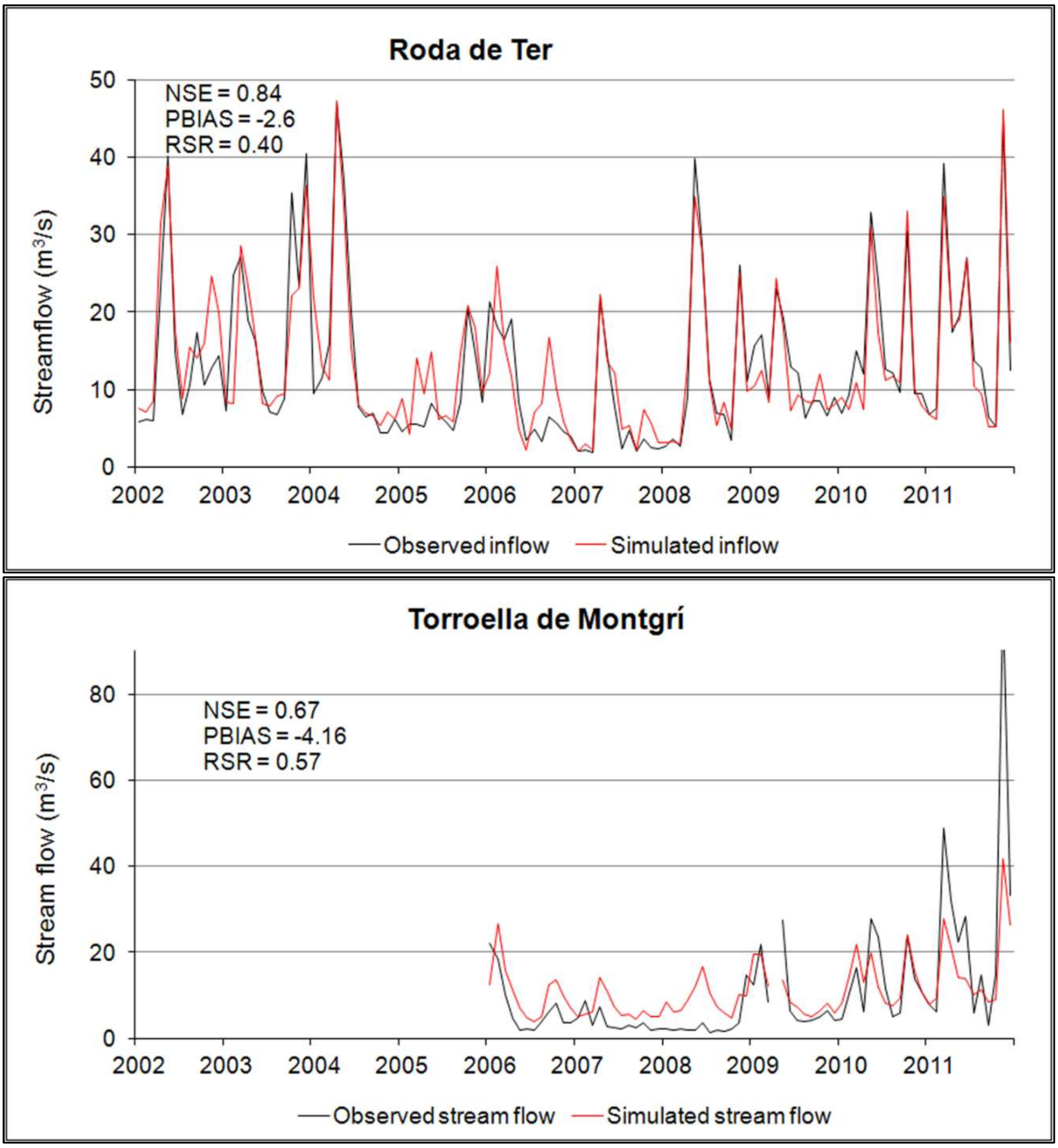

Figure 14. Calibration results: observed (black line) and simulated (red line) dam inflow or stream flow at two points of the basin: Roda de Ter (headwaters) and Torroella de Montgrí (river mouth).

Table 12 compares simulated and measured dam inflow and stream flow data per gauging station. In Roda and Torroella, the two stations have different results: slight underestimation in Roda de Ter (-2.29%) and high overestimation in Torroella de Montgrí (19.8). The NSE, PBIAS and RSR statistics show very good performance ratio for Roda de Ter gauging stations, while for the other stations only is able to get good/satisfactory ones (Moriasi et al. 2007).

	Simulated Qm ($m^{3/}s$)	Observed Qm (m3/s)	Statistics		
			NSE	PBIAS	RSR
Roda de Ter	13.26	12.92	0.84	-2.6	0.4
Torroella de Montgrí	11.20	10.62	0.67	-4.16	0.57

Table 12. Calibration results at a monthly time step: dam inflow or stream flow values (Qm) from both simulated and observed data and statistics in each gauging station. Yellow color identifies unsatisfactory performance ratio for the statistic, yellow identifies satisfactory, light green good and dark green very good, following Moriasi et al. (2007).

Calibration of Segre basin

Figure 15 shows calibration outputs for monthly stream flow and reservoir inflow (m^3/s and Hm^3, respectively) for five gauging stations: in the Valira river (La Seu d'Urgell), in the Segre river (Organyà and Seròs), Noguera Pallaresa (Escaló) and in Noguera Ribagorzana river (Escales Dam inflow). This figure shows that RHESsys is able to simulate the streamflow in a satisfactory way with a clear underestimation in some high flows, being the more representative one in 2008. Generally and knowing the complexity of this basin the calibrations can be regarded as satisfactory/good.

Table 13 compares simulated and measured stream flow data per gauging station and dam inflow in the case of Escales Dam. Simulations underestimated mean stream flow values in all the cases (3.45% in Escalés, 13.9% in Escaló, 2.9% in Organyà and 12.71% in Valira) except in Seròs gauging station, where the simulation overestimated stream flows in a 25%. The statistics show satisfactory results what talks about the complexity of this basin. Indeed, the calibration in lowland (Seròs) is in the limit to be an unsatisfactory calibration, explained with the mismatch in the last two years of calibration. The statistics in this station are much better for the period 2002-2010 (NSE: 0.6, PBIAS: 18%, RSR: 0.64) and for the period 2002-2009 (NSE: 0.74, PBIAS: 10.4%, RSR: 0.5). The observed data in 2010 delays the peak streamflow of spring, while in 2009 is practically non-existent, what the model is not able to replicate. A part from this, the model show a clear adjust the first five years.

	Simulated Qm ($m^{3/}s$)	Observed Qm (m3/s)	Statistics		
			NSE	PBIAS	RSR
Escalés (Hm^3)	37.74	39.09	0.61	3.456	0.62
Escaló	8.58	9.96	0.64	13.9	0.6
Organyà	20.36	21.24	0.59	2.939	0.64
Valira	6.12	7.01	0.66	12.71	0.59
Seròs	57.44	48.39	0.52	-25.00	0.69

Table 13. Calibration results at a monthly time step: dam inflow or stream flow values (Qm) from both simulated and observed data and statistics in each gauging station. Yellow color identifies satisfactory performance ratio for the statistic, light green good and dark green very good, following Moriasi et al. (2007).

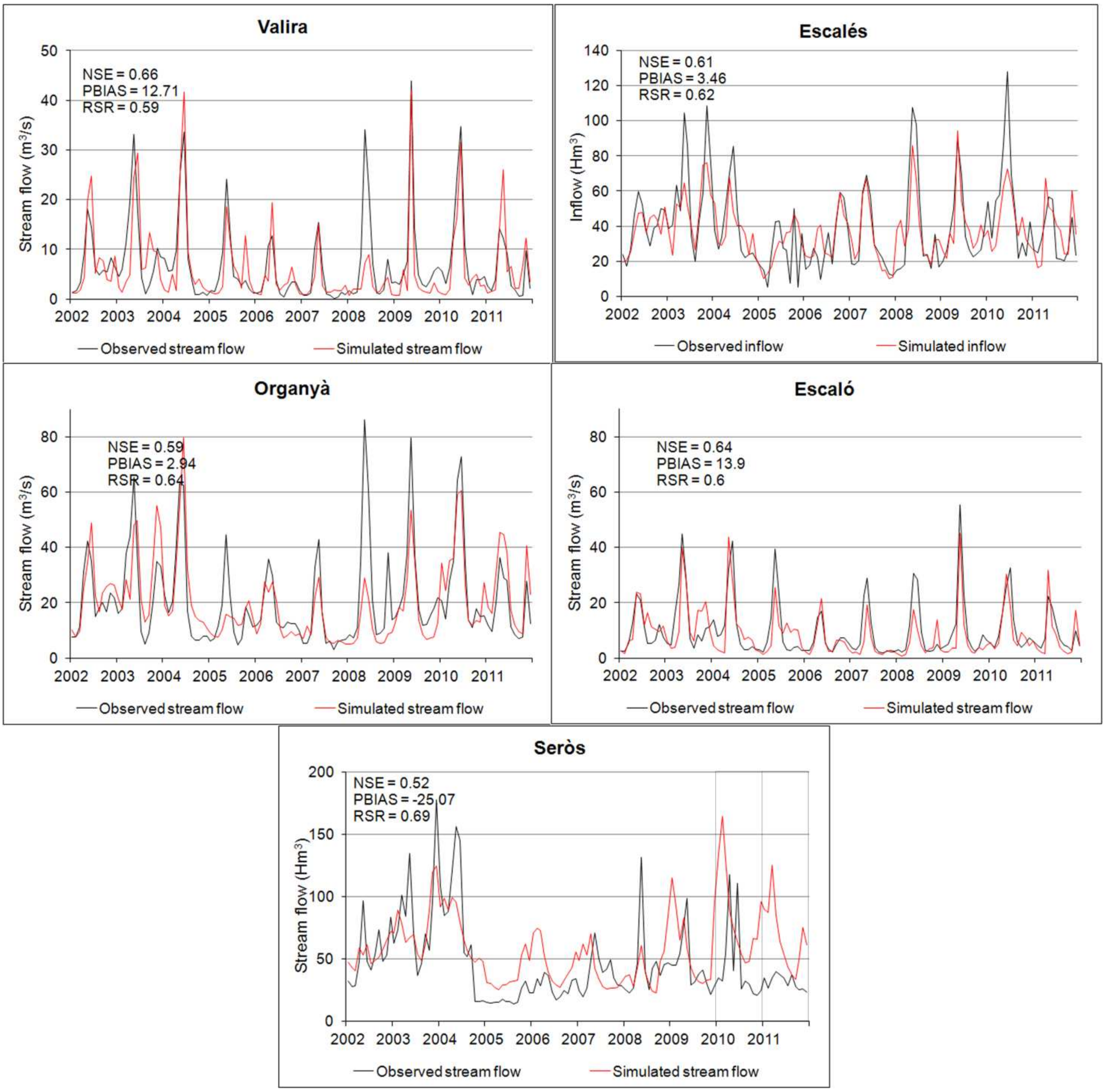

Figure 15. Calibration results: observed (black line) and simulated (red line) dam inflow or stream flow at five points of the basin: Valira, Escalés, Escaló, Organyà and Seròs.

4.4.2. SWAT model

Climate, topography, land use, soil type data were introduced in SWAT model. Previously to calibration, some steps were accomplished. First, we divided each basin in sub-basins with quite homogeneous topographic characteristics. Sub-basins delimitation was based on elevation, creating units with similar area. We identified 14 sub-basins in Muga basin, 20 in Ter and 55 in Segre (Figure 16). The sub-basins are used by the model to assign a specific climate. To do so, SWAT model uses the data from the meteorological station nearest the centroid of each sub-basin. As some meteorological stations were located at low altitude, the precipitation data used in some sub-basins in mountainous areas were underestimated. For this reason, climate series were corrected for the effects of topography using GIS techniques. The relationship between climate and topography was derived from the digital elevation model (DEM, 30 m spatial resolution) of Catalonia (Catalan Cartographic Institute, ICC, 2012) and the Digital Climatic Atlas of Catalonia (Ninyerola et al. 2000).

Secondly, we introduced reservoir data into the model, including: 1) reservoir capacity to the principal and emergency spillway (hm^3); 2) reservoir surface area when the reservoir is filled to the principal and emergency spillway (ha); 3) reservoir volume at the beginning of the simulation period (hm^3), 4) year the reservoir became operational; and 5) management data. Management data were measured daily outflow of each reservoir in m^3/s. For Boadella, Sau and Susqueda reservoirs, daily outflow data was only available from 2003. For 2002, we estimated the mean daily outflow from 2003 to 2011 and assigned to 2002.

Finally, we introduced abstraction data into the model. SWAT works removing the consumptive water use from the basin, considering the water to be lost from the system. Besides, SWAT allows water to be removed from the shallow aquifer or deep aquifer, the reach or the pond within any sub-basin. Water also may be removed from reservoirs for consumptive use (Arnold et al. 2012). Existent water abstractions were classified by source (aquifer, reach or pond) and sub-basin. Water for urban and industrial use is mostly returning to the basin after treatment plants. ACA quantifies that the 80% of the urban and industrial water returns. Therefore, we included into SWAT the 20% of the urban and industrial abstraction, except in the cases in which the abstracted water ends out of the basin (as for example the supply to the Metropolitan Region of Barcelona). On the contrary, only the 20% of the irrigation water is supposed to return to the basin. Then, we considered that the 80% of the irrigation consumptive water was lost from the system.

Calibrations were performed at monthly time step. Muga basin was calibrated with the Castelló d'Empúries gauging station. Ter was calibrated in two steps, first the headwaters with Roda de Ter station and second the medium and low courses with Torroella de Montgrí station. Segre, with 13,000 km^2 of surface and 7 reservoirs, was the most difficult to calibrate. We divided the basin in 6 parts and calibrate each part with Pont de Suert and Canelles reservoir inflow (Noguera Ribagorzana), Talarn reservoir inflow (Noguera Pallaressa), and Organyà, Oliana reservoir inflow and Seròs (Segre).

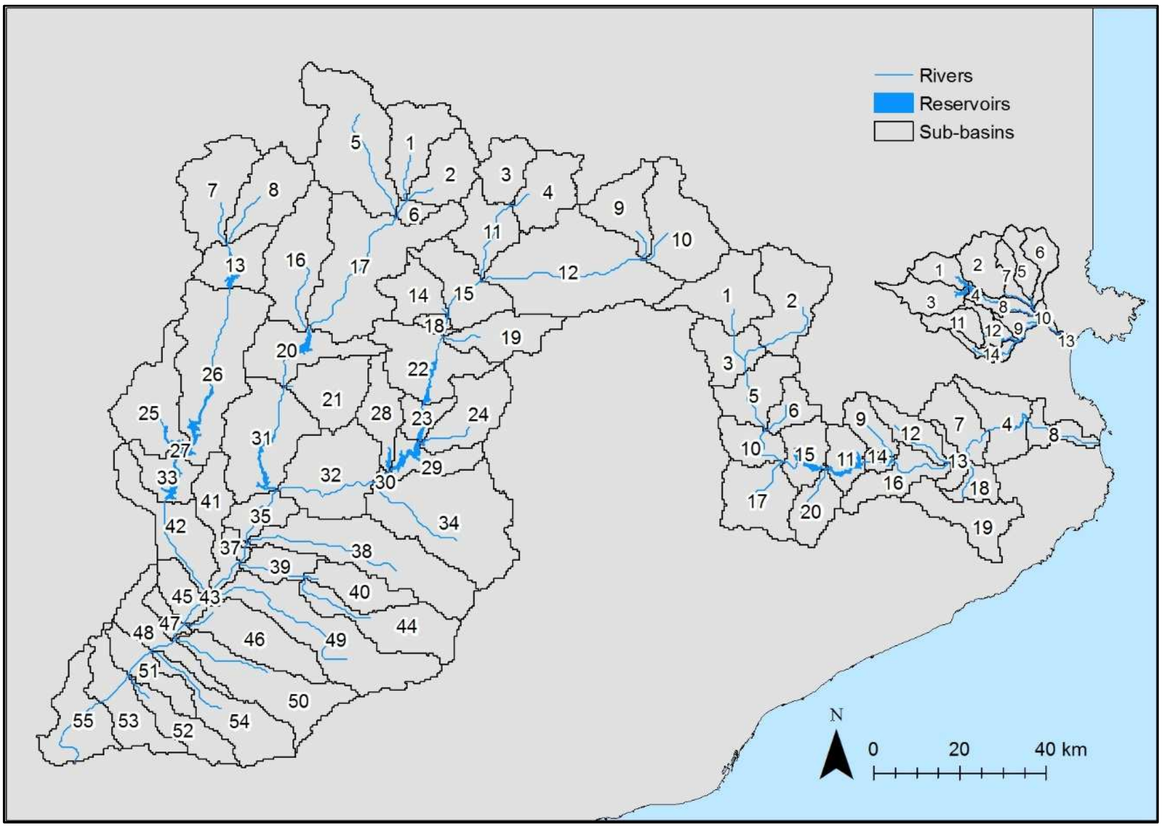

Figure 16. Delimitation of sub-basins by SWAT model.

Sensitivity analysis and preliminary model trials were developed using the Sensitivity Analysis Tool provided by SWAT (Van Griensven 2005) to identify the most influential parameters, which were adjusted during the calibration. These were parameters related to base flow generation, surface runoff, soil parameters, orographic correction and catchment response.

Calibration was performed through the SWAT Calibration and Uncertainty Program (SWAT-CUP, Abbaspour 2013) in 10-year periods. Parameters related to groundwater (groundwater delay time, base flow alpha factor, groundwater revap coefficient...), soil (available water capacity of the soil, saturated hydraulic capacity …), land cover (plant uptake and soil compensation factor, curve number …) or orographic correction (precipitation and temperature lapse rate) were adjusted using SWAT-CUP, estimating the best fit possible.

Calibration of Muga basin

Figure 17 shows calibration outputs for monthly stream flow and reservoir inflow (m^3/s) for three gauging stations: Boadella reservoir (in the headwaters, 190.7 km^2 upstream surface area and 25.0% of the total area), Peralada (in Llobregat d'Empordà Muga affluent, 304.3 km^2 and 39.9%) and Castelló d'Empúries (in the river mouth, 755.5 km^2 and 99.1%). The graphical comparison between simulated and observed data showed a good fit, although in Peralada and Castelló simulations underestimated high flood peaks and slightly overestimated base flows. One explanation could be the high spatial variability of the precipitation in the area, where the complex mountainous landscape causes orographic precipitation or convective phenomena that affect the climate (Barrera-Escoda and Cunillera 2011). This means that the precipitation measured in the meteorological station may be different than the total registered in the upstream area of the gauging station. Another reason can be the low capacity of the SWAT model structure to adequately account for hydrological extreme events (Ndomba et al. 2008).

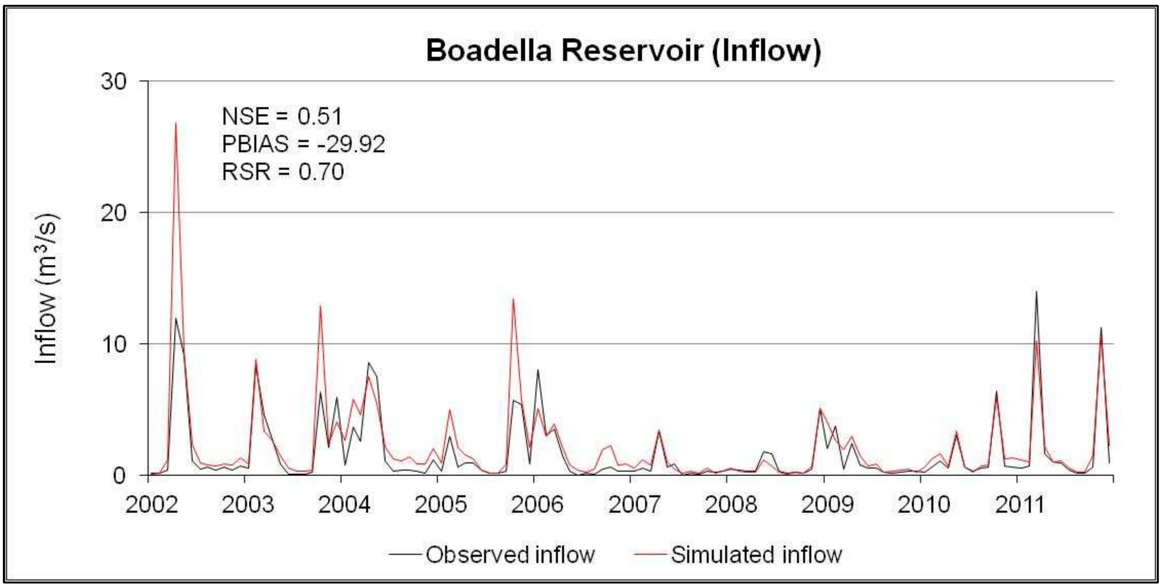

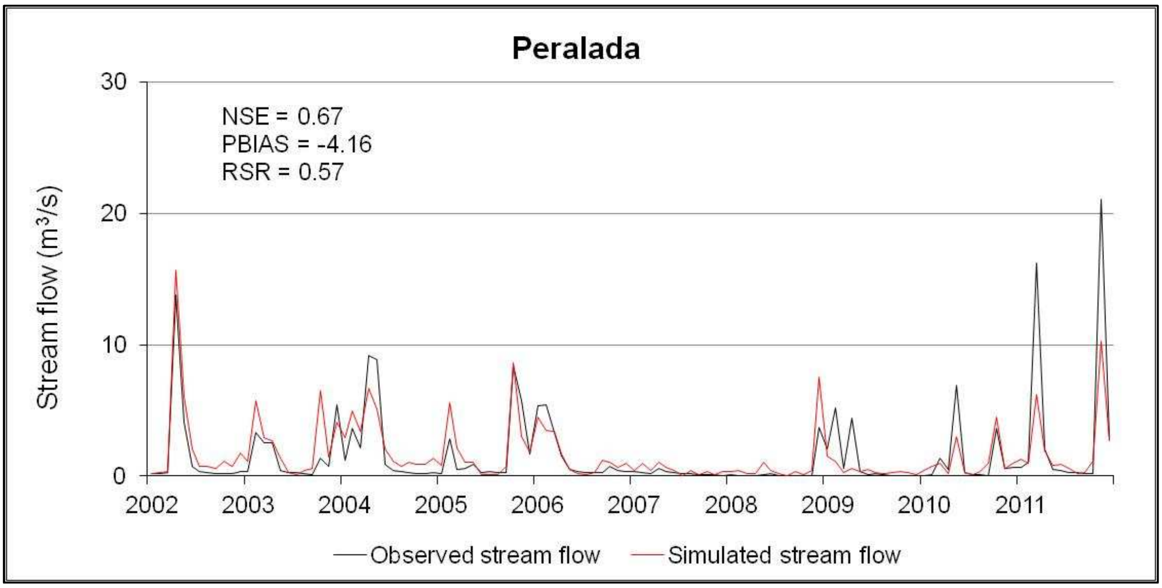

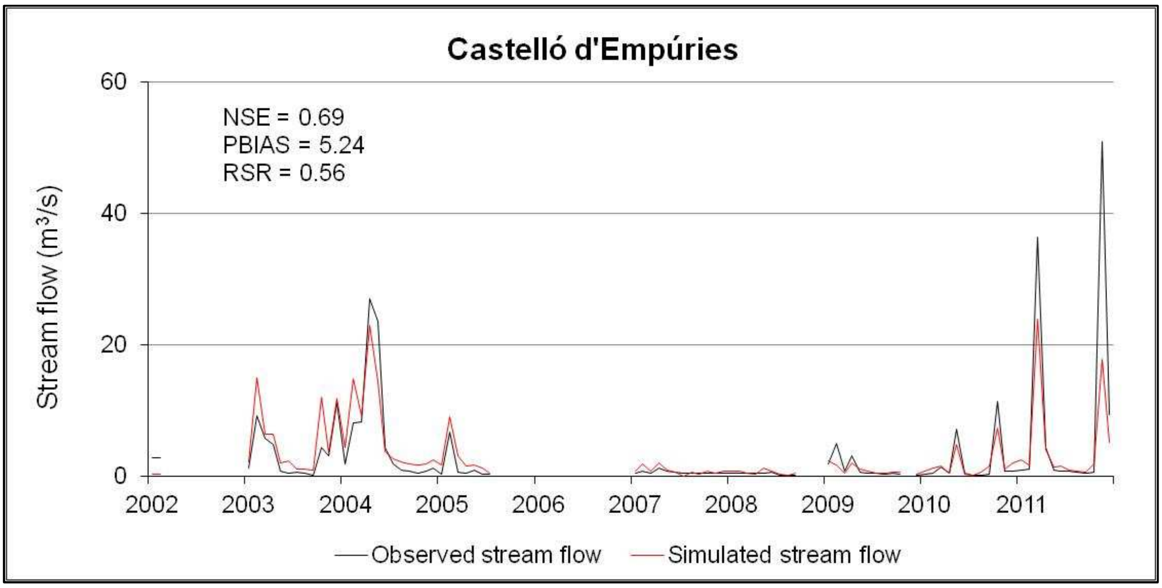

Figure 17. Calibration results: observed (black line) and simulated (red line) dam inflow or stream flow at three points of the basin: Boadella reservoir (headwaters), Peralada (Llobregat d'Empordà) and Castelló d'Empúries (river mouth).

Table 14 compares simulated and measured dam inflow and stream flow data per gauging station. In Boadella and Peralada, simulations overestimated mean stream flow values (by 29.9 and 4.2%, respectively). In Castelló, simulations underestimated observed data in a 5.2%. It is worthy to remember than Muga basin was fully calibrated with Castelló stations, so mean values and statistic were adjusted to the best fit in this station. The NSE, PBIAS and RSR statistics show a satisfactory fit for Boadella and a good or very good for Peralada and Castelló (Moriasi et al. 2007).

	Simulated Qm (m^3/s)	Observed Qm (m^3/s)	Statistics		
			NSE	PBIAS	RSR
Boadella Reservoir	2.18	1.68	0.51	-29.92	0.70
Peralada	1.62	1.56	0.67	-4.16	0.57
Castelló d'Empúries	3.08	3.25	0.69	5.24	0.56

Table 14. Calibration results at a monthly time step: dam inflow or stream flow values (Qm) from both simulated and observed data and statistics in each gauging station. Orange color identifies unsatisfactory performance ratio for the statistic, yellow identifies satisfactory, light green good and dark green very good, following Moriasi et al. (2007).

Calibration of Ter basin

Figure 18 shows calibration outputs for monthly stream flow and dam inflow (m^3/s) for five gauging stations: Roda de Ter (in the headwaters, 1,388 km^2 upstream surface area and 47.0% of the total area), Sau reservoir (1,525 km^2 and 51.7%), Susqueda reservoir (1,770.5 km^2 and 60.0%), Girona (2,232 km^2 and 75.6%) and Torroella de Montgrí (in the river mouth, 2,952.25 km^2 and 100.0%). The graphical comparison between simulated and observed data showed a good fit, although at the end of the calibration period the simulations tend to overestimate peak flows, meanwhile the opposite trend is observed at the beginning of the period.

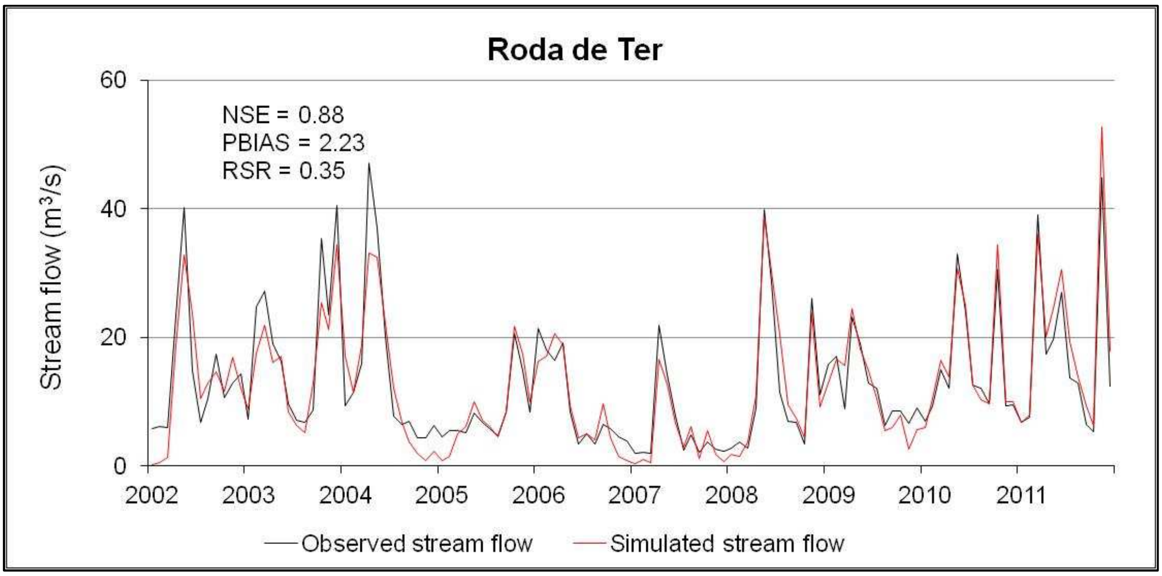

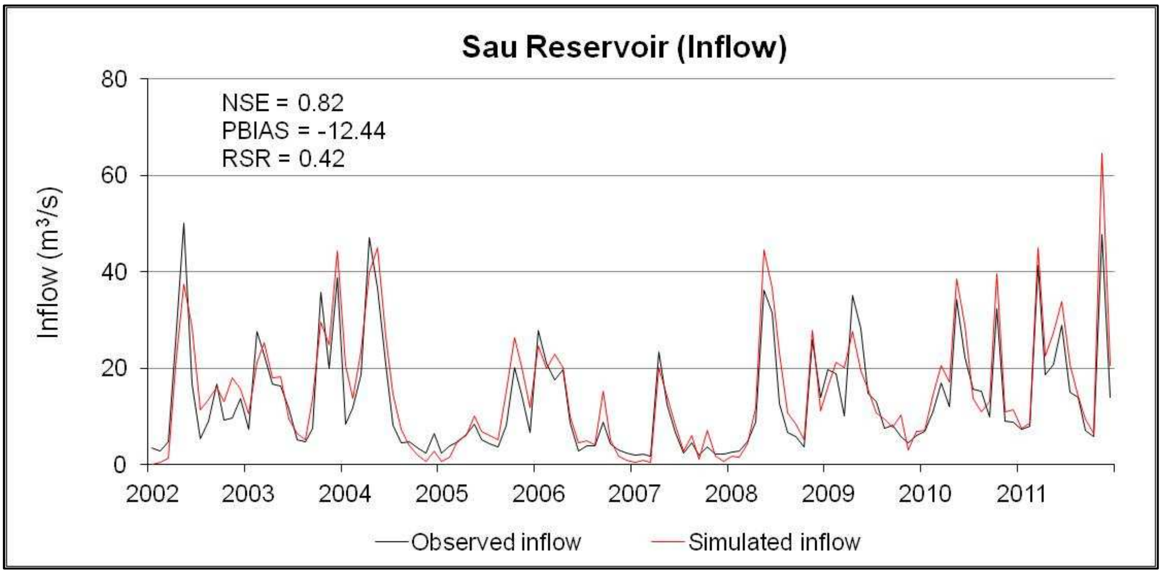

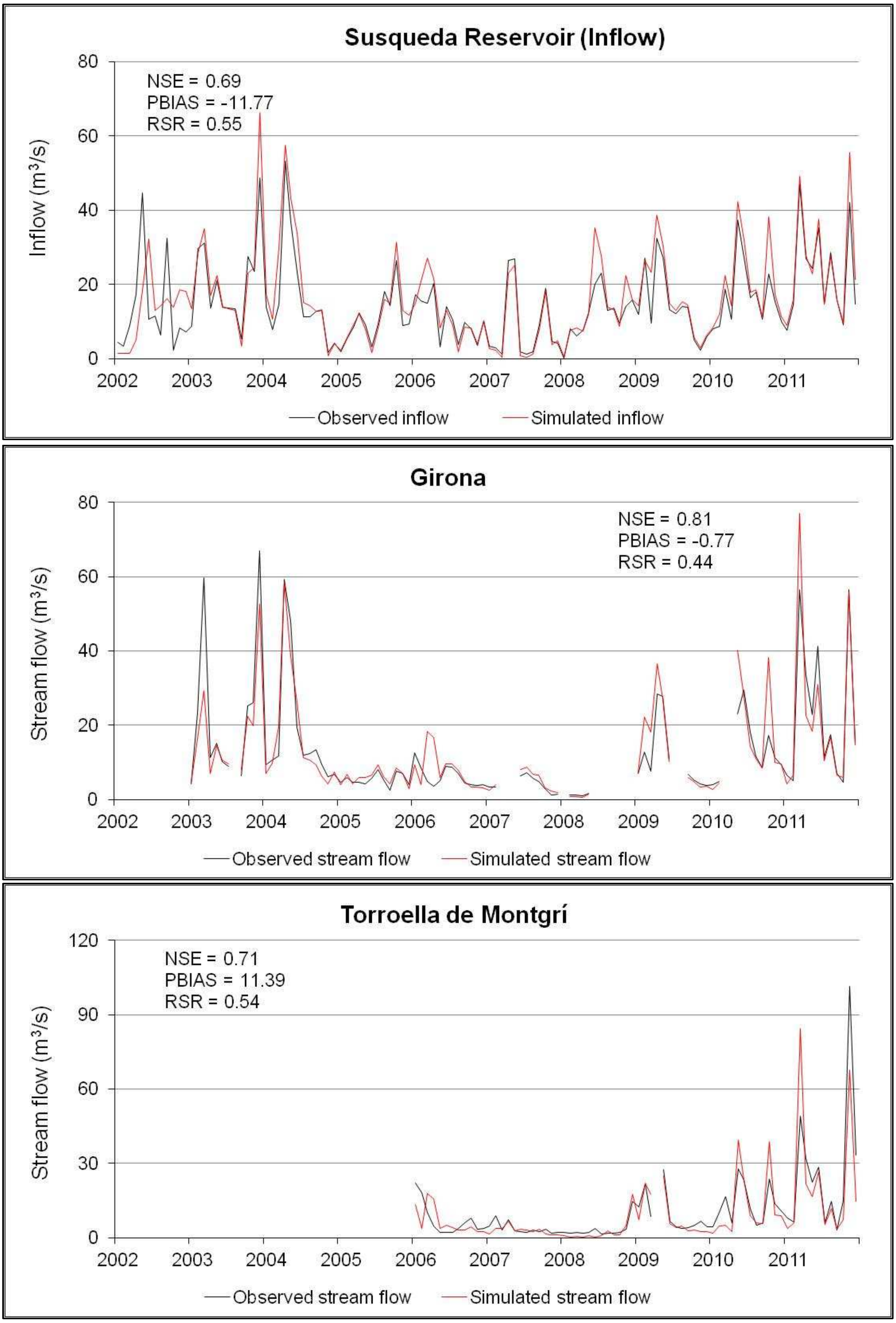

Figure 18. Calibration results: observed (black line) and simulated (red line) dam inflow or stream flow at five points of the basin: Roda de Ter (headwaters), Sau and Susqueda dams, Girona and Torroella de Montgrí (river mouth).

Table 15 compares simulated and measured dam inflow and stream flow data per gauging station. In Roda and Torroella, the two stations used in this calibration, simulations underestimated mean stream flow values (by 2.2 and 11.4%, respectively). The NSE, PBIAS and RSR statistics show good or very good performance ratio for all the gauging stations (Moriasi et al. 2007).

	Simulated Qm (m^3/s)	Observed Qm (m^3/s)	Statistics		
			NSE	PBIAS	RSR
Roda de Ter	12.63	12.92	0.88	2.23	0.35
Sau Reservoir	14.87	13.23	0.82	-12.44	0.42
Susqueda Reservoir	16.51	14.77	0.69	-11.77	0.55
Girona	12.90	12.80	0.81	-0.77	0.44
Torroella de Montgrí	9.41	10.62	0.71	11.39	0.54

Table 15. Calibration results at a monthly time step: dam inflow or stream flow values (Qm) from both simulated and observed data and statistics in each gauging station. Light green color identifies good performance ratio for the statistic and dark green identifies very good, following Moriasi et al. (2007).

<u>Calibration of Segre basin</u>

Figure 19 shows calibration outputs for monthly stream flow and reservoir inflow (m^3/s) for eight gauging stations: in the Noguera Ribagorzana river, Pont de Suert (in the headwaters, 545.8 km^2 upstream surface area and 4.1% of the total area) and Santa Anna Reservoir (1,761.5 km^2 and 13.3%); in the Noguera Pallaresa river: Talarn Reservoir (1,913 km^2 and 14.5%) and Camarassa Reservoir (2,816.8 km^2 and 21.3%); and in the Segre river: Organyà (headwaters, 2,381.3 km^2 and 18.0%), Oliana Reservoir (2,695.3 km^2 and 20.4%) and Rialb Reservoir (3,320 km^2 and 25.1%), and Seròs (river mouth, 12,941.8 km^2 and 98%).

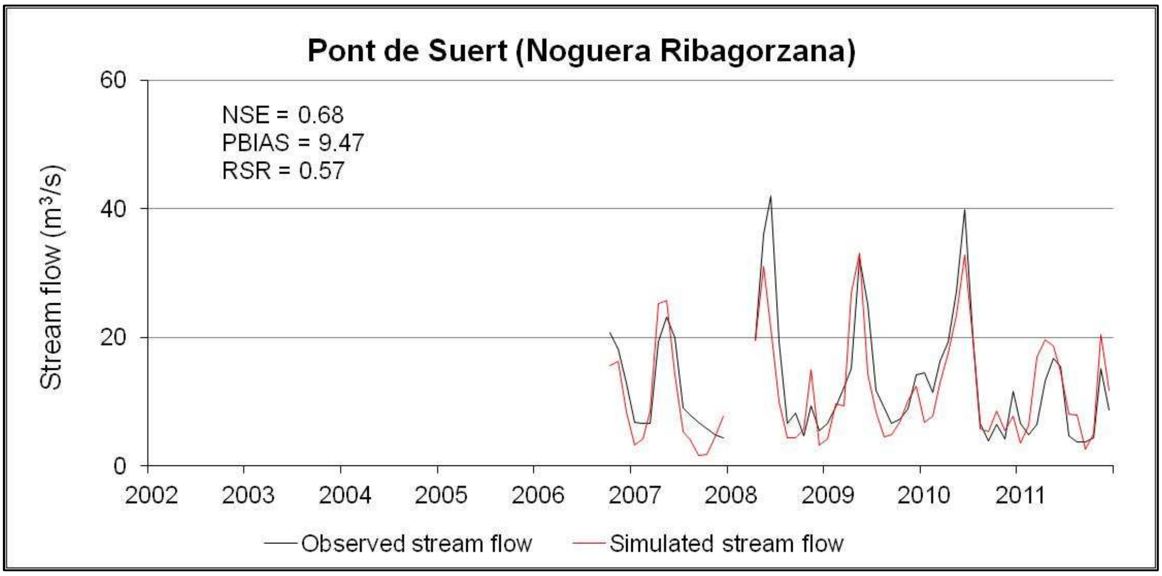

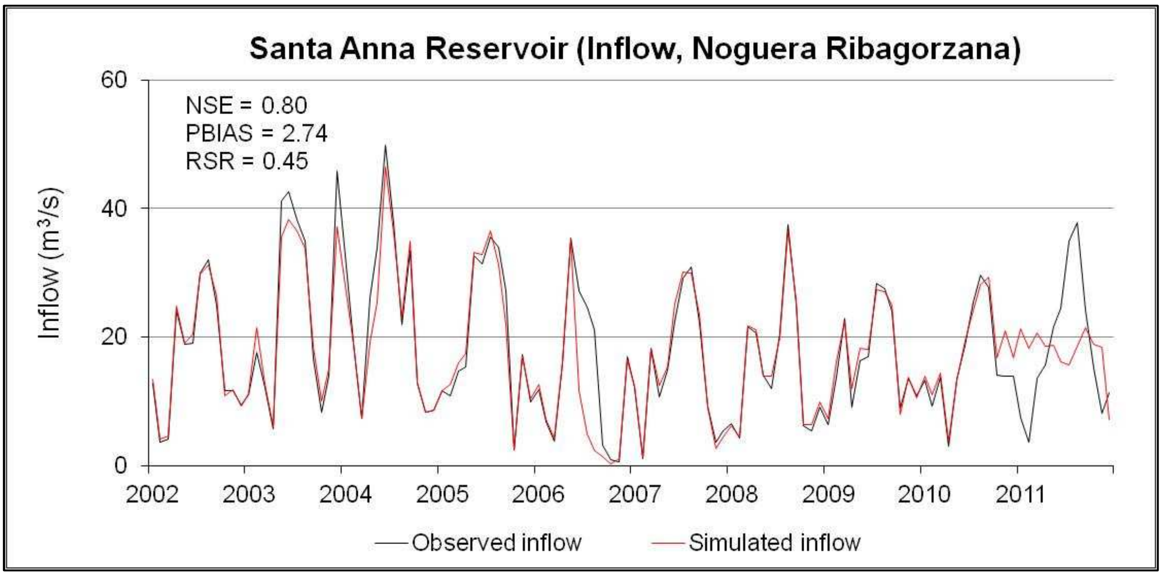
Santa Anna Reservoir (Inflow, Noguera Ribagorzana)
NSE = 0.80
PBIAS = 2.74
RSR = 0.45
Inflow (m³/s)
0
20
40
60
2002
2003
2004
2005
2006
2007
2008
2009
2010
2011
Observed inflow
Simulated inflow

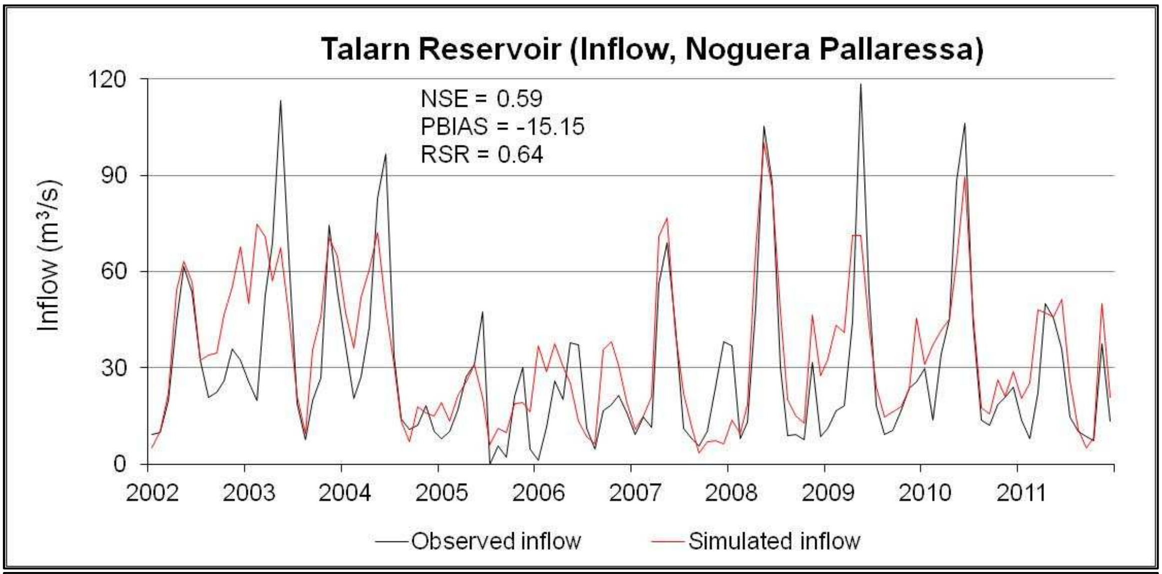
Talarn Reservoir (Inflow, Noguera Pallaressa)
NSE = 0.59
PBIAS = -15.15
RSR = 0.64
Inflow (m³/s)
0
30
60
90
120
2002
2003
2004
2005
2006
2007
2008
2009
2010
2011
Observed inflow
Simulated inflow

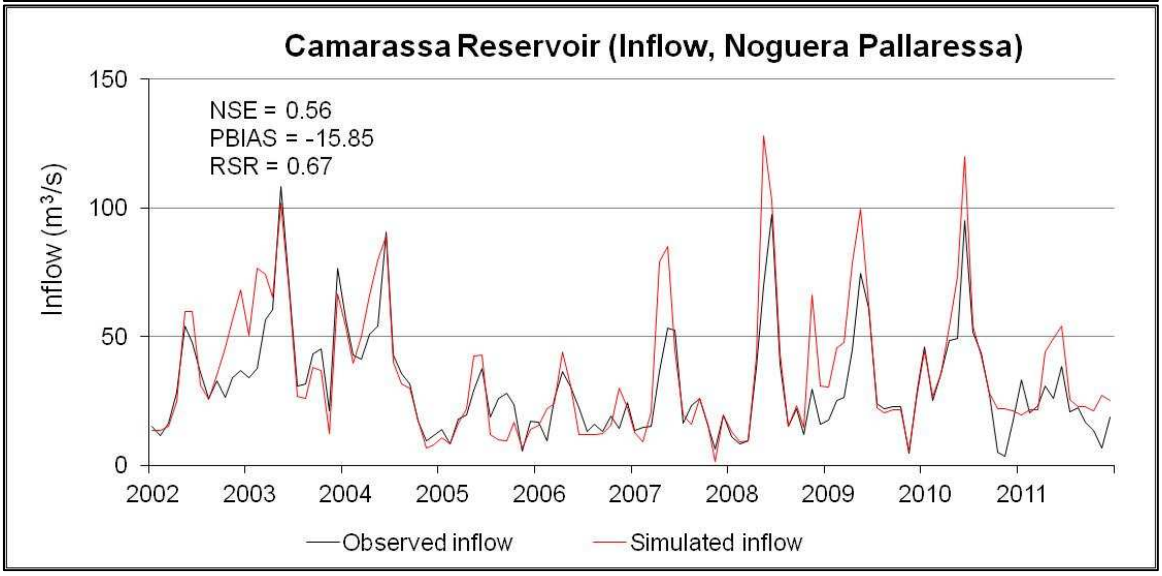
Camarassa Reservoir (Inflow, Noguera Pallaressa)
NSE = 0.56
PBIAS = -15.85
RSR = 0.67
Inflow (m³/s)
0
50
100
150
2002
2003
2004
2005
2006
2007
2008
2009
2010
2011
Observed inflow
Simulated inflow

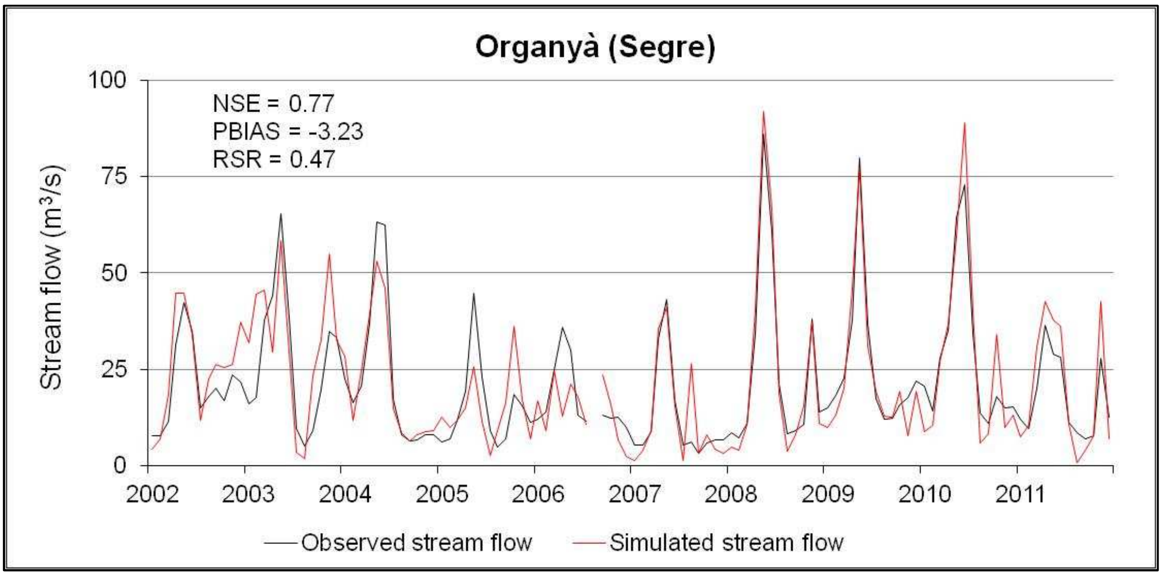
Organyà (Segre)
NSE = 0.77
PBIAS = -3.23
RSR = 0.47
Stream flow (m³/s)
0
25
50
75
100
2002
2003
2004
2005
2006
2007
2008
2009
2010
2011
Observed stream flow
Simulated stream flow

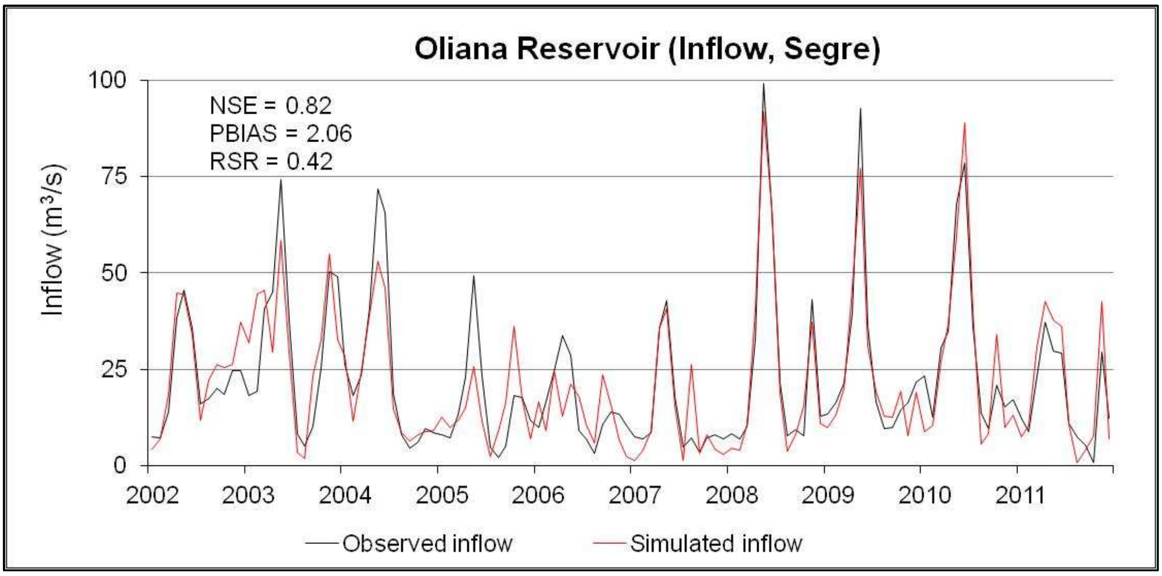
Oliana Reservoir (Inflow, Segre)
NSE = 0.82
PBIAS = 2.06
RSR = 0.42
Inflow (m³/s)
0
25
50
75
100
2002
2003
2004
2005
2006
2007
2008
2009
2010
2011
Observed inflow
Simulated inflow

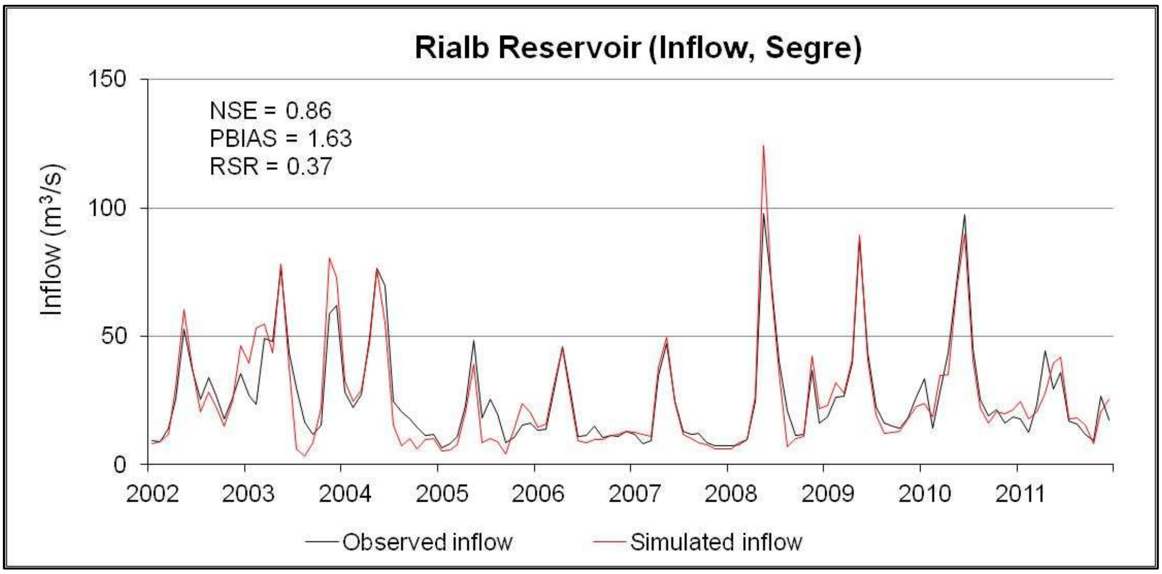
Rialb Reservoir (Inflow, Segre)
NSE = 0.86
PBIAS = 1.63
RSR = 0.37
Inflow (m³/s)
0
50
100
150
2002
2003
2004
2005
2006
2007
2008
2009
2010
2011
Observed inflow
Simulated inflow

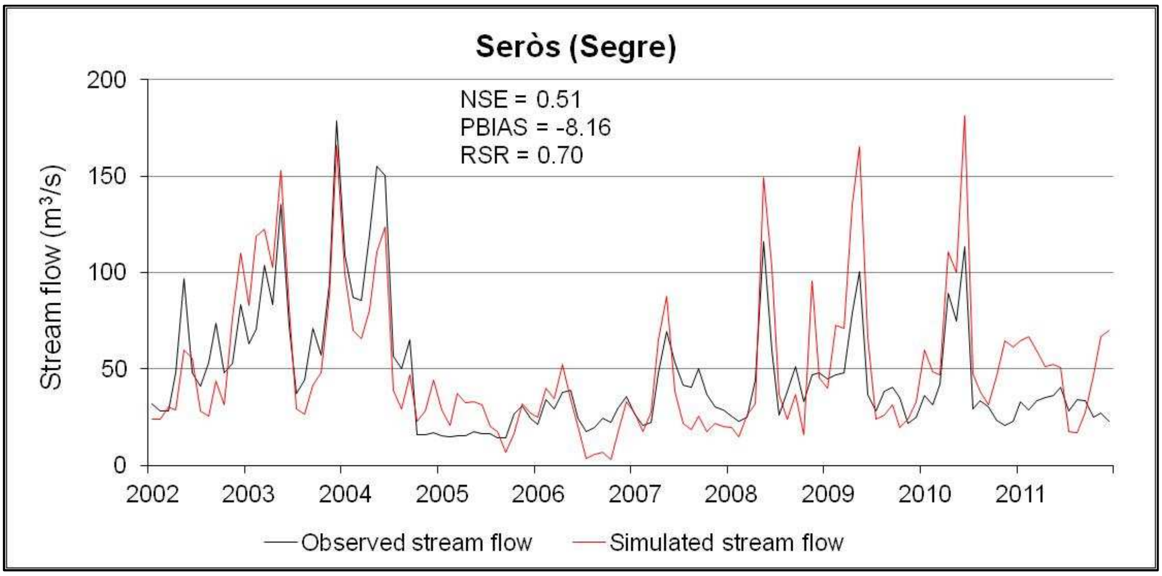

Figure 19. Calibration results: observed (black line) and simulated (red line) dam inflow or stream flow at eight points of the basin, ordered by rivers: Noguera Ribagorzana river: Pont de Suert (headwaters) and Santa Anna Reservoir; Noguera Pallaresa river: Talarn and Camarassa Reservoirs; Segre river: Organyà (headwaters), Oliana and Rialb Reservoirs, and Seròs (river mouth).

Table 16 compares simulated and measured dam inflow and stream flow data per gauging station. Simulations underestimated mean stream flow values in the Noguera Ribagorzana river (9.5% in Pont de Suert and 2.7 in Santa Anna Reservoir) and overestimated in the Noguera Pallaresa (15.1 and 15.9% in Talarn and Camarassa respectively). In Seròs, the river mouth of the Segre basin, the simulation overestimated stream flows in a 8.2% The NSE, PBIAS and RSR statistics show a majority of good or very good performance ratio for Noguera Ribagorzana and Segre gauging stations (except for Seròs). The Noguera Pallaresa was the most difficult to adjust.

	Simulated Qm (m^3/s)	Observed Qm (m^3/s)	Statistics		
			NSE	PBIAS	RSR
Pont de Suert (Noguera Ribagorzana)	11.60	12.81	0.68	9.47	0.57
Santa Anna Reservoir (Noguera Ribagorzana)	17.57	18.06	0.80	2.74	0.45
Talarn Reservoir (Noguera Pallaresa)	33.88	29.42	0.59	-15.15	0.64
Camarassa Reservoir (Noguera Pallaresa)	35.82	30.92	0.56	-15.85	0.67
Organyà (Segre)	22.02	21.33	0.77	-3.23	0.47
Oliana Reservoir (Segre)	21.88	22.34	0.82	2.06	0.42
Rialb Reservoir (Segre)	26.07	26.50	0.86	1.63	0.37
Seròs (Dam)	50.57	46.75	0.51	-8.16	0.70

Table 16. Calibration results at a monthly time step: dam inflow or stream flow values (Qm) from both simulated and observed data and statistics in each gauging station. Yellow color identifies satisfactory performance ratio for the statistic, light green good and dark green very good, following Moriasi et al. (2007).

4.5. Validation of the hydrological models

The validation measures the model prediction capacity through the comparison between simulated results and observed data in a time period different from the calibration. At this point we only have validated the Muga basin, but the other validation will come soon.

4.5.1. RHESSys model

Validation of Muga basin

The validation was arranged for the period 1991-2001 for the Boadella-Darnius Dam inflow (m^3/s) as is showed in Figure 20. The validation shows a very good result except the period 1998-2000, where the streamflow is very low and the model trends to overestimate. The statistics reveals that RHESsys reproduces the dam inflow quite well, being good/very good as is explained in Moriasi et al. 2007.

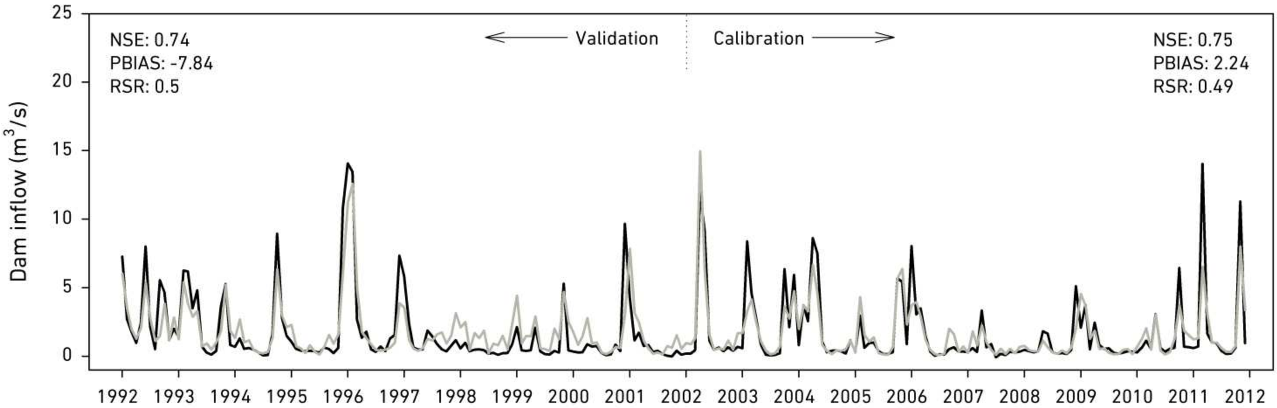

Figure 20. Simulated (in grey) and Observed (in black) data after parameter calibration.

In Figure 21 is showed the mean monthly precipitation, observed and simulated streamflow. The model can predict in a very good way the streamflow seasonality. Both of them reflect the good correlation between precipitation and streamflow, especially in the calibration period. Although the precipitation shows different patterns between the two periods, the model can predict how the streamflow responds to this variability. The main difference between calibration and validation is that in the first, the streamflow is underestimated, unlike the way it works in the validation.

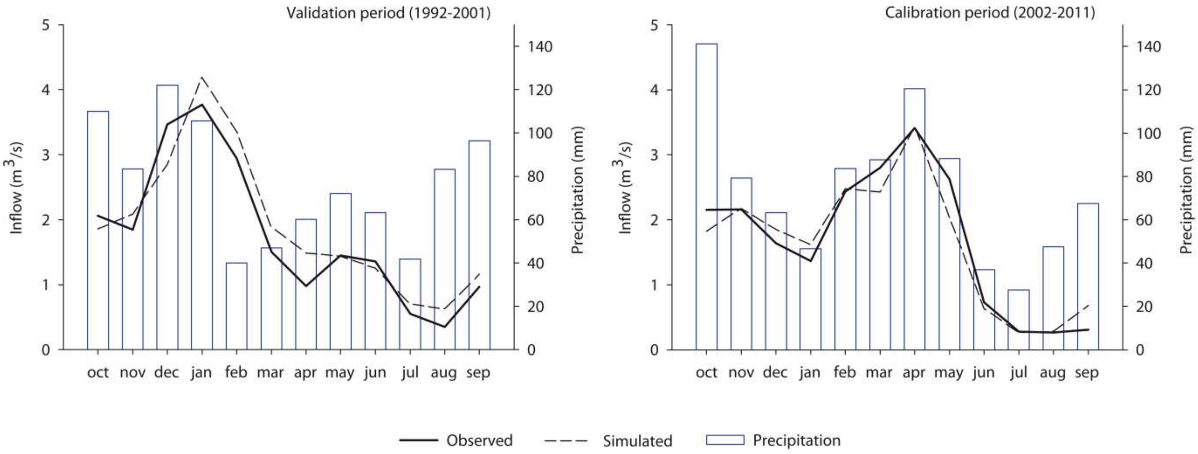

Figure 21. Mean monthly streamflow and precipitation for calibration/validation periods.

The validation at this point (dam inflow) has a great value in this basin, because the Boadella-Darnius dam was built to manage the water resources of the basin, characterized with a high tourism and agricultural pressure in an area that has changed from being considered a basin without water resources problems to be a basin with a high drought sensitivity.

4.5.2. SWAT model

<u>Validation of Muga basin</u>

The validation was performed within the 1991-2001 period (11 years). Land cover map and water abstraction data were as in the calibration. Reservoir was simulated at monthly time-step and outflow data was obtained from ACA (available monthly data from 1971-2008).

Figure 22 shows validation outputs for monthly stream flow and dam inflow (m^3/s) for the same three gauging stations of the calibration. The graphical comparison between simulated and observed data shows a fit less satisfactory than the calibration. It is difficult to interpret the validation outputs since water abstraction data was not adapted to the period due to the lack of data. Besides, daily reservoir outflows were not available and validation outputs after Boadella reservoir may be wrong. But then, we can use Boadella Reservoir (Inflow) as indicator of the model validation. In this case, simulations overestimated stream flow values in a 33.5%. The NSE and and RSR statistics show a very good performance ratio for Boadella and satisfactory for Peralada and Castelló. PBIAS statistic was unsatisfactory for the three gauging stations (Table 17).

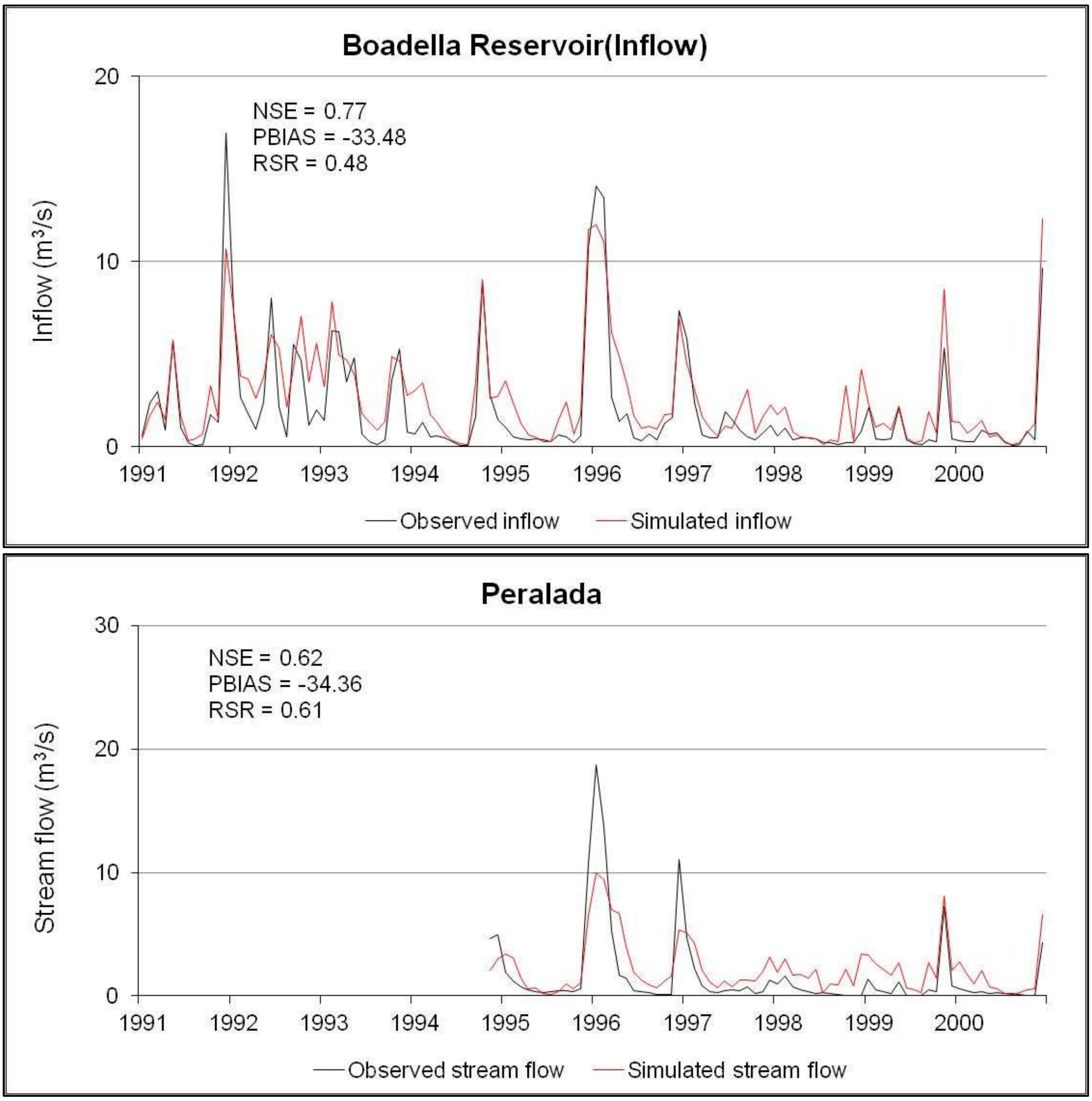

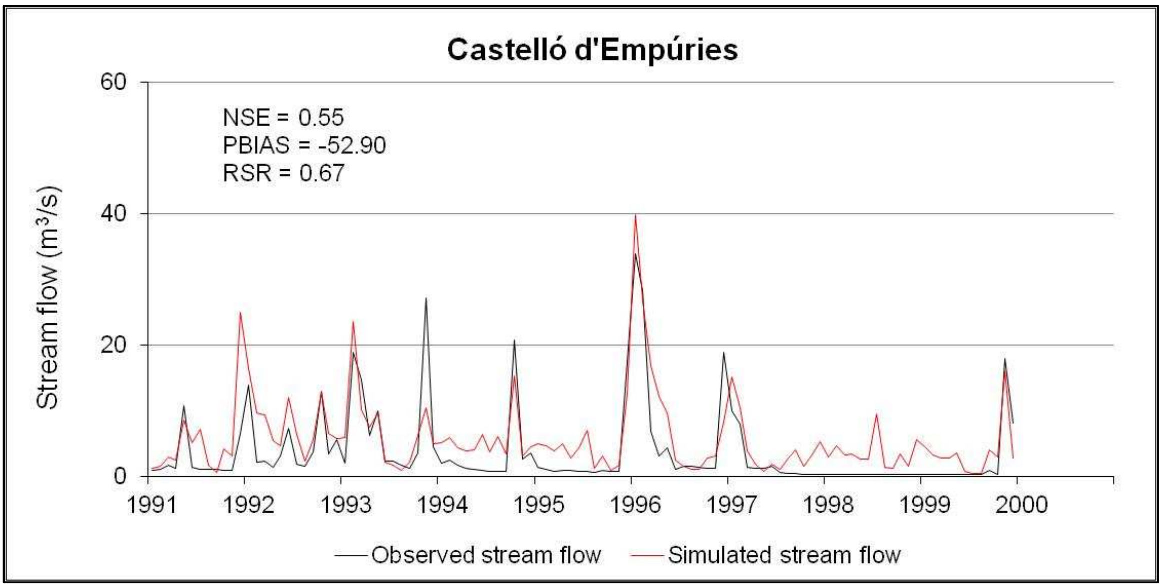

Figure 22. Validation results: observed (black line) and simulated (red line) dam inflow or stream flow at three points of the basin: Boadella reservoir (headwaters), Peralada (Llobregat d'Empordà) and Castelló d'Empúries (river mouth).

	Simulated Qm (m^3/s)	Observed Qm (m^3/s)	Statistics		
			NSE	PBIAS	RSR
Boadella Reservoir	2.49	1.86	0.77	-33.48	0.48
Peralada	2.07	1.54	0.62	-34.36	0.61
Castelló d'Empúries	5.80	3.79	0.55	-52.90	0.67

Table 17. Validation results at a monthly time step: dam inflow or stream flow values (Qm) from both simulated and observed data and statistics in each gauging station. Orange color identifies unsatisfactory performance ratio for the statistic, yellow identifies satisfactory, light green good and dark green very good, following Moriasi et al. (2007).

4.6. Impact of climate and socioeconomic scenarios on hydrology

Once that we have our hydrological models calibrated and validated and the climate and socioeconomic scenarios defined and created, we combined all these information to assess the impacts of these scenarios on the water resources of the three case-study basins.

For this purpose, we introduced the climate change scenario (RCP4.5), the land cover scenarios (AFOR and FIREFOR) and the socioeconomic scenarios (AFOR+RATUS, AFOR+DEMINC, FIREFOR+RATUS, FIREFOR+DEMINC) into the hydrological models. Results were analyzed for the reference period (2002-2011) and for two time horizons (short term 2021-2030 and long term 2041-2050) at two spatial areas (headwaters and river mouths). The results are available at *Deliverable 14 Impacts of climate and global change on the ecological, hydrological and agriculture systems in the LIFE MEDACC case study basins* (Pascual et al. 2016).

5. Agriculture modelling

5.1. Introduction

Agricultural production is sensitive to variations in climate and can be expected to be influenced markedly by climate change (Rotter et al. 2013). Within the context of climate change and the expected increase in extreme events (IPPC 2014) we could therefore expect a rapid evolution of the regional suitability of specific crops. Consequently, assessing which crops are adequate for the climate of a given area appears essential for planners, land managers, farmers and plant breeders who can then propose and apply adaptation strategies to improve and sometimes maintain agriculture in some regions (Caubel et al. 2015)

The consequences of global warming impacts on agriculture, water resources management and ecosystems pose particular concern in the Mediterranean climates in the transition zone between the arid climate of North Africa and the temperate climate of central Europe. The Mediterranean region, characterized by a double stress (long and hot summers and cold or very cold wet winters; Terradas and Savé, 1992), is potentially highly vulnerable to existing adverse trends of warming and rainfall reduction and will likely be the region within Europe to firstly experience severe economical and sociological consequences from climate change. Management and allocation of water are thus particularly sensitive issues in the local agricultural context (Valverde et al. 2015).

To assess agriculture suitability, net irrigation needs (NIR) of major crops was estimated in the three basins for the reference period and two future periods under climate change conditions.

Moreover, to better understand and manage the risks posed by climate change a set of agroclimatic parameters that are capable of indicating the consequences of climate change for crop production and growing cycle (Tian et al., 2013) was calculated.

A general diagram (Figure 27) of the methodology performed in the agriculture modelling can be seen in Annex 2.

5.2. Methodology for the estimation of net irrigation requirements (NIR)

Daily crop potential evapotranspiration (ETc, mm day^{-1}) was calculated for major crops (those occupying more than 1% of agriculture surface at sub-basin level) in the three basins according to FAO procedure in FAO-56 document (Allen et al., 1998): first, daily potential evapotranspiration (ET_0, mm day^{-1}) was calculated as usual using the FAO Penman-Monteith equation from the meteorological parameters regionalized by SWAT at the sub-basin level (see section 4.4.2); second, ETc was calculated for each crop in each sub-basin from the general ET_0 of the sub-basin and a crop coefficient (Kc, dimensionless) modified by crop phenological stage, as:

$$ETc=ET0*Kc$$

Kc coefficients of most of the major crops used in the three basins were those presented in ACA and IRTA (2008), a compilation of different studies related to Kc coefficients from different crops in Catalonia (Girona et al. 2002, 2004, 2011, Marsal et al. 2013). Kc coefficients are given in relation to accumulated growing degree days (GDD) and were adapted to different base temperatures depending of the crop typology. Because ACA and IRTA (2008) assume 7.2ºC as a base temperature for all the crops, GDD were recalculated to the most suitable base temperature for each crop (Annex 2, from Figure 28 to Figure 40). For example, a base temperature of 5ºC was adopted for winter cereals such as wheat or barley and a base temperature of 10ºC for vines or olives. Following consistency with ACA and IRTA (2008) the recalculation of GDD were performed using temperature data from different weather stations from Catalonia and Aragon for the years 2005, 2006 and 2007.

Since, the reference surface considered for ET_0 is a hypothetical grass reference crop that resembles an extensive surface of green, well-watered grass of uniform height, actively growing and completely shading the ground (Allen et al. 1998), ETc of grassland and other herbaceous crops like ray-grass were consider to be equal to ET_0. In the case of Alfalfa and Olive, ETc was estimated with a fixed Kc value 0.78 and 0.65, respectively. Those Kc coefficients of major crops not undescribed in ACA and IRTA, 2008 were adopted from (Allen et al. 1998).

Under FAO procedure, ETc corresponds to the crop evapotranspiration under standard conditions. These standard conditions refer to crops grown in large fields under excellent agronomic and soil water conditions. However, ETc may actually be limited by available water coming from rain and soil water content. In this case, ETc is reduced to the so called actual evapotranspiration (ETa, mm $month^{-1}$). Then, for the land surface occupied by each crop in each sub-basin, a monthly water balance was recurrently calculated from effective precipitation (Pef, mm $month^{-1}$), ETa of previous month and soil water content (SWC, mm $month^{-1}$) surplus (water remaining in the soil at the end of the previous month), as follows:

$$\text{If } ETc > SWC_{\text{previous month surplus}} + Pef; \quad \begin{cases} ETa = SWC_{\text{previous month surplus}} + Pef \\ \text{and} \\ SWC_{\text{surplusfor the next month}} = 0 \end{cases}$$

$$\text{If } ETc < SWC_{\text{previous month surplus}} + Pef; \quad \begin{cases} ETa = ETc \\ \text{and} \\ ^{(1)}SWC_{\text{surplusfor the next month}} = SWC_{\text{previous month surplus}} + Pef - ETc \end{cases}$$

(1) In this calculation, a maximum SWC was established as readily available water (RAW, water that a crop can extract from the root zone without suffering water stress, mm). RAW was calculated for each crop and sub-basin from Total Available Water for each basin (TAW, see section 4.3.4 Soil data) and a depletion factor (p) for each crop:

$$RAW = p\ TAW$$

Theoretically, p ranges from 0 to 1. However, it normally varies from 0.30 for shallow rooted plants at high rates of ETc (> 8 mm d-1) to 0.70 for deep rooted plants at low rates of ETc (< 3 mm d-1). A value of 0.50 for p is commonly used for many crops. Values for p are listed in Table 22 in Allen et al. (1998).

Hence, after calculation RAW, SWC surplus for the next month is calculated as:

$$\text{if } SWC_{\text{previous month surplus}} + Pef > RAW; \quad SWC_{\text{surplusfor the next month}} = RAW$$

$$\text{if } SWC_{\text{previous month surplus}} + Pef < RAW; \quad SWC_{\text{surplusfor the next month}} = SWC_{\text{previous month surplus}} + Pef$$

Effective precipitation (Pef) was calculated following the method defined in the next equation, originating from the USDA Soil Conservation Service (USDA-SCS) (Clarke 1998), where Pt is the total monthly precipitation (mm) (Valverde et al. 2015):

$$\text{Pef} \quad \begin{cases} Pef = \frac{Pt(125-0.2Pt)}{125} \quad ; (Pt<250mm) \\ Pef = 125 + 0.1Pt \quad ; (Pt\geq 250mm) \end{cases}$$

Finally, the monthly net irrigation requirements of the crops (NIR, mm $month^{-1}$) were calculated as the difference between ETc and ETa:

$$NIR = ETc - ETa$$

NIR does not take in consideration water inefficiencies coming from irrigation system or water pipes.

5.3. Agroclimatic Indicators

Agroclimatic indicators related with phenology were calculated to assess crop development and growth in crops for the reference period and short and long term under RCP4.5 climate change scenario. A set of general indicators affecting different crops were estimated (Savé et al., 2012): (i) number of days with temperature lower than 0 ºC in March and April to estimate the effect of low temperature after germination of cereals like maize and flowering in woody crops; (ii) number of days with temperature higher than 30 ºC in July and August to estimate the effect of high temperatures in blossom and grain formation of cereals like maize; (iii) days with temperatures higher than 35 ºC in July and August to estimate heat effect of fruit in orchards and (iv) day when daily mean temperature begins to be higher than 5ºC (for winter cereals, fruit orchards, etc.) and 10ºC (for maize, sunflower, sorghum, olive, grapevine, etc.) suggesting the beginning of the cycle of most of the crops.

Some crop-specific indicators were estimated for some of the most relevant major crops. In Maize: day when 2076 GDD and 2126 GDD (Tbase=10ºC) were reached from 1^{st} January to assess the cycle duration of FAO cycle grain maize varieties of 600 and 700, respectively. In grapevine for Muga and Segre Basins: days to reach GDD accumulated from 1^{st} January to each phenological stage. In apple for lower Ter basin: flowering time estimation following Funes et al., (2016). In Wheat: days to reach GDD (Tbase=5ºC) accumulated from 1^{st} January to each phenological stage (Spike: 714 GDD; Anthesis: 1295 GDD; Maturation: 1956).

5.4. Input data

5.4.1. Agriculture land use map

A crop map at species level was created for each basin from mainly two sources: (i) Declaration of eligible agricultural area for Common Agricultural Policy payments of Government of Catalonia for 2013 (**DUN 2013**) and (ii) Farming Land Geographical Information System for 2013 (**SIGPAC 2013**, acronym in Spanish).

DUN 2013 is composed only by alphanumeric information, not vector data. Each agricultural plot presents information such as reference code, type of crop (species level), type of crop (crop group: arable land, orchards, citric, etc.), water regime, surface and other attributes.

SIGPAC 2013 is a geographical information system, vector data, composed by polygons that spatially represent the agricultural plots. Each feature has associated attributes as a reference code, type of crop (crop group), water regime, surface, slope, and other geographical attributes.

Both sources were related through the reference code of each agricultural plot by joining the alphanumeric information of DUN 2013 at the features of SIGPAC 2013 thus obtaining a crop map at species level (vector map).

Some problems were found when crossing both information sources:

- DUN 2013 presented multiple registrations for the same agricultural plot. The same plot could be registered more than once because it had two different owners or because it had more than one type of crop or by error. This problem was solved by eliminating duplicities and only considering the record for this plot with more surface declared hence leaving a single record per plot with a unique reference code. The multiple registrations in DUN 2013 for the basin studied only supposes 10% of declared agricultural surface.
- There were some agricultural plots of SIGPAC 2013 without declaration in DUN2013. Those plots without declaration in DUN were plots with small surface supposing 6.6% of the agricultural land. To this plots a type crop (species level) was assigned by estimating the most likely crop from the information at municipality level.
- Some inconsistences were found between both sources of information mainly in the common main fields: type crop (crop group) and water regime. These inconsistences were solved giving priority always to DUN information because this information is supposedly

updated annually by owners. These inconsistences supposed less than 1% of declared surface.

- Some geometry problems in SIGPAC 2013 like records without geometry, polygons with self-interactions or empty spaces were solved using the ArcGIS tool Repair geometry.

DUN 2013 and SIGPAC 2013 cover the Catalan surface of the basins (most of the basins surface), however Segre basin slightly extends in its upper course to France and Andorra and Muga basin to France territory. In both cases, different regional sources were used depending of the nationality of the territory. For the French zone we used two sources of information: the French RGP 2012 (acronym in French of Graphic plot register) and Corine 2006. For the Andorran zone we used the farm register information of the Andorra government for the year 2014. Moreover, Segre basin extends to Aragon territory. In this case, the crop map was completed from SIGPAC (2014) and Declaration of eligible agricultural area for Common Agricultural Policy payments of the Government of Aragon (2014) (Figure 23).

Figure 23. Basins and political delineation of territory.

5.4.2. Soil data

For each basin the soil class map (see in section 4.3.4) was intersected with the sub-basin map and the crop map in order to calculate the surface of each soil class corresponding to the agricultural land in each sub-basin. In this way, we could estimate a soil class surface-weighted mean value of the agricultural soils attributes: **Maximun rooting depth of soil profile** (variable name in SWAT: SOL_ZMX, mm) and **Available water capacity of the soil layer** (variable name in SWAT: SOL_AWC, mm H2O/mm soil) for each sub-basin. The water available to the plant, also referred as available water capacity (AWC), is calculated by subtracting the fraction of water present at permanent wilting point (WP, the soil water content at soil matric potential of -0.033 MPa) from that present at field capacity (FC, the soil water content at soil matric potential of -1.5 MPa), AWC=FC-WP (Arnold et al., 2011).

By multiplying both values (SOL_ZMX and SOL_AWC) at sub-basin level, a mean value of soil water capacity was estimated and it is the value used in the monthly water balance (section 5.2) as the **maximum soil water capacity** (mm) or **Total Available Soil Water** (TAW).

5.4.3. Meteorological data

Some meteorological parameters at daily level were needed in order to estimate NIR and agroclimatic indicators: temperature, precipitation, relative humidity, solar radiation and wind speed. Temperature, precipitation and solar radiation were regionalized at subbasin level from the weather stations data and from climate change projections through SWAT modelling (see section 4.4.2). Relative humidity and wind speed are not so evenly recorded across weather stations. Both are important variables in order to estimate ET_0 following the modified Penman-Monteith methodology (Allen et al. 1998), which is currently the standard and widely recommended method to estimate ET_0 because of its higher accuracy (Lopez-Moreno et al. 2009), although its data demand is relatively high, making it suitable for computing evapotranspiration with data from automatic weather stations, but harder to use with global climate datasets which often provide a limited set of climate variables. However, in our case we were able to estimate both parameters through SWAT statistical methods for missing data.

5.5. Impact of climate scenarios on agriculture

The impacts of climate change on agriculture were evaluated estimating NIR and the set of agroclimatic indicators of major crops at the three basins and at the sub-basin level for the reference period (2002-2011) and for the both future period under climate change conditions: short term (2021-2030) and long term (2041-2050) (RCP 4.5; see section 2). The impacts of climate change on agriculture evaluate in this study only assess changes in climate conditions not socieconomical changes affecting crop distribution, i.e., agriculture modelling performed is based only in the crop distribution estimated by using DUN and SIGPAC information for the year 2013. The results are available at *Deliverable 14 Impacts of climate and global change on the ecological, hydrological and agriculture systems in the LIFE MEDACC case study basins* (Pascual et al. 2016).

6. Forest modelling

6.1. Introduction

In the current context, forests are experiencing an abiotic environment that changes much faster than during the past several hundred years. Abiotic factors determining forest dynamics range from temperature limitations in northern boreal and high mountain elevations, to water limitation in the continental and Mediterranean contexts, and include large-scale disturbances such as wind throw, insect infestations and fires. Changes in the climate may therefore have a wide range of effects across Europe (Lindner et al., 2010). Forest management across such large geographical scales thus needs to be adaptive to changing conditions. It is essential to develop and use tools able to explore forest ecosystems' responses to different climate change projections.

Several previous studies (Vayreda et al. 2012) remark than, despite Mediterranean forests are, in general, currently performing as carbon sinks, during the second half of this century, some of them may become net carbon sources. The main cause of this change would be driven by an increased aridity according to climate change scenario projections. Furthermore, for the same reason, the relative amount of evapotranspiration will be also increased due to a rising atmospheric evaporative demand. However, adaptive forest management to climate change would help to increase water use efficiency by forests, as well as to maintain positives its carbon balances.

In the other hand, one of the most important regional vulnerabilities of Mediterranean forests is the fire risk. Observational studies have found very consistent correlations between climatic variables and the rate of forest fire risk and the number of fires and burned area (Piñol et al. 1998). Future climate scenarios foreseen an increase in forest fire risks (Moriondo et al. 2006).

In this work we used GOTILWA+ model (Gracia et al. 2004), a forest growth process-based model that allows to explore the effects of different climate change scenarios on forests. The main aim is to explore the functional response until 2050 horizon of the MEDACC forest species (selected forests species in each MEDACC pilot area in the B2 Action) using this modelling tool. We also have used the Drought Code (DC) index of the Canadian Forest Fire Weather Index System to assess future fire risk in the forests of the three case-study basins.

6.2. Methodology

6.2.1. GOTILWA+ model

GOTILWA+ (Growth Of Trees Is Limited by Water www.creaf.uab.cat/gotilwa) is a process-based forest growth model that has been implemented to simulate the forest growth processes and to explore how these processes are influenced by climate, tree stand structure, soil properties, management techniques and climate change. It was iniatlly developed for Mediterranean forests but it has become a generalist tool which has been successfully applied to all tree species, deciduous or evergreen, in boreal, temperate or Mediterranean regions. GOTILWA+ simulates forest growth considering water dynamics the main driving factor in forest functioning. Water is, very often, the limiting factor for plant growth (Piñol et al. 1991, Joffre and Rambal 1993, Rodà et al. 1999).

GOTILWA+ describes production, carbon allocation and respiration processes and explores how these processes are conditioned by climate, forest structure, forest management and soil properties (Figure 24). Consequently, the model is an useful tool to test forest variable responses to input parameters.

Simulated processes in GOTILWA+ model are tree based. The forest is described as a population of individuals each of them having its particular size (DBH). The total population density (trees/ha) and the distribution of trees in DBH classes are used to define the initial structure of the population. It can only simulate one single species forest. Interaction between different tree species growing in a particular stand are out of the scope of GOTILWA+ and, consequently, it does not distinguish horizontal spatial heterogeneity.

In a standard simulation climatic data are daily analyzed. From the interaction between daily rainfall and the forest structure the amount of intercepted water by the canopy layer, throughfall and stemflow are also estimated. This effective rainfall increases the water stored in the soil which is used by the trees. The proportion of sapwood to heartwood, the leaf area of each tree and, consequently, the leaf area index (LAI) of the forest are all highly dependent on water availability in the model.

Evapotranspiration is related to temperature and water availability. Water availability is a limiting factor for growth and production. When soil moisture decreases then there is a tree water uptake reduction: stomatal conductance decreases as well as photosynthesis and transpiration.

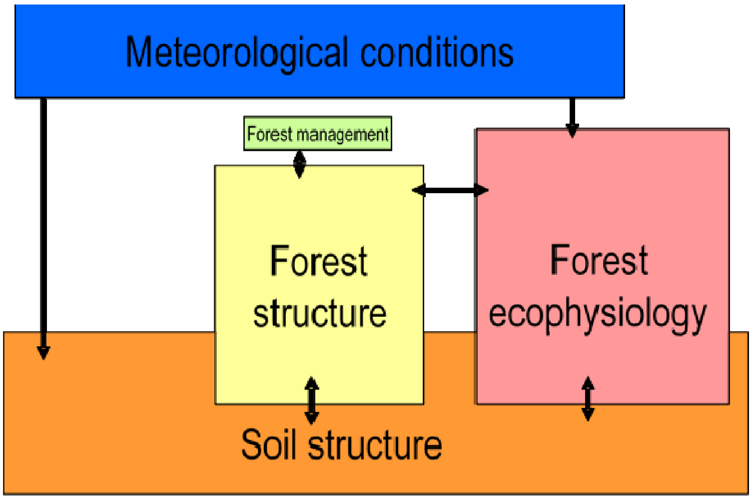

Figure 24. Main compartments and relationships considered by GOTILWA+.

The carbon uptake by the trees is computed by using the Farquhar model of photosynthesis (Farquhar and von Caemmerer 1982). The pool of carbon gained leads to an increase, primarily, in the mobile carbon stored in the plant. A fraction of this carbon compensates the maintenance respiration, while the remaining carbon, if any, constitutes the net primary production (NPP). Associated to the formation of new biomass components there is a metabolic cost which constitutes the growth respiration.

NPP allocation in GOTILWA+ is regulated by the pipe model theory (Shinozaki 1964) which considers a constant relationship between leaf area and sapwood area. The balance between the maintenance respiration, the NPP and the metabolic cost associated to the formation of new biomass, determines the processes of leaf formation and leaf fall, tree ring formation, the rate of change of sapwood into heartwood and, consequently, the changes in tree structure within each size class. These changes will affect in turn the hydrological fluxes which will subsequently take place in what might be described as a feed-back process (Figure 25).

The time resolution used in the model is: a) for physiological processes (Photosynthesis, Stomatal Conductance, Respiration) 1 hour time step. Integrated to produce daily values and b) for structural values (tree ring formation, biomass) 1 day time step. The output of the model is produced at three levels: daily, monthly and yearly.

GOTILWA+ has been successfully applied in different simulation experiments, showing a good performance in real data comparison and model benchmarking (Kramer and Mohren 2001, Sabaté et al. 2002, Kramer et al. 2002, Morales et al. 2005, Keenan et al 2009, Sabaté et al. 2014).

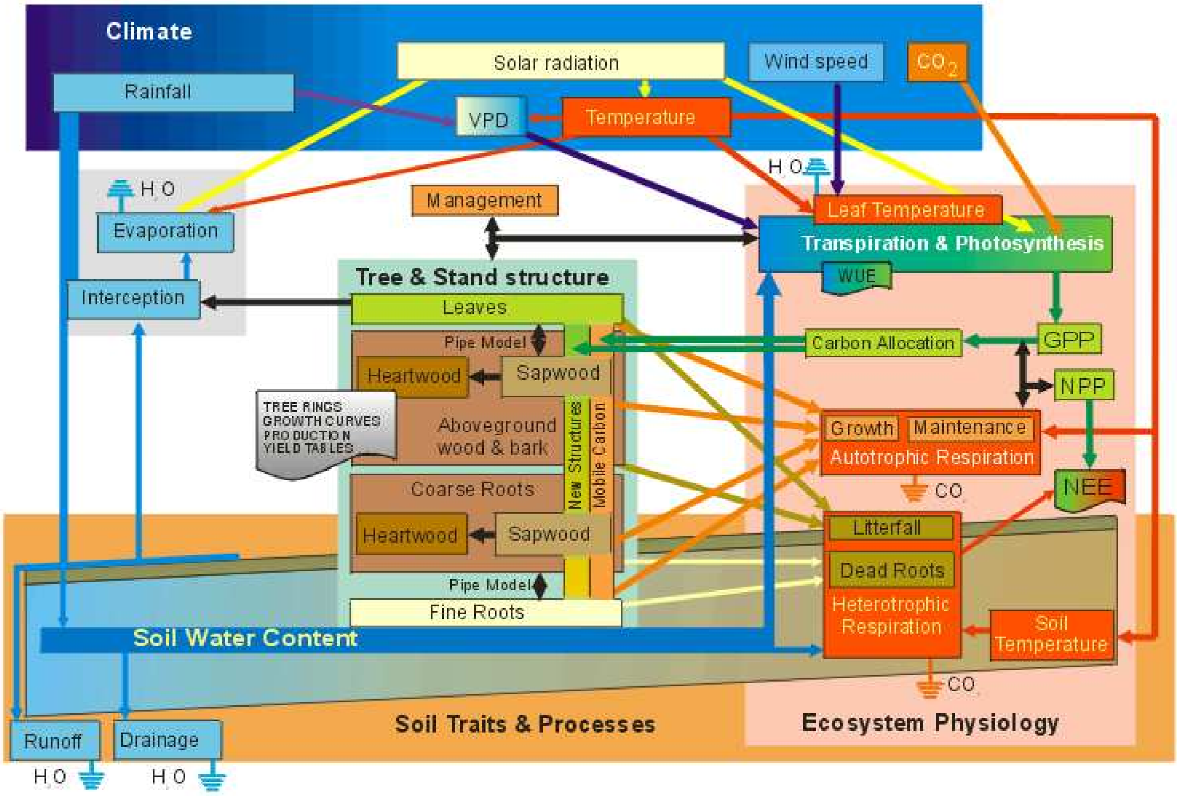

Figure 25. Schematic representation of the climate, physiological processes, soil traits, tree and stand structure and management regimes in the GOTILWA+ model.

6.2.2. Meteorological fire risk

We have adopted the Drought Code (DC) index of the Canadian Forest Fire Weather Index System (http://cwfis.cfs.nrcan.gc.ca/en_CA/background/summary/fwi).

The DC index is an estimator of accumulated drought of the forest combustible based on the maximum daily temperature and rainfall. Because it is estimated only with meteorological data, it is considered an estimator of the meteorological fire risk, and it does not take into account other drivers of fire risk, such as the forest structure, the slope, the extinction means … Recent studies in Catalonia establish a significant correlation between the DC index values and the exponential increase of the observed burned area. One of this studies (Loepfe et al. 2010) points out a threshold value of 600-800 DC to consider that the risk of a large fire is very high.

We have estimated the DC values for each sub-basin of the case-study basins, using as input data the RCP4.5 scenario. We obtained then daily DC values per subbasin. Afterwards, we have calculated the number of days per year and sub-basin with DC values higher than 800, when a risk of large fires exists. These data have been processed to make results understandable. We have calculated the mean number of days per year with DC>800 per sub-basin for three periods: reference (2002-2011), short term (2021-2030) and long term (2041-2050). Finally, we have assigned these mean values to the forest land cover existent in 2005 per sub-basin.

6.3. Input data

6.3.1. GOTILWA+ model

GOTILWA+ model requires different type of basic input parameters: (1) some of them refer to the structure and ecophysiology of plants, (2) some are descriptors of environmental conditions (climatic and topographic data), and finally (3) those parameters related to soil water and carbon fluxes. Optionally, the model can incorporate information on forest management regimes.

Data from the initial forest structure comes from field inventories in pilot sites (see *Deliverable 11. Description of the demonstrative adaptation measures implemented in the project*): the number of trees per hectare and their distribution in DBHs classes. The functional parameters (related to the forest cover ecophysiological responses) include information about photosynthesis and stomatal conductance. For each species these parameters are derived, either from the literature or from field measurements.

Soil information includes parameters related to the functions describing soil hydrological flows and carbon fluxes. In the model, soil is divided into two layers: the organic layer and the mineral one with a transfer rate between them. Hydrologically, the soil is a single compartment with homogeneous properties that determine the water stored in soil (Table 18).

Climate data include daily values of maximum and minimum temperatures (ºC) precipitation (mm day -1), solar radiation (MJ day-1), average wind speed (m s-1) and the vapour pressure deficit measured at dawn (kPa) (Table 19). The model is able to estimate these last two variables if they are not available or incomplete. The model also includes annual atmospheric CO_2 concentration data.

Process	Parameter	Symbol	Units
Soil Carbon Fluxes	Initial SOC in organic horizons		g/cm^2
	Initial SOC in mineral horizons		% of dry weight
	Bulk density		g/cm^3
	Decomposition rate of OM in LF h.	k(LF)	day^{-1}
	Decomposition rate of OM in AB h.	k(AB)	day^{-1}
	Soil temperature effect factor	Q10	---
	LF to AB transfer rate	$t_{o \Rightarrow m}$	---
		W min	mm
		W max	mm
Soil Hydraulic Conductivity	Hydraulic gradient		m/m
	Soil Hydraulic Conductivity		m/day
	Mean Soil Depth		m
	Minimum Water Usable		mm/m
	Stones volume		%

Table 18. Components of the soil hydraulic conductivity and soil organic matter.

	Variables	Symbol	Units
Climate	Solar radiation	Q	MJ/m2/day
	Max. Daily temperature	Max T	ºC
	Min. Daily temperature	Min T	ºC
	Rainfall	P	mm/day
	Wind speed		m/s
	CO2		ppm
	Vapour Pressure Deficit	VPD	kPa

Table 19. Climate variables

<u>Initial parameterization of ecophysiological processes</u>

Most of the functional and ecophysiological parameter values have been obtained or derived from previous work where the selected species (*Quercus ilex*, *Pinus nigra* and *Pinus sylvestris* have been simulated (Table 20). Theses reference values for these and other species, as well as its biological significance, can be reviewed in www.creaf.uab.cat/gotilwa+

Parameters	Symbol	Units	Q. ilex	P. nigra	P.sylvestris
LEAF PHOTOSYNTESIS					
Maximum rate of carboxilation at 25ºC	V_c max	µmols m^{-2} s^{-1}	62	93	90
Activation energy of V_c max	E_a	J mol^{-1}	75330	72000	75330
Intercellular partial pressure of CO_2	C	ppmv	222500	222600	222500
Maximum rate of oxygenation at 25ºC	V_o max	µmols m^{-2} s^{-1}	13.02	19.53	18.9
Activation energy of V_o max	E_a	J mol^{-1}	75330	72000	75330
Intercellular partial pressure of O_2	C	ppmv	222500	222600	222500
Potential electron transport rate	J max	µmols m^{-2} s^{-1}	115	115	150
Activation energy of J max	E_a	J mol^{-1}	57000	42000	57000
Curvature parameter of J max	E_d	J mol^{-1}	220000	220000	220000
Electron-transport temperature response parameter	S	J mol^{-1} K^{-1}	710	710	710
Curvature of response of electron transport to irradiance	ψ	An/PPFD	0.7	0.7	0.7
Michaelis-Menten constant of Rubisco for CO_2 at 25ºC	K_c	Pa	404	404	404
Activation energy for K_c max	E_a	J mol^{-1}	84200	59400	84200
Michaelis-Menten constant of Rubisco for O_2	K_o	Pa	248000	248000	248000
Activation energy for K_o max	E_a	J mol^{-1}	15200	36000	15200
Dark respiration rate at 25ºC	R_d	µmols m^{-2} s^{-1}	0.63	0.7	1.35
Temperature effect factor at 25ºC	Q_{10}	--	2	2	2
STOMATAL CONDUCTANCE					
Residual (Cuticular) conductance		µmols m^{-2} s^{-1}	0.01	0.01	0.01
Leuning Constant	g1	--	10.5	10.5	10.5
Factor of gs vs VPD responses	gsDO	kPa	1.5	1.5	1.5
SWC at which gs=0	Sgso	m^3 m^{-3}	5	5	5
SWC at which gs=gsmax	Sgsmax	m^3 m^{-3}	45	45	45
Leaf characteristical dimension	D	m	0.04	0.002	0.002
X parameter (ellipsoidal distribution)	X	v h^{-1}	1.46	0.92	20
Hypostomatous/Amphistomatous			Hypo	Amphi	Amphi

Table 20. Photosynthetic parameters and stomatal conductance parameters used in initial parametrization for the simulation of the selected species (Quercus ilex, Pinus nigra and Pinus sylvestris)

Climate

For this simulation experiment RCP4.5 climate scenario was used. These data were obtained from SWAT hydrological model outputs, which makes an estimation of the climate scenario per sub-basin. As it was explained in section 4.4.2, SWAT model takes the data from the meteorological station nearest the centroid of each sub-basin. These data is then corrected for the effects of topography using GIS techniques. The outputs are daily series of meteorological variables (precipitation, minimum and maximum temperature, solar radiation and wind), corrected by the altitude and fulfilled if gaps are existent.

Soil

Soil data and hydrological characteristics for each simulated site were obtained from the soil map created in the project for each river basin and soil surveys in the pilot experiment sites (Vicente-Serrano et al. 2014).

Forest structure

GOTILWA+ has simulated the forest dynamics for each forest selected in the pilot sites. Initial forest structure data comes from field inventories in pilot sites (see *Deliverable 11. Description of the demonstrative adaptation measures implemented in the project*). It includes DBH class distribution of the trees and other structural parameters. Initial parameterization (Table 20) was assigned according to the dominant species of each site (Requesens, Montesquiu and Solsonès).

Model benchmarking

Given the difficulties in validating GOTILWA + with instrumental data, a benchmarking exercise was performed using model outputs from GOTILWA+ and SWAT. Actual evapotranspiration results from the forest model were compared with the same variable simulated by SWAT for the same site cover. Actual evapotranspiration in GOTILWA+ model is estimated using Penman-Monteith method.

The benchmarking exercise was satisfactory performed, with a high degree of convergence between the results provided by the two models, with correlation coefficients between the results of the two models for the reference period (2002-2011) of 0.92 (Figure 26).

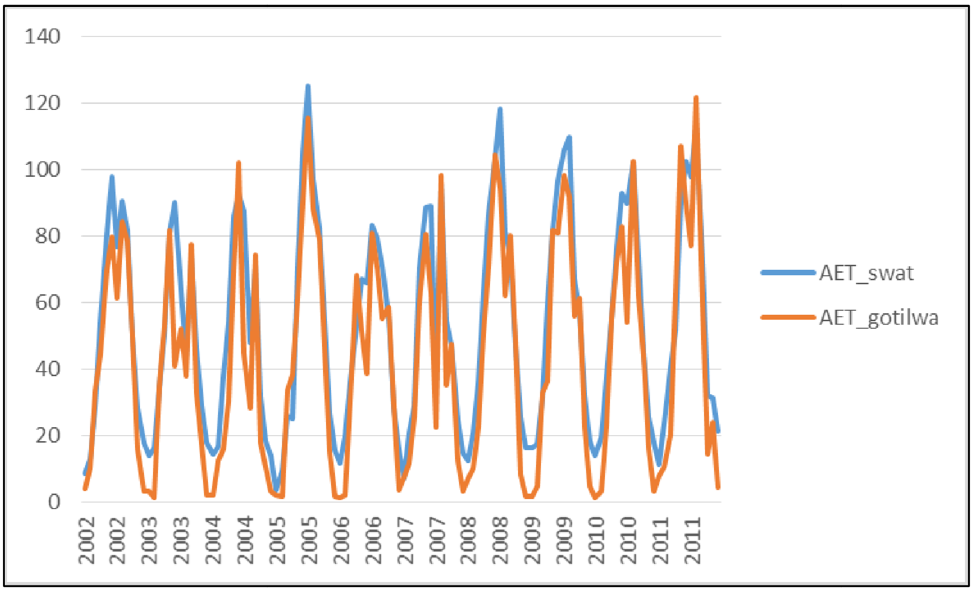

Figure 26. Model benchmarking between SWAT and GOTILWA+ models for actual evapotranspiration (AET) in Ter river basin (Montesquiu site).

6.3.2. Meteorological fire risk

Input data include daily precipitation and maximum temperature for the RCP4.5 climate scenario. These data were obtained from SWAT hydrological model outputs, which makes an estimation of the climate scenario per sub-basin. As it was explained in section 4.4.2, SWAT model takes the data from the meteorological station nearest the centroid of each sub-basin. These data is then corrected for the effects of topography using GIS techniques. The outputs are daily series of meteorological variables (precipitation and minimum and maximum temperature), corrected by the altitude and fulfilled if gaps are existent. Forest areas per sub-basin were identified using the land cover map of 2005 (Figure 6).

6.4. Impact of climate scenarios on forests

The impacts of climate change on forests were evaluated inducing climate change into the GOTILWA+ model and estimating future daily DC values per sub-basin for the climate series. Results were analyzed for the reference period (2002-2011) and for two time horizons (short term 2021-2030 and long term 2041-2050). The impacts of climate change on forest evaluate in this study only assess changes in climate conditions not socieconomical changes affecting forest distribution or species changes.The results are available at *Deliverable 14 Impacts of climate and global change on the ecological, hydrological and agriculture systems in the LIFE MEDACC case study basins* (Pascual et al. 2016).

7. References

Abbaspour KC (2013) SWAT-CUP 2012: SWAT Calibration and Uncertainty Programs - A User Manual. Switzerland: EAWAG.

ACA, IRTA (2008) Pla per a l'eficiencia en l'ús de l'aigua per a reg agrícola. Agencia Catalana de l'aigua and Institut de recerca i tecnología agroalimentaria. Government of Catalonia.

Allen RG et al. (1998) Crop evapotranspiration guidelines for computing crop water requirements. FAO Irrigation and Drainage Paper 56. FAO, Rome, p. 300.

Archer KJ, Kimes RV (2008) Empirical characterization of random forest variable importance measure. Computational Statistics & Data Analysis 52(4), 2249-2260.

Arnold JG, Srinivasan R, Muttiah RS, Williams JR (1998) Large-area hydrologic modeling and assessment: Part I. Model development. Journal American Water Resources Association, 34(1), 73-89.

Arnold JG et al. (2011) Soil and Water Assesment Tool. Input/Output File Documentation. Version 2009. Texas Water Resources Institute Technical Report No.365. Texas A&M University System.College station, Texas 77843-2118.

Arnold JG, Kiniry JR, Srinivasan R, Williams JR, Haney EB, Neitsch SL (2012) Input / Output Documentation – Version 2012 – Soil & Water Assessment Tool. Texas Water Resources Institute, TR-439.

Band, L.E., Patterson, P., Nemani, R. and Running, S.W., 1993. Forest ecosystem processes at the watershed scale: incorporating hillslope hydrology. Agricultural and Forest Meteorology, 63: 93-126.,

Barrera-Escoda A, Cunillera J (2011) Climate change projections for Catalonia (NE Iberian Peninsula). Part I: regional climate modeling. Tethys, 8, 75–87.

Bates BC et al. Eds (2008) Climate change and water. Geneva: IPCC Secretariat, Technical Paper of the Intergovernmental Panel on Climate Change Breiman L (2001). Random forests. Machine Learning 45(1), 5-32.

Brotons L, Aquilué N, de Cáceres M, et al (2013) How fire history, fire suppression practices and climate change affect wildfire regimes in Mediterranean landscapes. PLoS One 8:e62392.

Burriel JA, Ibáñez JJ, Pons X (2001) El Mapa de Cubiertas del Suelo de Cataluña: Herramienta para la gestión y la planificación territorial. In III Congreso Forestal Español.

Caubel J, García de Cortázar-Atauri I, Launay M, Noblet-Ducoudré N, Huard F, Bertuzzi P, Graux AI (2015) Broadening the scope for ecoclimatic indicators to assess crop climate suitability according to ecophysiological, technical and quality criteria. Agricultural and Forest Meteorology 207:94-106.

Christensen, L, Tague, C and Baron, J. (2008). Spatial patterns of simulated transpiration response to climate variability in a snow dominated mountain ecosystems. Hydrological Processes, 22: 3576-3588.

Clarke D (1998) CROPWAT for Windows: User Guide. FAO, Rome.

Clarke L, Edmonds J, Jacoby H, PitcherH, Reilly J,Richels R (2007) CCSP Synthesis and Assessment Product 2.1, Part A: Scenarios of Greenhouse Gas Emissions and Atmospheric Concentrations.U.S. Government Printing Office.Washington, DC.

CREAF (2009). Mapa de cobertes del sòl de Catalunya v4. Centre de Recerca Ecològica i Aplicacions Forestals, Departaments d'Agricultura, Ramaderia, Pesca, Alimentació i Medi Natural, Interior i Territori i Sostenibilitat. Generalitat de Catalunya. http://www.creaf.uab.es/MCSC/

EEA, European Environment Agency (2012) Climate change, impacts and vulnerability in Europe. Copenhagen: European Environment Agency.

Farquhar GD, Von Caemmerer S. (1982) Modeling of photosynthetic response to environment. In: Lange OL, Nobel PS, Osmond CB, Ziegler H (eds). Encyclopedia of plant physiology, Vol 12B, Physiological Plant Ecology II, Water relations and carbon assimilation. Springer, Berlin, pp 549-587

Funes I, Aranda X, Biel C, Carbó J, Camps F, Molina AJ, de Herralde F, Grau B, Savé R (2016) Future climate change on apple flowering data in a Mediterranean Subbasin. Agricultural Water Management 164:19-27.

Gassman PW, Reyes MR, Green CH, Arnold JG (2007) The soil and water assessment tool: Historical development, applications, and future research directions. Transactions of the ASABE, 50 (4), 1211-1250.

Gil-Tena A, Aquilué N, Duane A, de Cáceres M, Brotons L (2016) Mediterranean fire regime effects on pine-oak forest landscape mosaics under global change in NE Spain. Eur J Forest Res (2016) 135: 403. doi:10.1007/s10342-016-0943-1

Girona J, Luna M, Arbones A, Mata M, Rufat J, Marsal J (2002) Young olivet rees responses (Olea europea, cv "Arbequina" to different water supplies. Water function determination. Proceeding of the four international symposium on olive growing Vols 1 and 2. Acta Horticulturae, 586:277-280.

Girona J, Marsal J, Mata M, et al. (2004) Pear crop coefficients obtained in a large weighing lysimeter. Proceedings of the IVth International symposium on irrigation of horticultural crops. Acta Horticulturae , 664: 277-281

Girona J, del Campo J, Mata M, Lopez G, Marsal J (2011) A comparative study of apple and pear tree water consumption measured with two weighing lysimeters. Irrigation Science 29: 55-63.

Gislason PO, Benediktsson JA, Sveinsson JR (2006) Random Forests for land cover classification. Pattern Recognition Letters 27, 294-300.

Godsey, S.E., Kirchner, J.W., Tague, C.L. (2014). Effects of changes in winter snowpacks on summer low flows: Case studies in the Sierra Nevada, California, USA. Hydrological Processes, 28 (19): 5048-5064.

Gracia CA, Pla E, Sánchez A, Sabaté S (2004) GOTILWA+: Un modelo de crecimiento forestal basado en procesos ecofisiológicos. Cuadernos de la Sociedad Española de Ciencias Forestales. 18: 21-28.

ICC, Institut Cartogràfic de Catalunya, 2012 [online]. Available from: http://www.icc.cat/eng/Home-ICC/Inici/Inici.

Iglesias A et al. (2007) Challenges to manage the risk of water scarcity and climate change in the Mediterranean. Water Resources Management, 21, 775–788. doi:10.1007/s11269-006-9111-6

IPCC (2007a) Climate change 2007: the physical science basis. S. Solomon, et al., eds. Contribution of Working Group I to the Fourth Assessment Report of the Intergovernmental Panel on Climate Change. Cambridge, UK: Cambridge University Press.

IPCC (2007b) Climate change 2007: synthesis report. In: Core Writing Team, R.K. Pachauri and A. Reisinger, eds. Contribution of Working Groups I, II and III to the Fourth Assessment Report of the Intergovernmental Panel on Climate Change. Geneva: IPCC Secretariat.

IPCC (2014) Climate Change 2014. Synthesis Report. www.ipcc.com

James G, Witten D, Hastie T, Tibshirani R (2013) An introduction to statistical learning, with applications in R. Springer, New York.

Joffre R, Rambal S (1993) How Tree Cover Influences the Water Balance of Mediterranean Rangelands. Ecology, 74: 570–582. doi:10.2307/1939317

Kamusoko C, Gamba J (2015) Simulating urban growth using a Random Forest-Cellular Automata (RF-CA) model. ISPRS International Journal of Geo-Information 4. 447-470

Keenan T, Niinemets Ü, Sabaté S, Gracia C, Peñuelas J (2009) Process based inventory of isoprenoid emissions from European forets: model comparisons, current knowledge and uncertainties. Atmospheric Chemistry and Physics 9: 4053-4076.

Koutroulis AG et al. (2013) Impact of climate change on water resources status: a case study for Crete Island, Greece. Journal of Hydrology, 479, 146–158. doi:10.1016/j.jhydrol.2012.11.055

Kramer K, Mohren GMJ (2001) Long-term effects of climate change on carbon budgets of forests in Europe. Wageningen, ALTERRA, Green World Research. Report 194. 290 pp.

Kramer K, Leinonen I, Bartelink HH, Berbigier P, Borghetti M, Bernhofer C, Cienciala E, Dolman AJ, Froer O, Gracia CA, Granier A, Grünwald T, Hari P, Jans W, Kellomäki S, Loustau D, Magnani F, Markkanen T, Matteucci G, Mohren GMJ, Moors E, Nissinen A, Peltola H, Sabaté S, Sánchez A, Sontag M, Valentini R, Vesala T (2002) Evaluation of six process-based forest growth models using eddy-covariance measurements of CO2 and H2O fluxes at six forest sites in Europe. Global Change Biology, 8(3), 213-230.

Lindner M, Maroschek M, Netherer S, Kremer A, Barbati A, Garcia-Gonzalo J, Seidl R , Delzon S, Corona P, Kolström M, Lexer MJ (2010) Climate change impacts, adaptive capacity, and vulnerability of European forest ecosystems. Forest Ecology and Management, 259(4), 698-709.

Loepfe L, Martínez-Vilalta J, Oliveres J, Piñol J, Lloret F. (2010) Feedbacks between fuel reduction and landscape homogenisation determine fire regimes in three Mediterranean areas. Forest Ecology and Management 259: 2366–2374.

López-Moreno JI, Hess TM, White SM (2009) Estimation of reference Evapotranspiration in a mountainous mediterranean site using the Penman-Monteith equation with limited meteorological data. Pirineos,164: 7-31, ISSN 0373-2568.

López-Moreno, J.I., Zabalza, J., Vicente-Serrano, S.M., Revuelto, J., Gilaberte, M., Azorín-Molina, C., Morán-Tejeda, E., García-Ruiz, J.M. and Tague, C.L. (2014). Impact of Climate and land use change on water availability and reservoir management: Scenarios in the Upper Aragón River, Spanish Pyrenees. Science of the Total Environment, 493: 1222-1231.

Ludwig R et al. (2011) Towards an inter-disciplinary research agenda on climate change, water and security in Southern Europe and neighboring countries. Environmental Science Policy, 14 (7), 794–803. doi:10.1016/j.envsci.2011.04.003

Mariotti A et al. (2008) Mediterranean water cycle changes: transition to drier 21st century conditions in observations and CMIP3 simulations. Environmental Research Letters, 3, 044001. doi:10.1088/1748-9326/3/4/044001

Marsal J, Girona J, Casadesus J, Lopez G, Stöckle CO (2013) Crop coefficient (Kc) for apple: comparison between measurements by a weighing lysimeter and prediction by CropSyst. Irrigation Science, 31:455–463. DOI 10.1007/s00271-012-0323-7.

Javier Martin-Vide (coord). Tercer Informe sobre el canvi climàtic a Catalunya. 2016. IEC

Mitchell, S., Csillag, F. and Tague, C. (2005). Impacts of spatial partitioning in hydroecological models: predicting grassland productivity with RHESSys. Transactions in GIS, 9(3): 421-442.

Mohammed, I.N. and Tarboton, D.G. (2014). Simulated watershed responses to land cover changes using the Regional Hydro-Ecological Simulation System. Hydrological Processes, 15: 4511-4528.

Molowny-Horas R, Basnou C, Pino J (2015) A multivariate fractional regression approach to modeling land use and cover dynamics in a Mediterranean landscape. Computers, Environment and Urban Systems 54, 47-55.

Morales P, Sykes MT, Prentice I, Smith P, Smith B, Bugmanns H, Zierl B, Friedlingstein P, Viovy N, Sabaté S, Sánchez A, Pla E, Gracia C, Sitch S, Arneth A, Ogee J (2005). Comparing and evaluating process-based ecosystem model predictions of carbon and water fluxes in major European forest biomes. Global Change Biology, 11. 2211-2233.

Morán-Tejeda E, Zabalza J, Rahman K, Gago-Silva A, López-Moreno JI, Vicente-Serrano S, Lehmann A, Tague CL, Beniston M (2015) Hydrological impacts of climate and land-use changes in a mountain watershed: uncertainty estimation based on model comparison. Ecohydrol., 8: 1396–1416. doi: 10.1002/eco.1590.

Moriondo M, Good P, Durao R., Bindi M, Gianakopoulos C, Corte-Real J (2006) Potential impact of climate change on fire risk in the Mediterranean area. Climate Research, 31, 85-95.

Richard Moss, Mustafa Babiker, Sander Brinkman, Eduardo Calvo, Tim Carter, Jae Edmonds, Ismail Elgizouli, Seita Emori, Lin Erda, Kathy Hibbard, Roger Jones, Mikiko Kainuma, Jessica Kelleher, Jean Francois Lamarque, Martin Manning, Ben Matthews, Jerry Meehl, Leo Meyer, John Mitchell, Nebojsa Nakicenovic, Brian O'Neill, Ramon Pichs, Keywan Riahi, Steven Rose, Paul Runci, Ron Stouffer, Detlef van Vuuren, John Weyant, Tom Wilbanks, Jean Pascal van Ypersele, and Monika Zurek, (2008). Towards New Scenarios for Analysis of Emissions, Climate Change, Impacts, and Response Strategies. Technical Summary. Intergovernmental Panel on Climate Change, Geneva, 25 pp

Ndomba P, Mtalo F, Killingtveit A (2008) SWAT model application in a data scarce tropical complex catchment in Tanzania. Physics and Chemistry of the Earth, Parts A/B/C, 33, 626–632. doi:10.1016/j.pce.2008.06.013

Neitsch SL et al. (2005) Soil and water assessment tool - Theoretical documentation - Version 2005. USA: Agricultural Research Service and Texas Agricultural Experiment Station.

Ninyerola M, Pons X, Roure JM (2000) A methodological approach of climatological modelling of air temperature and precipitation through GIS techniques. International Journal of Climatology, 20, 1823-1841.

Nunes JP, Seixas J, Pacheco NR (2008) Vulnerability of water resources, vegetation productivity and soil erosion to climate change in Mediterranean catchments. Hydrological Processes, 22 (16), 3115-3134.

Pascual D, Pla E, López-Bustins JA, Retana J, Terradas J (2015) Impacts of climate change on water resources in the Mediterranean Basin: a case study in Catalonia, Spain. Hydrological Sciences Journal, Vol. 60, Iss. 12. http://dx.doi.org/10.1080/02626667.2014.947290

Pascual D, Zabalza Martinez J, Funes I, Vicente-Serrano SM, Pla E, Save R, Aranda X, Biel C (2016) Impacts of climate and global change on the ecological, hydrological and agriculture systems in the LIFE MEDACC case study basins. Deliverable 14. LIFE MEDACC.

Piñol J, Lledó MJ, Escarré A (1991) Hydrological balance of two Mediterranean forested catchments (Prades, northeast Spain). Hydrological Sciences Journal 36:95-107

Piñol J, Terradas J, Lloret F (1998) Climate Warming, Wildfire Hazard, and Wildfire Occurrence in Coastal Eastern Spain. Climate Change 38, 345–357.

R Core Team (2016). R: A language and environment for statistical computing. R Foundation for Statistical Computing, Vienna, Austria. https://www.R-project.org/.

Reynolds J, Wesson K, Desbiez ALJ, Ochoa-Quintero JM, Leimgruber P (2016) Using remote sensing and Random Forests to assess the conservation status of critical cerrado habitats in Mato Gross do Sul, Brazil. Land 5(2) 12.

Rodà F, Retana J, Gracia C, Bellot J (eds) (1999) Ecology of Mediterranean evergreen oak forests. Springer, Berlin, pp. 253-269.

Rodrigo A, Retana J, Picó FX (2004) Direct regeneration is not the only response of Mediterranean forests to large fires. Ecology 85:716–729.

Rodriguez-Galiano VF, Ghimire B, Rogan J, Chica-Olmo M, Rigol-Sanchez JP (2012) An assessment of the effectiveness of a random forest classifier for land-cover classification. ISPRS Journal of Photogrammetry and Remote Sensing 67, 93-104.

Rötter RP, Höhn J, Trnka M, Fronzek S, Carter TR, Kahiluoto H (2013) Modelling shifts in agroclimate and crop cultivar response under climate change. Ecology and Evolution, 3(12), 4197–4214. http://doi.org/10.1002/ece3.782.

Sabaté S., Gracia C, Sánchez A. (2002). Likely effects of Climate Change on growth of Quercus ilex, Pinus halepensis, Pinus pinaster, Pinus sylvestris and Fagus sylvatica forests in the Mediterranean Region. Forest Ecology and Management. 5906:1-15.

Sabaté S., Nadal-Sala D., Gracia C. (2014). Proyecciones sobre la evolución de los balances de carbono y agua para los bosques españoles en el contexto del cambio climático. En: Herrero A, Zavala MA, editores. Impactos, Vulnerabilidades y Adaptación de los Bosques y la Biodiversidad de España frente al cambio climático. MAGRAMA, Madrid.

Savé R, de Herralde F, Aranda X, Pla E, Pascual D, Funes I, Biel C (2012) Potential changes in irrigation requirements and phenology of maize, apple trees and alfalfa under global change conditions in Fluvià watershed during XXIst century: Results from a modeling approximation to watershed-level water balance. Agricultural Water Management, 114: 78– 87.

Senatore A, et al (2011) Regional climate change projections and hydrological impact analysis for a Mediterranean basin in Southern Italy. Journal of Hydrology, 399, 70–92. doi:10.1016/j.jhydrol.2010.12.035

Shinozaki K., Yoda K., Hozumi K., Kira T. (1964). A quantitavie analysis of plant form- pipe model theory. I. Basic analyses. Japanese Journal of Ecology. 14:97-105.

Smith SJ, Wigley TML (2006) Multi-Gas Forcing Stabilization with the MiniCAM. Energy Journal SI3:373-391.

Tague, C., and Band, L. (2004) RHESSys: Regional Hydro-Ecologic Simulation System: An object-oriented approach to spatially distributed modeling of carbon, water and nutrient cycling. Earth Interactions, 8, 1:42.

Terradas and Savé (1992) The influence of summer and winter stress and water relationships on the distribution of Quercus ilex L. Vegetatio 99/100:137-146.

Tian Z, Yang X, Sun L, Fischer G, Lianga Z, Pang J (2014) Agroclimatic conditions in China under climate chage scenarios projected from regional climate models. International Journal of Climatology, 34: 2988-3000.

Valverde P, Serralheiro R, de Carvalho M, Maia R, Oliveira B, Ramos V (2015) Climate change impacts on irrigated agriculture in the Guadiana river basin (Portugal). Agricultural Water Management, 152:17–30.

Van Griensven A (2005) Sensitivity, auto-calibration, uncertainty and model evaluation in SWAT2005. Unpublished report

Vayreda J, Martínez-Vilalta J, Gracia M, Retana J (2012) Recent climate changes interact with stand structure and management to determine changes in tree carbon stocks in Spanish forests. Global Change Biology 18: 1028-1041 DOI: 10.1111/j.1365-2486.2011.02606.x.

Vicente-Serrano SM, Zabalza Martínez J, Pla E, Pascual D, Serrano R, Borràs G, Savé R, Biel C (2014) Protocol of database quality and homogeneity. Deliverable 4. LIFE MEDACC. http://www.medacc-life.eu/document/deliverable-4-protocol-database-quality-and-homogeneity

Vicente-Serrano, S.M., Camarero, J.J., Zabalza, J., Sangüesa-Barreda, G., López-Moreno, J.I. and Tague, C.L. (2015). Evapotranspiration déficit controls net primary production and growth of silver fir: implications for Circum-Mediterranean forests under forecasted warmer and drier conditions. Agricultural and Forest Meteorology, 206: 45-54.

Vicente-Serrano SM, Pascual D, Pla E, Zabalza Martínez J, Borràs G, Cantos G, Savé R, Biel C, Funes I (2016). Historical trends in climate, land use and water demands. Deliverable 12. LIFE MEDACC. http://www.medacc-life.eu/document/deliverable-12-historical-trends-climate-hydrology-and-land-use

Wessels KJ, van den Bergh F, Roy DP, Salmon BP, Steenkamp KC, MacAlister B, Swanepoe D, Jewitt D (2016) Rapid land cover map updates using change detection and robust Random Forest classifiers. Remote Sensing 8(11), 888.

Wise M, Calvin K, Thomson A, ClarkeL, SandsR, SmithSJ, JanetosA, Edmonds J (2009) The Implications of Limiting CO2 Concentrations for Agriculture, Land-use Change Emissions, and Bioenergy. Technical Report. [PNNL-17943].

Wright MN (2016) Ranger: A Fast Implementation of Random Forests. R package version 0.5.0. https://CRAN.R-project.org/package=ranger

8. Annexes

8.1. Annex 1. Minutes of the meeting for the design of socioeconomic scenarios

LIFE MEDACC PROJECT
Reuniósobre escenaris socioeconòmics - 19 de maig de 2015
Seu de l'OCCC, Barcelona

Participants

Salvador Samitier (OCCC), Gabriel Borràs (OCCC), Gemma Cantos(OCCC), Robert Savé(IRTA), Sergio Vicente(IPE), Javier Retana(CREAF), Eduard Pla(CREAF), Diana Pascual (CREAF), Francesc Reguant (economista, assessor DAAM),

1. Introducció

Explicació del projecte a en Francesc Reguant.

Àmbits dels escenaris: Demografia (comptarem amb l'Anna Ribas, UdG), consums d'aigua, energia, usos del sòl i alimentació.

Objectiu en aquest darrer àmbit a Catalunya a futur: autosuficiència del 40%?

2. Aportacions d'en Francesc Reguant

Futur de tensió en funció de què prioritzem (energia? alimentació?...). Falta un vector important que és la desigualtat: afecta a les tensions alimentàries, que alhora afecta a canvis migratoris.

Com alimentarem a aquesta població? Els factors determinants de la suficiència alimentaria de Catalunya seran l'aigua i la població. Per una autosuficiència del 40%, el factor limitant és disposar també de sòl suficient. Des d'un punt de vista agrícola, les muntanyes no permeten competir amb algun país pla. Les grans crisis catalanes van ser per fam. No hi havia menjar suficient.

El G20 comença a parlar d'intensificació sostenible que ha de pivotar sobre tres pilars: ambiental, econòmic i social. Sostenible vol dir regadiu i ciència-tecnologia, però també admetre sostres ambientals.

Hem espatllat massa coses per resoldre-les anant marxa enrere, només cal artificialitzar: artificialitzar el bosc i l'aigua. Això no vol dir maltractar-los. Boscos trencats per camps agrícoles, ramaderia no productiva, sinó per obrir els boscos. Catalunya era un país d'ovelles a principis de segle. L'oví només es pot recuperar des d'un punt de vista ambiental. Dues agricultures. Xarxes per optimizar l'aigua i l'energia.

Gestió del sòl: Hem d'integrar en una única unitat decisòria la gestió dels usos del sòl. Es prenen decisions contradictòries.

La seguretat alimentària millorarà amb la reducció del malbaratament i el reciclatge.

Revolució biotecnològica: OMG (organismes millorats genèticament). Hi renunciarem a l'any 2050?

Anirà a més la producció d'insectes per alimentació, bioenergia càrnia, mar (algues, bioenergia, ...)

No hi ha sòl suficient però ens hem d'alimentar. Catalunya va fer dues coses: comprar la terra i l'aigua que no tenim en forma de gra, transformar-lo (alimentant al bestiar) i vendre'l de nou per pagar el gra. Però ens surt a zero perquè obtenim guanys de la venda del producte. Som molt competitius en ramaderia intensiva, que es mantindrà així perquè tot i que el preu de gra pugi, també pujarà el de la venda de la carn. Això funciona i funcionarà mentre la gent vulgui menjar carn. Aquest model intensiu ens dóna estabilitat en temes alimentaris i som competitius.

Hem de ser més sostenibles en el consum: menjant menys carn, això passarà però no cal avançar-nos.

Produccions agrícoles: Hauríem d'anar transformant-nos en funció del preu dels productes; anirem cap a conreus més transformadors en termes econòmics (l'horta, no fer horta és un luxe, un hivernacle de tomàquets produeix 44 vegades més que un camp de secà de Lleida. Si regues el blat, multipliques per 2, no per 44, un préssec per 12, ...). Tot amb reg molt eficient, menys agressiu pel medi perquè implica menys fertilitzacions (encara que unitàriament consumeixin més). L'agricultura tornarà a pujar la muntanya. Els preus dels aliments han pujat (van lligats al preu del petroli). Zones que no eren competitives ara comencen a ser-ho.

Dues agricultures: 1) no competitiva, que està en extensió: secà i muntanyes, , 2) potencialment competitiva en la qual basem el nostre abastament (90% del consum): vinya, horta i ramaderia intensiva. Polítiques rurals, ambientals i sostenibles a la primera, polítiques productives a la segona. Per defensar la primera agricultura, és necessari que la gent visqui en aquella terra i se'ls pagui per aquests serveis: això vol dir canviar radicalment el sistema d'ajuts de l'agricultura. L'agricultura intensiva abusa d'aquests ajuts que no els necessita. Els ajuts han d'anar a aquesta agricultura més residual i a cobrir els riscos associats a la volatilitat dels productes.

Reflexions:

- Canviarem la forma de consum quan pugin molt els preus (carn)
- No estem a la frontera del desert, si hi ha un producte que no funciona es podran trobar d'altres a partir de la tecnologia, etc ...
- Fer recomanacions que la gent canviï una cosa que serà rendible en 20 anys no funciona perquè encara tenim temps
- No hi ha transferència dels esforços que s'han de fer per produir aliments

El PIB destinat a l'agricultura: 1,7% del valor afegit del PIB agricultura. 3,8% incloent l'industria agroalimentària. És la indústria que més contribueix al PIB (farmacèutiques 3,4%). Per produir una poma, es necessiten uns serveis afegits (assessorament, energia, compra de molts productes, genera serveis de bancs, transport, ...). En conjunt, l'agricultura, la indústria, la distribució dels aliments, el cuiner i cambrer del restaurant, la botiga i el Mercabarna, és el 30,5% de l'economia. Sense intermediaris ni serveis, el pes de l'agricultura catalana en el PIB és del 15% (agricultura i indústria). L'energia és el 1,8%, els cotxes és el 2,7%.

3. Debat posterior

- Polítiques europees. La PAC està canviant, ens ha canviat el paisatge (hi ha més pèsols, cigrons, colza ...). Està en procés de nacionalització, està patint la mateixa crisi europea. Espanya ha fet un exercici de maquillatge sense canviar res. L'UE vol treure la traçabilitat dels productes segons registres històrics (si mantens el producte des de fa molts anys, cobres més). A Europa aniran perdent els ajuts plans i històrics i es destinaran més a l'agricultura en dificultat i la volatilitat. L'afegitó és que els ajuts a Europa serveixen com aranzel ocult, que s'estan reduint al món i es mantenen a Europa de manera oculta. És un aranzel molt car, perquè s'han de pagar. Politiques clares: recuperar les proteaginoses (lleguminoses, colza, ...). Més condicionants ambientals. Hi ha una evolució molt positiva cap ala reducció de productes químics o l'ús de substàncies menys contaminants. La PAC fa el discurs correcte però la despesa incorrecta (es paga el blat de moro). El paquet gros és el pagament únic i a Espanya s'aplica com es venia aplicant des de fa temps, pagant a tots el mateix com a aranzel ocult.
- A nivell mundial, expectativa de increment de preus. En produccions estàndards, els preus són globals.
- Tornem cap a la muntanya: Es pot modificar la tendència d'aforestació massiva o seguirà així com a futur? La propera llei agrària inclourà la recuperació de terrenys abandonats. Fins a 1991, la població rural queia en picat excepte les comarques de regadiu històric, on no s'ha reduït la població des de 1850, de fet s'ha incrementat. Al 91, va començar a créixer un 20%, i aquests darreres anys s'ha frenat però no disminuït. Aquesta gent viu de productes de valor afegit en mercats de proximitat.
- Diferència entre menjar i alimentar-se. Reaprofitament d'aliments descartats per calibre o preu.
- Directiva marc de l'aigua. Problema de lixiviats. La cabana ramadera és catalana, no es porten els porcellets d'Europa, s'engreixen aquí i es venen fora (ens quedem amb les dejeccions). GESFER: empresa que coordinés la bona gestió de les dejeccions ramaderes, però que per pressions va ser una empresa sense objectius.
- Revolució tecnològica: Tant sols ha servit per incidir en malalties, lo qual tant sols genera un 6% de pèrdues en productivitat en el primer mon. No son descartables el OMG, però tenen moltes limitacions
- Malbaratament: existeix realment? No és resultat d'una sobreproducció? Associat a la forma de producció?
- Podem seguir amb el model actual de producció d'un 20% de superfície agrícola intensiva (és la superfície regable)? No. Anirem cap a conreus més transformadors i reduint el malbaratament de l'aigua, hi haurà més hivernacles, més horticultura i fructicultura. Tenim els cereals a França molt a prop.
- Tindrem limitació tèrmica en agricultura, però la tecnologia ho pot equilibrar.
- Fruits secs en regadiu: des d'un punt de vista de mercat és bo, però a llarg termini, no és el seu lloc, ja que no són competitius en aquestes condicions.
- Els departaments d'agricultura i medi ambient s'haurien d'ajuntar per prendre decisions úniques.
- Hi haurà una pressió mundial en el tema alimentari, si hi ha una crisi, potser França no ens vol vendre el gra. Els països productors poden tancar fronteres

perquè si hi ha crisis s'encareix el preu i la seva gent pot morir. Hem de tenir productes propis.

- Escenaris del projecte per 2050. El que hem vist als últims 30 anys, hi ha hagut una densificació del bosc, increment del regadiu, reducció del secà. Els regadius en quina mesura la superfície s'incrementarà i l'eficiència del reg hi serà. No es veu possible incrementar la superfície de regadiu a excepció del ja planificat o en marxa (Segarra Garrigues), la majoria ja estan fets. En un futur aquests regadius estan pensants per ser més eficients. 160.000 ha noves respecte a la situació de l'any 2000. També hi ha moltes obres d'eficiència però que com que s'estalviava aigua, aquesta s'inverteix en noves zones de regadiu (efecte rebot). Però a Catalunya no hi ha espai per transformar més en regadiu. Sí que hi haurà connexions entre conques per assegurar garanties, però no grans ampliacions.
- Maresme: amb l'increment de la temperatura, és una zona molt factible per recuperació de l'horta, com era fa anys, que hi havia taronges.
- Els rendiments de l'agricultura no han pujat tant com l'increment de la població amb la revolució verda? No està demostrat.

<u>Cloenda</u>:
Quan parlem de sobirania alimentària, tots els factors són igual d'importants i part del problema.
Les grans crisis alimentaries de 2007, 2010 i 2012 tenen el segell de canvi climàtic. 2007: es va projectar per llei una demanda espectacular d'hidrocarburs per reduir l'impacte del CO2. 2010: crisis de calor a Rússia, no registrada als últims 120 anys. 2012: causada per grans sequeres de les planes del Mississippí.

4. Escenaris socioeconòmics

<u>Hipòtesis</u>

- Sense increment de la superfície de regadiu (fora dels ja planificats). El manteniment de la superfície, les conseqüències son diferent per conca: la Muga ja es deficitària, per tant les tensions seran més gran. Al Segre, quan tot Segarra – Garrigues i Urgell estigui modernitzat, no serà necessària tota la concessió.
- Conreus de secà: Es mantindran ja que estan molt ben aprofitats (normalment estan associats a granges a on reutilitzen els nitrats, és un subproducte). Si s'abandonen les granges, s'abandonarà el secà. Continua havent-hi abandonament de secans a fons de vall. Plausible reducció de la superfície de secà en les zones marginals molt lleu. Ens pot passar corbes de taxes d'abandonament de camps de conreu.
- Es millora l'eficiència: es reduiran les demandes (si es modernitza el Urgell, sinó no).
- Zones de muntanyes:
    - Augment de la població: Que consumeix i afavoreix la producció local, augment del preu.

- o Recuperació del sector jove a l'agricultura en general i també en les zones de muntanya .
- o Principalment remugants (oví, boví i sobretot equí).
- o Dos escenaris: Fre de la tendència a l'aforestació en zones de muntanya o continuïtat de les pèrdues actuals.
- o Cereals no es tornaran a sembrar, però patates, fruits secs, ... amb valor afegit.

<u>Pla de gestió de l'aigua de Catalunya (2016-2021).</u>

Els escenaris de demandes són pel 2050.

- 2021-2027: reducció del 5% dels recursos.
- 2045: reducció del 10% dels recursos.

En temes urbans, s'ha reduït un 90hm3/any en domèstic, i 8 hm3/any en agrícola entre 2007 i 2012.

Diagnosi 2012:

- Muga necessita font complementaria actual de 0,5 m3/s (8 hm3/any). Mesures internes com reutilització o recreixement de Boadella. A futur (2045), necessita font de 0,75 a 1 m3/s. Però perquè la demanda agrícola fixada per l'ACA són 60 hm3 (2 m3/s). Però si la demanda real és la meitat, no caldria recreixement de Boadella
- Ter: Actualment deficitària, dèficit de 2 m3/s (estimat el pitjor dels anys 2006-2008). La proposta actual és que el Pla Hidrològic Nacional digui allò que s'ha de fer. A 2045, el dèficit serà de 6 m3/s.

<u>Processos</u>

- Intensificació
- No increment de regadius
- Planificació de l'aigua: Problema en que sempre se sobreestima la demanda.
- Les projeccions demogràfiques han superat les previsions, però les demandes urbanes han disminuït 100 hm3. En l'agricultura es pensa que les demandes augmenten, però no és cert. A MEDACC, a la Muga l'estimació és de 15 hm3/any, però en el pla de gestió es mantenen les demandes de sempre (60 hm3) i es desembassen 29 hm3 de Boadella. Al Ter passa una cosa semblant però l'aigua que passa pels canals té un objectiu també ecològic.
- Increment de població que afecta a l'increment de consum de l'aigua, però no a l'increment de la superfície agrícola.
- Purins: Catalunya té una deficiència de nitrogen, el problema és com es reparteix. El problema amb els fertilitzacions és de gestió, està mal repartit (GESFER).
- Energia: El consum energètic augmenta any a any, independentment de l'eficiència. El preu de l'energia afecta al reg.

Eixos:

- Demografia + demandes associades
- Què passa amb el territori: matriu sistemes naturals. Transformació naturals del bosc, els roures comencen a desplaçar als pins.

Escenaris

- Parts baixes de les conques: saber què passa amb la demanda d'aigua. Escenaris de cobertes són petites, ja que no hi ha augment de la superfície de regadiu. Es pot jugar amb les demandes urbanes, excepte en el Segre (que importa l'agrícola).
- Capçaleres: Escenaris cobertes d'usos del sòl.
- Han de ser comuns
- Combinacions: 1) Com fins ara, 2) escenaris de baix i dalt i després veurem quins són versemblants o no.

8.2. Annex 2. Diagram of the methodology performed in the agriculture modelling

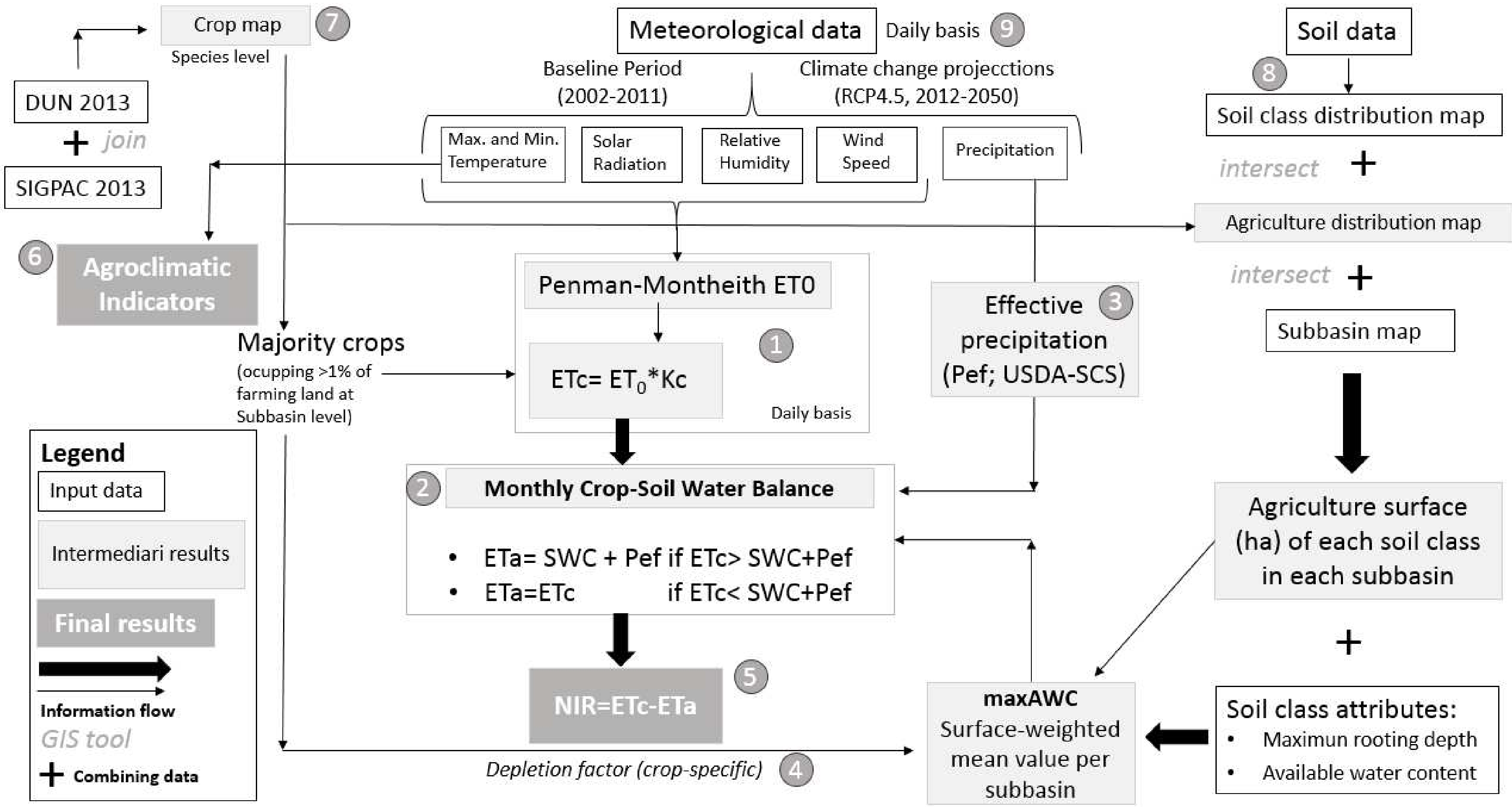

Figure 27. Diagram of agriculture modelling methodology. The method components are numbered according to the description in section 5.

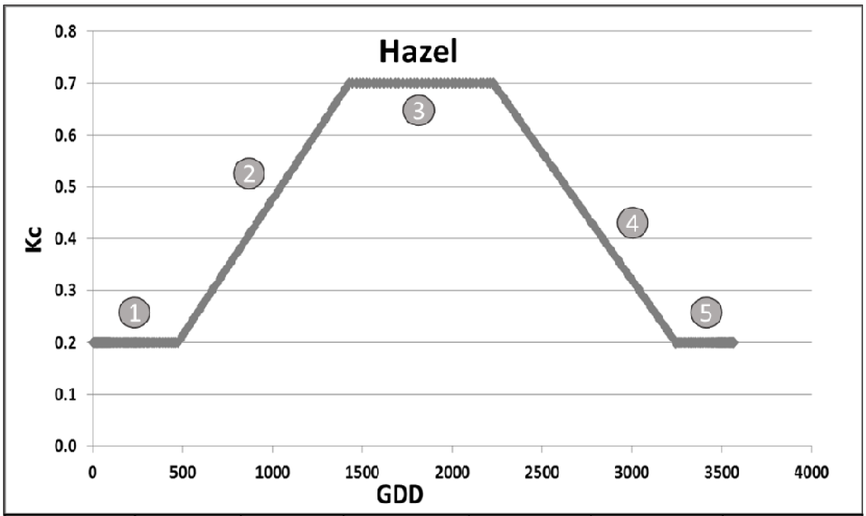

Function Section	$Kc_{initial}$	Kc_{final}	$GDD_{initial}$	GDD_{final}	a	b
1	0.2	0.2	0	474	0	0.2
2	0.2	0.7	474	1426	0.000525	-0.048822
3	0.7	0.7	1426	2230	0	0.7
4	0.7	0.2	2230	3247	-0.000492	1.7966817
5	0.2	0.2	3247	3567	0	0.2

Figure 28. Kc of Hazel as a function of GDD from 1st January. a and b values are slope and intercept, respectively, of each numbered lineal subfunction corresponding to each Kc function section. Calculated from ACA and IRTA (2008). See section 5.2 for details.

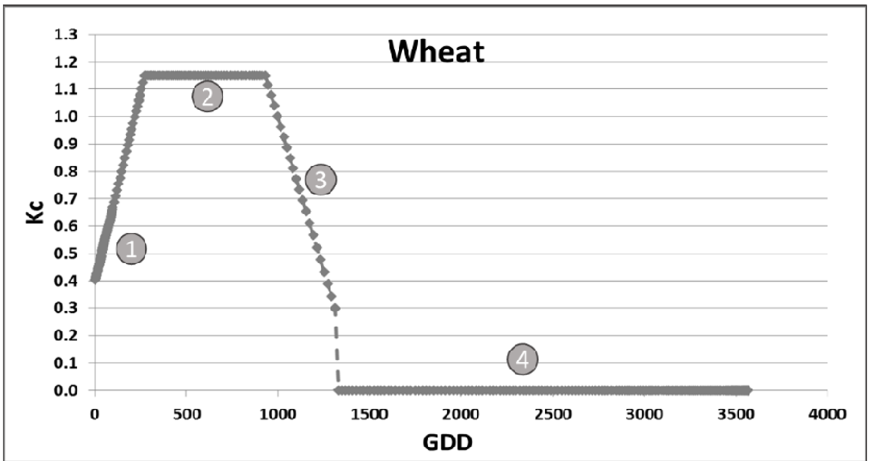

Function Section	$Kc_{initial}$	Kc_{final}	$GDD_{initial}$	GDD_{final}	a	b
1	0.4	1.15	0	272	0.002762	0.400000
2	1.15	1.15	272	930	0	1.15
3	1.15	0.3	930	1312	-0.002226	3.220624
4	0	0	1312	3500	0	0

Figure 29. Kc of Wheat as a function of GDD from 1st January. a and b values are slope and intercept, respectively, of each numbered lineal subfunction corresponding to each Kc function section. Triticale and winter cereals fodder crops Kc was calculated as wheat Kc. Calculated from ACA and IRTA (2008). See section 5.2 for details.

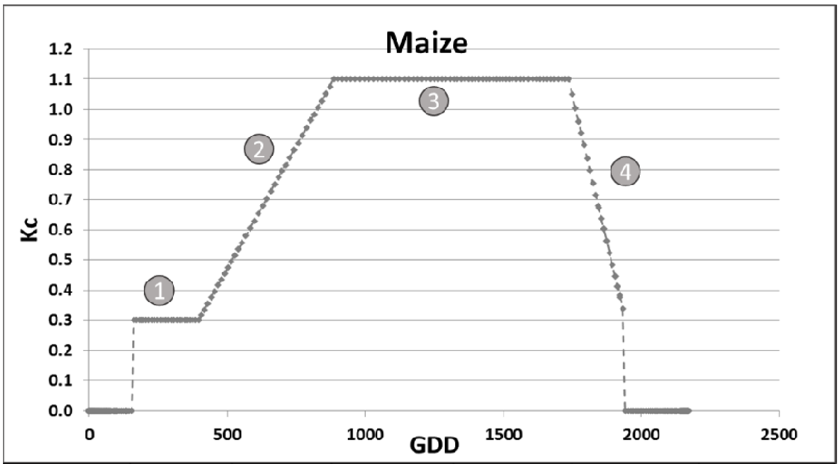

Function Section	Kc initial	Kc fina	GDD iritial	GDD final	a	b
1	0.3	0.3	154	396	0	0.3
2	0.3	1.1	396	886	0.001631	-0.345922
3	1.1	1.1	886	1736	0	1.1
4	1.1	0.3	1736	1942	-0.003873	7.823605

Figure 30. Kc of Maize as a function of GDD from 1st January. a and b values are slope and intercept, respectively, of each numbered lineal subfunction corresponding to each Kc function section. Calculated from ACA and IRTA (2008). See section 5.2 for details.

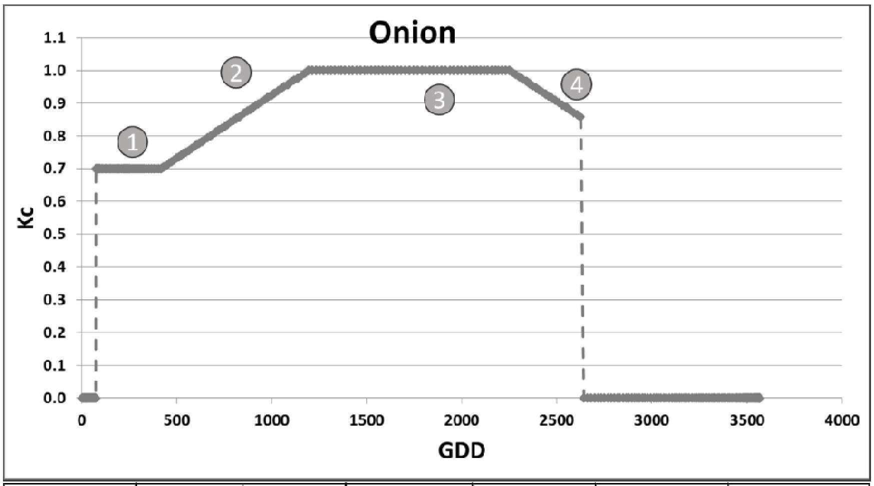

Function Section	Kc initia	Kc f nal	GDD initial	GDD final	a	b
1	0.7	0.7	75	416	0	0.7
2	0.7	1	416	1193	0.000386	0.539360
3	1	1	1193	2248	0	1
4	1	0.85	2248	2642	-0.000380	1.855182

Figure 31. Kc of Onion as a function of GDD from 1st January. a and b values are slope and intercept, respectively, of each numbered lineal subfunction corresponding to each Kc function section. Vegetables Kc was calculated as onion Kc because it is the vegetable more widespread over the three basins. Calculated from ACA and IRTA (2008). See section 5.2 for details.

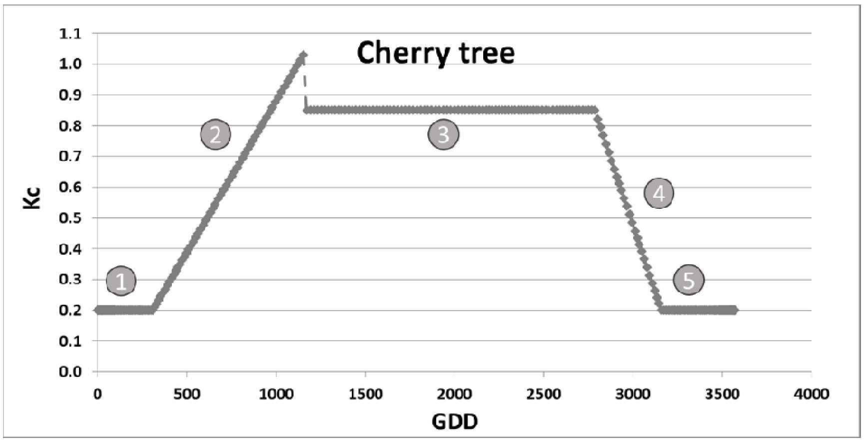

Function Section	Kc initial	Kc final	GDD initial	GDD final	a	b
1	0.2	0.2	0	309	0	0.2
2	0.2	1.05	309	1172	0.000984	-0.104011
3	0.85	0.85	1172	2785	0	0.85
4	0.85	0.2	2785	3157	-0.001747	5.715940
5	0.2	0.2	3157	3567	0	0.85

Figure 32. Kc of cherry tree as a function of GDD from 1st January. a and b values are slope and intercept, respectively, of each numbered lineal subfunction corresponding to each Kc function section. Vegetables Kc was calculated as onion Kc because it is the vegetable more widespread over the three basins. Calculated from ACA and IRTA (2008). See section 5.2 for details.

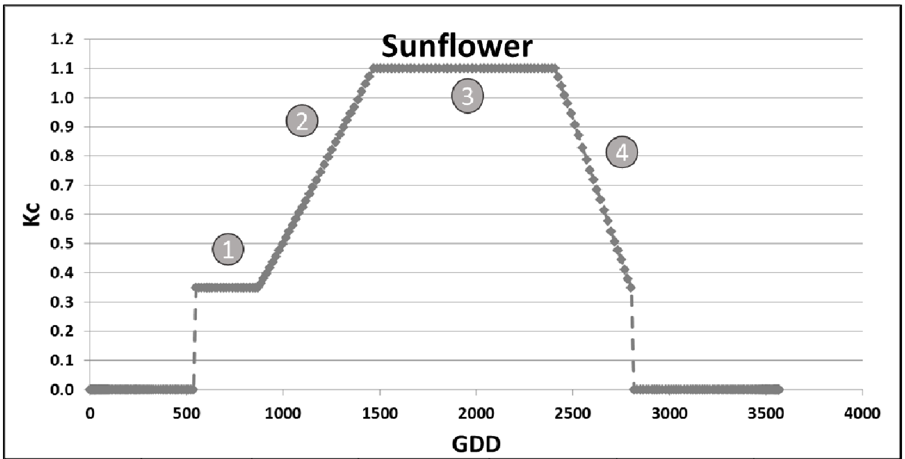

Function Section	Kc initial	Kc final	GDD initial	GDD final	a	b
1	0.35	0.35	144	356	0	0.35
2	0.35	1.1	356	787	0.001740	-0.270293
3	1.1	1.1	787	1488	0	1.1
4	1.1	0.35	1488	1772	-0.002641	5.029496

Figure 33. Kc of sunflower as a function of GDD from 1st January. a and b values are slope and intercept, respectively, of each numbered lineal subfunction corresponding to each Kc function section. Calculated from ACA and IRTA (2008). See section 5.2 for details.

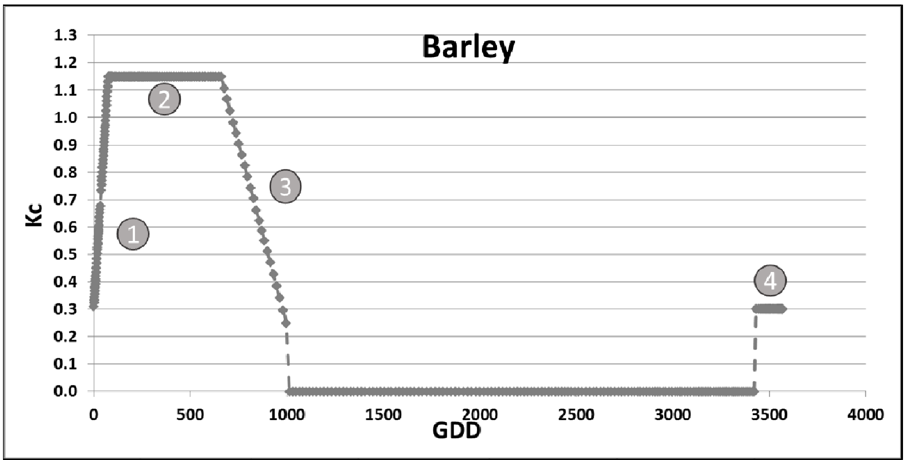

Function Section	Kc initial	Kc final	GDD initial	GDD final	a	b
1	0.3	1.15	0	75	0.011306	0.300000
2	1.15	1.15	75	660	0	1.15
3	1.15	0.25	660	997	-0.002675	2.915793
4	0.3	0.3	3420	3567	0	0.3

Figure 34. Kc of barley as a function of GDD from 1st January. a and b values are slope and intercept, respectively, of each numbered lineal subfunction corresponding to each Kc function section. Oats Kc was calculated as barley Kc. Calculated from ACA and IRTA (2008). See section 5.2 for details.

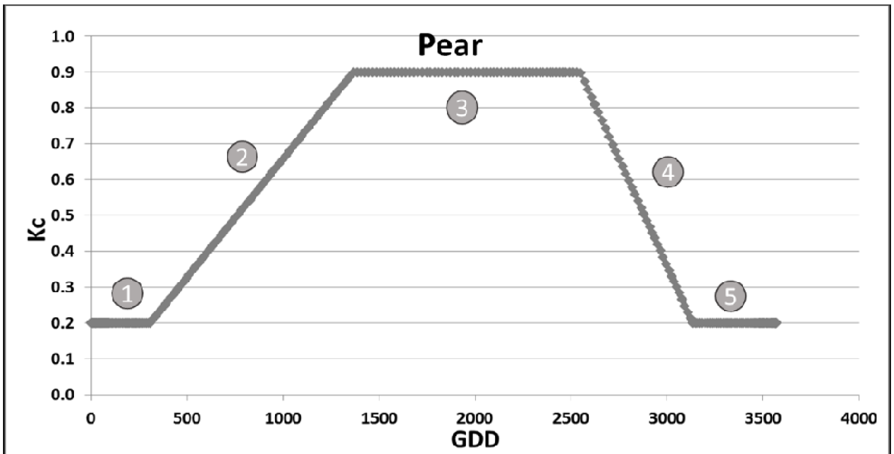

Function Section	Kc initial	Kc final	GDD initial	GDD final	a	b
1	0.2	0.2	0	309	0	0.2
2	0.2	0.9	309	1366	0.000662	-0.004444
3	0.9	0.9	1366	2549	0	0.9
4	0.9	0.2	2549	3133	-0.001199	3.956161
5	0.2	0.2	3133	3567	0	0.2

Figure 35. Kc of pear as a function of GDD from 1st January. a and b values are slope and intercept, respectively, of each numbered lineal subfunction corresponding to each Kc function section. Calculated from ACA and IRTA (2008). See section 5.2 for details.

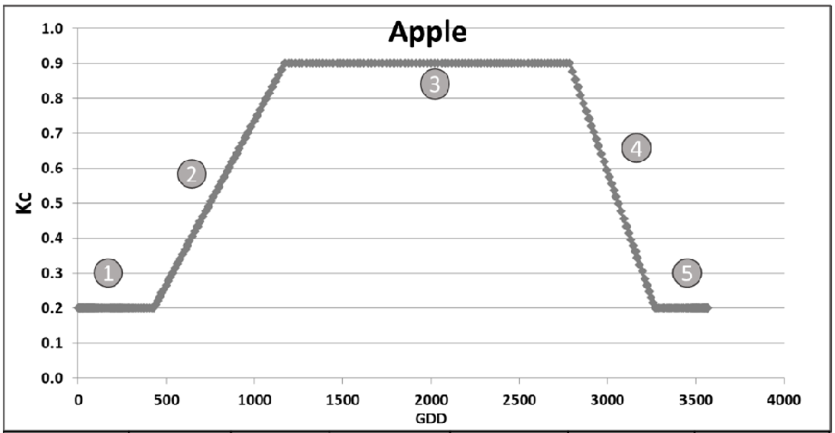

Function Section	Kc initial	Kc final	GDD initial	GDD final	a	b
1	0.2	0.2	0	428	0	0.2
2	0.2	0.9	428	1172	0.000941	-0.202784
3	0.9	0.9	1172	2785	0	0.9
4	0.9	0.2	2785	3268	-0.001448	4.932709
5	0.2	0.2	3268	3567	0	0.2

Figure 36. Kc of apple as a function of GDD from 1st January. a and b values are slope and intercept, respectively, of each numbered lineal subfunction corresponding to each Kc function section. Calculated from ACA and IRTA (2008). See section 5.2 for details.

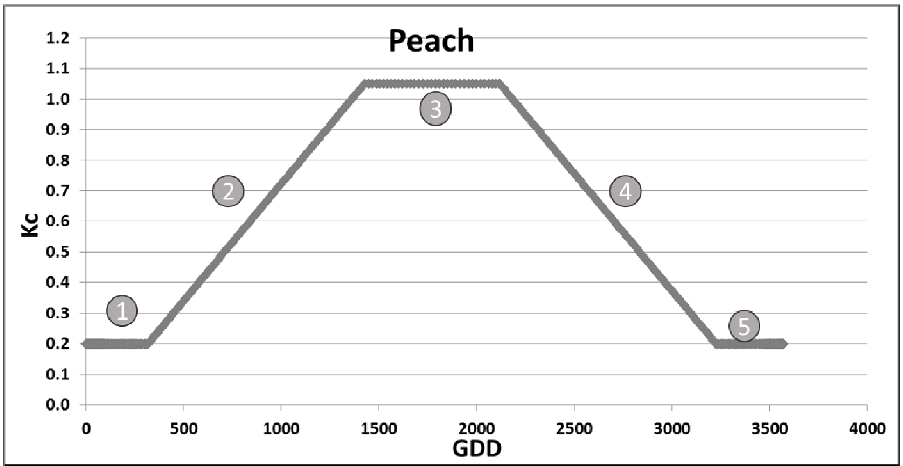

Function Section	Kc initial	Kc final	GDD initial	GDD final	a	b
1	0.2	0.2	0	319	0	0.2
2	0.2	1.05	319	1426	0.000768	-0.044839
3	1.05	1.05	1426	2117	0	1.05
4	1.05	0.2	2117	3223	-0.000768	2.675634
5	0.2	0.2	3223	3567	0	0.2

Figure 37. Kc of peach as a function of GDD from 1st January. a and b values are slope and intercept, respectively, of each numbered lineal subfunction corresponding to each Kc function section. Calculated from ACA and IRTA (2008). See section 5.2 for details.

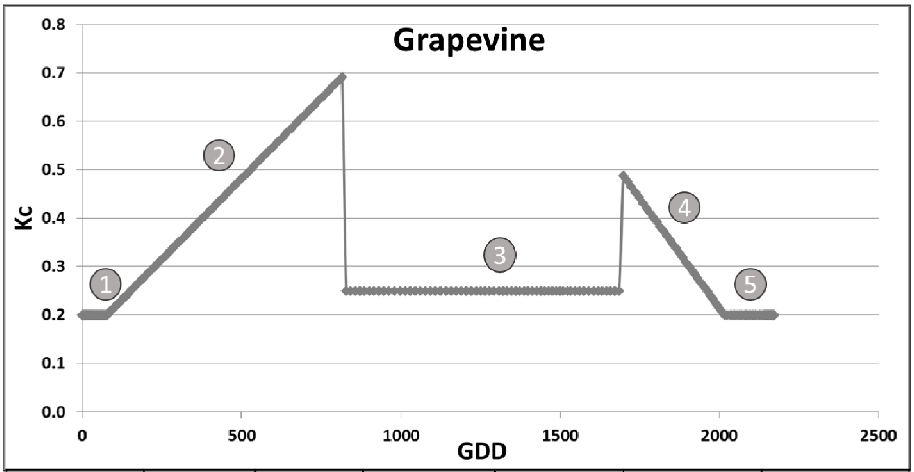

Function Section	Kc initial	Kc final	GDD initial	GDD final	a	b
1	0.2	0.2	0	77	0	0.2
2	0.2	0.7	77	829	0.000665	0.148907
3	0.25	0.25	829	1686	0	0.25
4	0.5	0.2	1686	2017	-0.000907	2.028240
5	0.2	0.2	2017	2171	0	0.2

Figure 38. Kc of grapevine as a function of GDD from 1st January. a and b values are slope and intercept, respectively, of each numbered lineal subfunction corresponding to each Kc function section. Calculated from ACA and IRTA (2008). See section 5.2 for details.

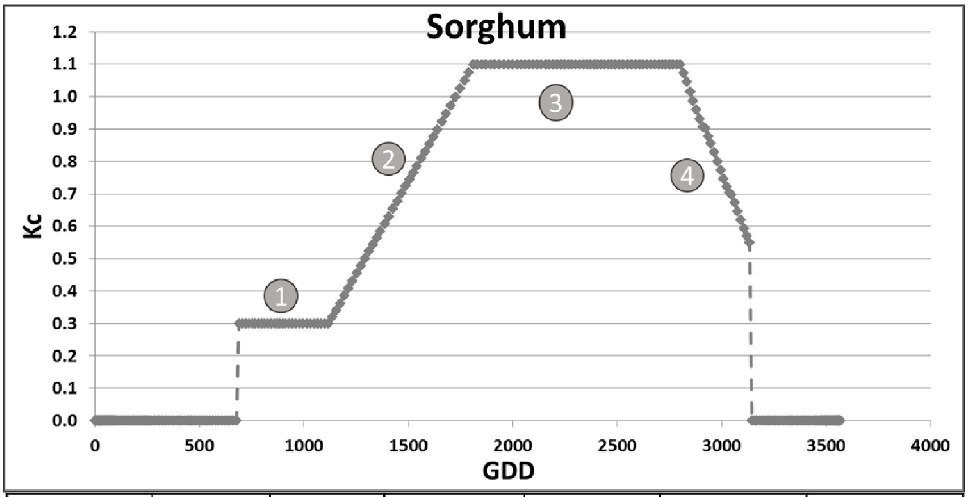

Function Section	Kc initial	Kc final	GDD initial	GDD final	a	b
1	0.3	0.3	236	528	0	0.3
2	0.3	1.1	528	1045	0.001545	-0.515382
3	1.1	1.1	1045	1772	0	1.1
4	1.1	0.55	1772	1979	-0.002659	5.812156

Figure 39. Kc of sorghum as a function of GDD from 1st January. a and b values are slope and intercept, respectively, of each numbered lineal subfunction corresponding to each Kc function section. Calculated from ACA and IRTA (2008). See section 5.2 for details.

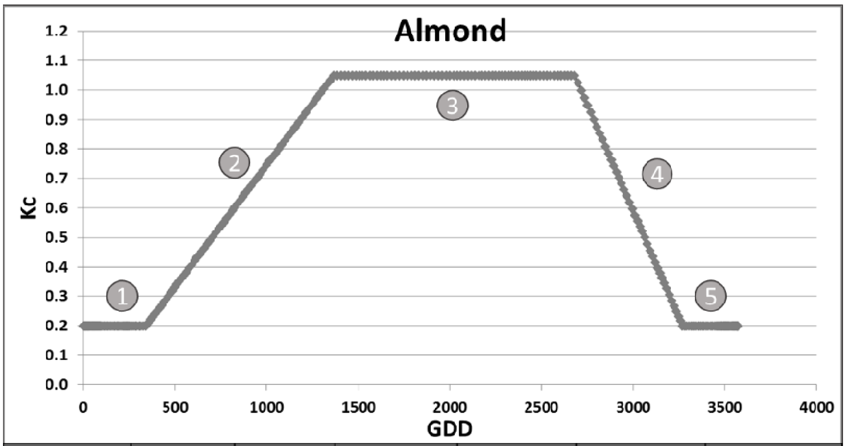

Function Section	Kc initial	Kc final	GDD initial	GDD final	a	b
1	0.2	0.2	0	342	0	0.2
2	0.2	1.05	342	1366	0.000830	-0.083842
3	1.05	1.05	1366	2680	0	1.05
4	1.05	0.2	2680	3268	-0.001444	4.921001
5	0.2	0.2	3268	3567	0	0.2

Figure 40. Kc of Almond as a function of GDD from 1st January. a and b values are slope and intercept, respectively, of each numbered lineal subfunction corresponding to each Kc function section. Calculated from ACA and IRTA (2008). See section 5.2 for details.